

Supporting information for:

Preparation of a Borane-Appended Co(III) Hydride: Evidence for Metal-Ligand Cooperativity in O–H Bond Activation

Joseph A. Zurakowski,^{a,¶} Brady J. H. Austen,^{a,¶} Maeve, C. Dufour,^a Moulika Bhattacharyya,^a

Denis M. Spasyuk,^b and Marcus W. Drover^{a,*}

*E-mail: marcus.drover@uwindsor.ca

^aDepartment of Chemistry and Biochemistry, The University of Windsor, 401 Sunset Avenue, Windsor, ON, N9B 3P4, Canada

^b Canadian Light Source Inc., 44 Innovation Blvd., Saskatoon, SK, S7N 2V3, Canada

[¶]These authors contributed equally

1. Experimental Section	S2
2. Preparation of Compounds	S3
3. Multinuclear NMR data	S11
4. Crystallography	S49
5. Computational Chemistry	S52

Experimental Section:

General Considerations. All experiments were carried out employing standard Schlenk techniques under an atmosphere of dry nitrogen employing degassed, dried solvents in a solvent purification system supplied by PPT, LLC. Non-halogenated solvents were tested with a standard purple solution of sodium benzophenone ketyl in tetrahydrofuran in order to confirm effective moisture removal. *d*₆-benzene was dried over molecular sieves and degassed by three freeze-pump-thaw cycles. HBCy₂¹ and BCy₂ⁿOct² were prepared using literature procedures. All other reagents were purchased from commercial vendors and used without further purification unless otherwise stated.

Physical methods. ¹H NMR spectra are reported in parts per million (ppm) and are referenced to residual solvent e.g., ¹H(C₆D₆): δ 7.16; ¹³C(C₆D₆): 128.06; coupling constants are reported in Hz. ¹³C, ¹¹B, and ³¹P NMR spectra were performed as proton-decoupled experiments and are reported in ppm.

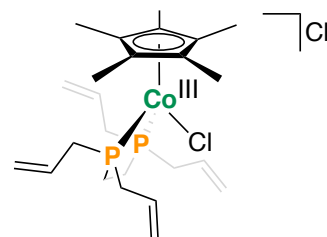
Electrochemistry. Electrochemical measurements were carried out using a BioLogic SP50: Single Channel Electrochemical Potentiostat. A freshly polished glassy carbon electrode was used as the working electrode, a platinum wire was used as the counter electrode, and a Ag wire/AgOTf solution (with electrolyte) was used as the reference electrode. All analytes (~2 mM) were measured in 4 mL THF in an N₂-filled glovebox containing electrolyte (0.25 M [ⁿBu₄N]PF₆). All reported potentials are referenced to the ferrocene/ferrocenium couple, [Cp₂Fe]⁺/Cp₂Fe, which was measured externally and internally to ensure consistency.

¹ A. Abiko, *Org. Synth.* 2002, **79**, 103.

² M.W. Drover, L.L. Schafer, J.A. Love. *Angew Chem., Int. Ed.* 2016, **51**, 3181.

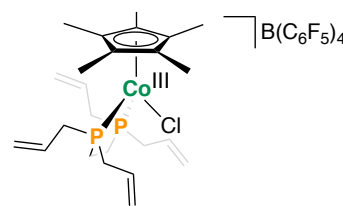
Preparation of Compounds:

[Cp*Co^{III}(tape)Cl]Cl ([1]Cl; C₂₄H₃₉Cl₂P₂Co, M_w = 519 g/mol): In the glovebox, [Cp*Co(μ-Cl)]₂ (20 mg, 0.09 mmol, 0.5 equiv.) and tape (22 mg, 0.09 mmol, 1 equiv.) were combined in a 20 mL scintillation vial equipped with a stir bar. Approximately 4 mL of hexanes was added and the solution was allowed to stir for 1 h at room temperature. The resulting solution was orange in color with ample brown precipitate ([1]Cl). The solution was decanted away from the solid and the solid was washed with additional hexanes (3 x 5 mL portions) and dried *in-vacuo* to provide [1]Cl (18 mg, 82%). For the isolation of **2**, solvent from the aforementioned hexane washings was removed *in-vacuo*, providing an orange solid that was once again dissolved in hexanes, filtered, and solvent removed to provide **2** (16 mg, 82 %). ¹H NMR (500 MHz, CDCl₃, 298 K): δ = 5.94 (m, 2H; CH(allyl)), 5.79 (m, 2H; CH(allyl)), 5.51-5.17 (m (two sets), 8H; CH₂(allyl)), 3.08 (br, 2H; P-CH₂(allyl)), 2.89 (br, 6H; P-CH₂(allyl)), 2.06 (br, 2H; P-CH₂-CH₂-P), 1.57 (br, 2H; P-CH₂-CH₂-P), 1.45 (s, 15H; Cp*H). ¹³C{¹H} NMR (125.8 MHz, CDCl₃, 298 K): δ = 130.4, 129.4, 123.1, 120.9, 98.6, 30.6, 30.4, 22.1, 11.0. ³¹P{¹H} NMR (202.5 MHz, CDCl₃, 298 K): δ = + 65.3. HRESI(+)-MS: calcd. 483.1548 exptl. 483.1555 for C₂₄H₃₉ClP₂Co [M]⁺.



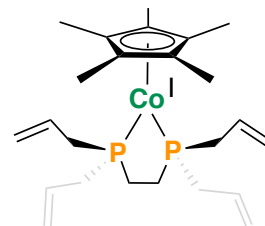
[Cp*Co^{III}(tape)Cl]B(C₆F₅)₄ ([1]B(C₆F₅)₄; C₄₈H₃₉BClF₂₀P₂Co, M_w = 1163 g/mol): In the glovebox, [Cp*Co^{III}(tape)Cl]Cl ([1]Cl) (17 mg, 0.03 mmol) was weighed into a 20 mL scintillation vial equipped with a stir bar. Approximately 4 mL of THF was added. To this solution was added dropwise, a 2 mL

solution of [Li(OEt)₂]B(C₆F₅)₄ (29 mg, 0.03 mmol, 1 equiv.) and the reaction was allowed to stir for 1 h at room temperature. The resulting orange solution was filtered through Celite® and the solvent was removed *in-vacuo* to give [1]B(C₆F₅)₄ as a brown solid (35 mg, 92%). ¹H NMR (500 MHz, CDCl₃, 298 K): δ = 5.77 (m, 4H; CH(allyl)), 5.43-5.20 (m (two sets), 8H; CH₂(allyl)), 3.05 (br, 6H; P-CH₂(allyl)), 2.54 (m, 2H; P-CH₂(allyl)), 1.83 (d, ³J_{H,P} = 9.5 Hz, 4H; P-CH₂-CH₂-P), 1.61 (t, ⁵J_{H,P} = 1.7 Hz, 15H; Cp*H). ¹³C{¹H} NMR (125.8 MHz, CDCl₃, 298 K): δ = 148.4 (dm, ¹J_{C,F} = 238 Hz; B(C₆F₅)₄), 138.4 (dm, ¹J_{C,F} = 238 Hz; B(C₆F₅)₄), 136.4 (dm, ¹J_{C,F} = 238 Hz; B(C₆F₅)₄), 128.9, 127.7, 122.5, 122.1, 99.4, 31.2 (m), 30.9 (m), 21.5 (t, J_{C,P} = 22 Hz), 10.3; B-C of B(C₆F₅)₄ not observed. ³¹P{¹H} NMR (202.5 MHz, CDCl₃, 298 K): δ = + 67.2. ¹¹B{¹H} NMR (160.5 MHz, CDCl₃, 298 K): δ = - 16.6.



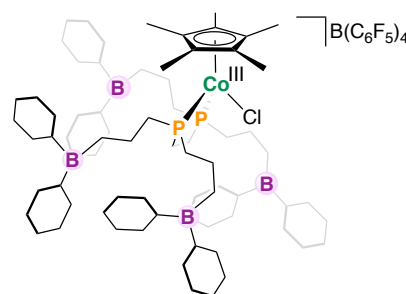
$^{19}\text{F}\{^1\text{H}\}$ NMR (470 MHz, CDCl_3 , 298 K): $\delta = -132.5$ (8F, F_{ortho}), -162.9 (t, $^3J_{\text{F,F}} = 21$ Hz; F_{para}), -166.8 (8F, F_{meta}). HRESI(+)-MS: calcd. 483.1548 exptl. 483.1534 for $\text{C}_{24}\text{H}_{39}\text{ClP}_2\text{Co}$ $[\text{M}]^+$.

[Cp*Co^I(tape)] (2; $\text{C}_{24}\text{H}_{39}\text{P}_2\text{Co}$, $M_w = 448$ g/mol): In the glovebox, $[\text{Cp}^*\text{Co}^{\text{II}}(\mu\text{-Cl})_2]$ (20 mg, 0.09 mmol, 0.5 equiv.) and tape (22 mg, 0.09 mmol, 1 equiv.) were combined in a 20 mL scintillation vial equipped with a stir bar. Approximately 4 mL of hexanes was added and the solution was allowed to stir for 1 h at room temperature. The resulting solution was orange in color with ample brown precipitate ($[\text{1}]\text{Cl}$). The solution was decanted away from the solid and the solid was washed with additional hexanes (3 x 5 mL portions) and dried *in-vacuo* to provide $[\text{1}]\text{Cl}$ (18 mg, 82%). For the isolation of **2**, solvent from the aforementioned hexane washings was removed *in-vacuo*, providing an orange solid that was once again dissolved in hexanes, filtered, and solvent removed to provide **2** (16 mg, 82%). ^1H NMR (500 MHz, tol-d_8 , 298 K): $\delta = 5.92$ (m, 4H; $\text{CH}(\text{allyl})$), 4.93 (dd, $^2J_{\text{H,H}} = 10$ Hz, $^3J_{\text{H,H}} = 17$ Hz, 8H; $\text{CH}_2(\text{allyl})$), 2.39 (m, 4H; $\text{CH}_2(\text{allyl})$), 2.30 (m, 4H; $\text{CH}_2(\text{allyl})$), 1.88 (s, 15H; Cp*H), 1.25 (d, $^3J_{\text{H,P}} = 12$ Hz, 4H; P- CH_2CH_2 linker). $^{13}\text{C}\{^1\text{H}\}$ NMR (125.8 MHz, tol-d_8 , 298 K): $\delta = 135.2, 115.3, 88.0, 37.6$ (m), 26.0 (m), 12.1. $^{31}\text{P}\{^1\text{H}\}$ NMR (202.5 MHz, tol-d_8 , 298 K): $\delta = +72.4$. Compound was isolated as an oil, elemental analysis was not performed. Clean ^1H and ^{31}P NMR data indicate >95% purity.



[Cp*Co^{III}(Cl)(P₂B^{Cy}₄)]B(C₆F₅)₄ ([3]B(C₆F₅)₄;

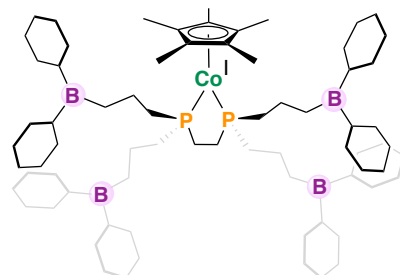
$\text{C}_9\text{H}_{131}\text{B}_5\text{ClP}_2\text{F}_{20}\text{Co}$, $M_w = 1875$ g/mol): In the glovebox, $[\text{Cp}^*\text{Co}^{\text{III}}(\text{tape})\text{Cl}]\text{B}(\text{C}_6\text{F}_5)_4$ ($[\text{1}]\text{B}(\text{C}_6\text{F}_5)_4$) (15 mg, 0.013 mmol) and HBCy_2 (9 mg, 0.052 mmol, 4 equiv.) were added to a 20 mL scintillation vial equipped with a stir bar. Approximately 4 mL of THF was added and the solution was allowed to stir for 30 min at room



temperature. The resulting orange solution was filtered through Celite[®] and the solvent was removed *in-vacuo* to give an orange oil (15 mg, 62%). ^1H NMR (500 MHz, CDCl_3 , 298 K): $\delta = 1.55$ (s, 15H, Cp* (located by ^1H - ^{13}C HSQC), 1.94-1.00 (multiple overlapping $\text{C}(\text{sp}^3)\text{-H}$ resonances). $^{13}\text{C}\{^1\text{H}\}$ NMR (125.8 MHz, CDCl_3 , 298 K): $\delta = 148.4$ (dm, $^1J_{\text{C,F}} = 238$ Hz; $\text{B}(\text{C}_6\text{F}_5)_4$), 138.4 (dm, $^1J_{\text{C,F}} = 238$ Hz; $\text{B}(\text{C}_6\text{F}_5)_4$), 125.2 (br), 98.6, 36.0, 35.9, 34.9, 27.6, 27.1, 25.5, 21.1, 19.6, 10.1; some overlapping, B-C of $\text{B}(\text{C}_6\text{F}_5)_4$ not observed. $^{31}\text{P}\{^1\text{H}\}$ NMR

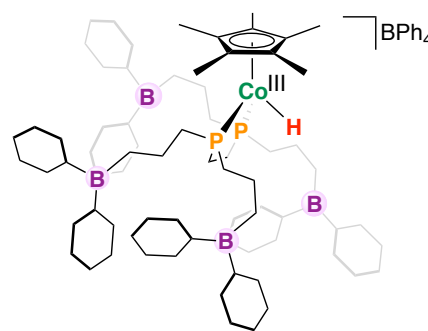
(202.5 MHz, CDCl₃, 298 K): $\delta = + 66.4$. ¹¹B{¹H} NMR (160.5 MHz, CDCl₃, 298 K): $\delta = + 83$ ($\Delta_{1/2} = 1230$ Hz), $- 16.6$ (B(C₆F₅)₄). ¹⁹F{¹H} NMR (470 MHz, CDCl₃, 298 K): $\delta = -132.6$ (8F, F_{ortho}), -164.9 (t, ³J_{F,F} = 21 Hz; F_{para}), -168.4 (8F, F_{meta}). **Anal. Calcd.** For C₉₆H₁₃₁B₅ClP₂F₂₀Co: C, 61.48; H, 7.04. Best Found: C, 59.87; H, 6.72; these results are outside the range viewed as establishing analytical purity, but are provided to illustrate the best values obtained to date. Clean ¹H and ³¹P NMR data indicate >95% purity.

[Cp*Co^I(P₂B^{Cy}₄)] (**4**; C₇₂H₁₃₁B₄P₂Co, M_w = 1161 g/mol): In the glovebox, [Cp*Co^I(tape)] (**2**) (10 mg, 0.022 mmol) and HBCy₂ (16 mg, 0.09 mmol, 4 equiv.) were added to a 20 mL scintillation vial equipped with a stir bar. Approximately 4 mL of toluene was added and the solution was allowed to stir for 30 min at room temperature. The resulting orange solution was filtered



through Celite[®] and the solvent was removed *in-vacuo* to give an orange oil (24 mg, 93%). ¹H NMR (500 MHz, tol-*d*₈, 298 K): $\delta = 2.04$ (s, 15H; Cp*), 2.00-1.02 (multiple overlapping C(sp³)-H resonances). ¹³C{¹H} NMR (125.8 MHz, C₆D₆, 298 K): $\delta = 87.6, 36.3, 36.1$ (m), 28.1, 28.0, 27.8, 27.6, 27.5, 20.6, 12.5. ³¹P{¹H} NMR (202.5 MHz, tol-*d*₈, 298 K): $\delta = + 82.5$. ¹¹B{¹H} NMR (160.5 MHz, tol-*d*₈, 298 K): $\delta = + 85$ ($\Delta_{1/2} = 1250$ Hz). Compound was isolated as an oil, elemental analysis was not performed. Clean ¹H and ³¹P NMR data indicate >95% purity.

[Cp*Co^{III}(H)(P₂B^{Cy}₄)]BPh₄ ([**5**]BPh₄: C₉₆H₁₅₂B₅P₂Co, M_w = 1481 g/mol): In the glovebox, [Cp*Co^I(P₂B^{Cy}₄)] (**4**) (16 mg, 0.01 mmol) was dissolved in 4 mL THF and [HNEt₃]BPh₄ (6 mg, 0.01 mmol, 1 equiv.) in 1 mL THF was added dropwise. The resulting orange solution was stirred for 30 min at room temperature and the solvent was removed *in-vacuo* giving an orange oil, which was washed with hexanes (20 mL) to provide a yellow powder (15 mg, 73%). Small yellow crystals of [**5**]BPh₄ could be grown from a hexanes-layered THF solution. ¹H NMR (500 MHz, THF-*d*₈, 298 K): $\delta = 7.27$ (br, 8H; BPh₄), 6.84 (t, 8H, ³J_{H,H} = 7.1 Hz; BPh₄), 6.70 (t, 4H, ³J_{H,H} = 7.1 Hz; BPh₄), 1.83 (s, 15H; Cp*), 1.80-1.10 (multiple overlapping C(sp³)-H resonances), -16.8 (t, ²J_{H,P} = 67.6 Hz; Co^{III}-H).

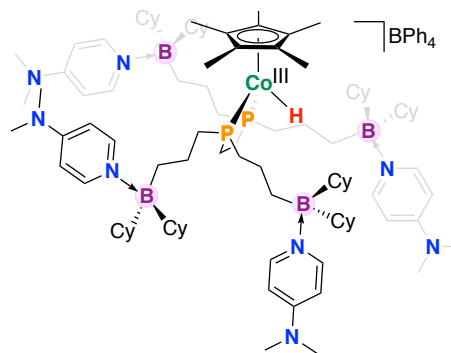


$^{13}\text{C}\{^1\text{H}\}$ NMR (125.8 MHz, THF- d_8 , 298 K): δ = 165.1 (q, $^1J_{\text{B,C}} = 50.9$ Hz; BPh_4^-), 135.4 (BPh_4^-), 123.8 (BPh_4^-), 119.9 (BPh_4^-), 94.3, 34.0, 33.8, 30.7, 27.0, 26.9 (2 signals), 26.8 (2 signals), 26.7 (2 signals), 26.3 (2 signals), 23.9, 19.1, 9.1. $^{31}\text{P}\{^1\text{H}\}$ NMR (202.5 MHz, THF- d_8 , 298 K): δ = + 80.0 (d, $^2J_{\text{H,P}} = 67.6$ Hz). $^{11}\text{B}\{^1\text{H}\}$ NMR (160.5 MHz, THF- d_8 , 298 K): δ = 85 ($\Delta_{1/2} = 1300$ Hz), - 6.5 (BPh_4^-). FT-IR (NaCl plate, cm^{-1}): 1937 (very broad, Co–H). Anal. Calcd. For $\text{C}_{96}\text{H}_{152}\text{B}_5\text{P}_2\text{Co}$: C, 77.85; H, 10.34. Best Found: C, 76.77; H, 11.17; these results are outside the range viewed as establishing analytical purity, but are provided to illustrate the best values obtained to date. Clean ^1H and ^{31}P NMR data indicate >95% purity.

$[\text{Cp}^*\text{Co}^{\text{III}}(\text{H})(\text{P}_2\text{BCy}_4)(\text{DMAP})_4]\text{BPh}_4$ ([6] BPh_4 :

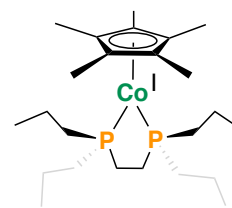
$\text{C}_{124}\text{H}_{192}\text{B}_5\text{P}_2\text{CoN}_8$, $M_w = 1969$ g/mol): In the glovebox, [5] BPh_4 (15 mg, 0.01 mmol) was dissolved in 3 mL THF and DMAP (5 mg, 0.04 mmol, 4 equivs.) was added. The reaction mixture was allowed to stir for 5 mins and then solvent was removed *in-vacuo* giving a yellow oil, which was washed with hexanes (20 mL) to provide a yellow powder (19 mg, 95%). ^1H NMR

(500 MHz, THF- d_8 , 298 K): δ = 7.96 (br, 8H; $\text{DMAP}|C\text{-H}_{\text{ortho}}$), 7.29 (br, 8H; BPh_4^-), 6.83 (t, $^3J_{\text{HH}} = 7.3$ Hz, 8H; BPh_4^-), 6.69 (t, $^3J_{\text{H,H}} = 7.3$ Hz, 4H; BPh_4^-), 6.58 (br, 8H; $\text{DMAP}|C\text{-H}_{\text{meta}}$), 2.99 (s, 24H; $\text{DMAP}|N\text{Me}_2$), 1.90 (s, 15H; Cp^*), 1.78-0.53 (overlapping $C(sp^3)\text{-H}$ resonances), -16.9 (t, $^2J_{\text{H,P}} = 68.4$ Hz; $\text{Co}^{\text{III}}\text{-H}$). $^{13}\text{C}\{^1\text{H}\}$ NMR (125.8 MHz, THF- d_8 , 298 K, select signal only): δ = 9.8 (Cp^* from $^1\text{H}\text{-}^{13}\text{C}$ HSQC). ^{31}P NMR (202.5 MHz, THF- d_8 , 298 K): δ = + 78.7 (d, $^2J_{\text{H,P}} = 68.4$ Hz). $^{11}\text{B}\{^1\text{H}\}$ NMR (160.5 MHz, THF- d_8 , 193 K): δ = -5.1 (RBCy_2DMAP) -6.5 (BPh_4^-). FT-IR (NaCl plate, cm^{-1}): 1937 (br, Co–H).



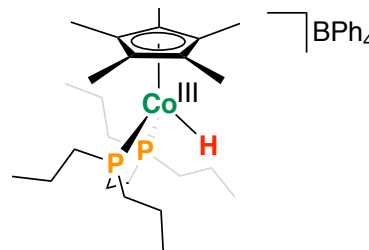
$[\text{Cp}^*\text{Co}^{\text{I}}(\text{dnppe})]$ (7; $\text{C}_{24}\text{H}_{47}\text{P}_2\text{Co}$, $M_w = 456$ g/mol):

In the glovebox, $[\text{Cp}^*\text{Co}^{\text{II}}(\mu\text{-Cl})_2]$ (30 mg, 0.07 mmol, 0.5 equiv.) and dnppe (34 mg, 0.14 mmol, 1 equiv.) were combined in a 20 mL scintillation vial equipped with a stir bar. Approximately 4 mL of hexanes was added and the solution was allowed to stir for 1 h at room temperature. The resulting solution was orange in color with ample brown precipitate. The solution was filtered away from the solid and the solid was washed with additional hexanes (3 x 5 mL portions). Combination of the hexanes washings and removal of solvent *in-vacuo* provided an orange solid that was one again dissolved in hexanes, filtered, and solvent removed to provide 7 (23 mg, 79%). ^1H NMR



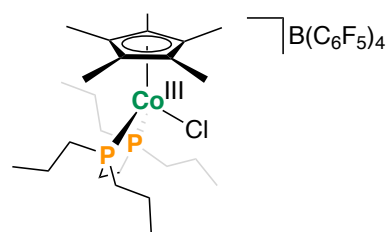
(500 MHz, THF- d_8 , 298 K): δ = 1.79 (s, 15H; Cp*H), 1.72 (m, 4H; under THF- d_8), 1.53 (m, 4H), 1.44 (m, 4H), 1.26 (m, 4H; P-CH₂CH₂ linker), 1.19 (m, 4H), 0.99 (t, $^3J_{H,H}$ = 7.3 Hz, 12H). $^{13}\text{C}\{^1\text{H}\}$ NMR (125.8 MHz, THF- d_8 , 298 K): δ = 87.4, 34.9 (m), 28.5 (m), 19.4, 16.4 (m), 12.1. $^{31}\text{P}\{^1\text{H}\}$ NMR (202.5 MHz, THF- d_8 , 298 K): δ = + 84.2. Compound was isolated as an oil, elemental analysis was not performed. Clean ^1H and ^{31}P NMR data indicate >95% purity.

[Cp*Co^{III}(H)(dnppe)]BPh₄ ([8]BPh₄: C₄₈H₆₈BP₂Co, M_w = 776 g/mol): In the glovebox, [Cp*Co^I(dnppe)] (7) (23 mg, 0.05 mmol) was dissolved in 4 mL THF and [HNEt₃]BPh₄ (19 mg, 0.045 mmol, 0.9 equiv.) in 1 mL THF was added dropwise. The resulting orange solution was stirred for 30 min at room temperature and the solvent was removed *in-*



vacuo giving an orange oil, which was washed with hexanes (20 mL) to provide a yellow powder. Yellow crystals of [8]BPh₄ could be grown from a hexanes-layered THF solution (34 mg, 87%). ^1H NMR (500 MHz, THF- d_8 , 298 K): δ = 7.27 (br, 8H; BPh₄), 6.85 (t, 8H, $^3J_{HH}$ = 7.1 Hz; BPh₄), 6.71 (t, 4H, $^3J_{H,H}$ = 7.1 Hz; BPh₄), 1.83 (m, 4H), 1.76 (s, 15H; Cp*), 1.70-1.14 (multiple overlapping C(sp³)-H resonances), 1.02 (t, $^3J_{H,H}$ = 7.3 Hz, 12H), -16.8 (t, $^2J_{H,P}$ = 67.6 Hz; Co^{III}-H). $^{13}\text{C}\{^1\text{H}\}$ NMR (125.8 MHz, THF- d_8 , 298 K): δ = 165.1 (q, $^1J_{B,C}$ = 50.9 Hz; BPh₄), 137.0 (BPh₄), 125.5 (BPh₄), 121.6 (BPh₄), 95.9, 30.7 (m), 30.1 (m), 18.7, 15.9 (m), 16.0 (m), 10.4. $^{31}\text{P}\{^1\text{H}\}$ NMR (202.5 MHz, THF- d_8 , 298 K): δ = + 81.4 (d, $^2J_{H,P}$ = 67.6 Hz). $^{11}\text{B}\{^1\text{H}\}$ NMR (160.5 MHz, THF- d_8 , 298 K): δ = - 6.5 (BPh₄). FT-IR (ATR, cm⁻¹): 1939 (Co-H). **Anal. Calcd.** For C₄₈H₆₈BP₂Co: C, 74.22; H, 8.82. Found: C, 74.31; H, 8.72.

[Cp*Co^{III}(Cl)(dnppe)]B(C₆F₅)₄ ([9]B(C₆F₅)₄; C₄₈H₄₇BClP₂F₂₀Co, M_w = 1171 g/mol): In the glovebox, [Cp*Co^{II}(μ-Cl)]₂ (30 mg, 0.07 mmol, 0.5 equiv.) and dnppe (34 mg, 0.14 mmol, 1 equiv.) were combined in a 20 mL scintillation vial equipped with a stir bar. Approximately 4 mL of hexanes was added and the solution was allowed to



stir for 1 h at room temperature. The resulting solution was orange in color with ample brown precipitate of [9]Cl. The solution was filtered away from the solid and the solid was washed with additional hexanes (3 x 5 mL portions) to remove 7. Crude [9]Cl was then dissolved in THF (4 mL) and [Li(OEt₂)₂]B(C₆F₅)₄ (58 mg, 0.07 mmol, 1 equiv.) was

added in a single portion. The reaction was allowed to stir for 1 h at room temperature. The resulting orange solution was filtered through Celite® and the solvent was removed *in-vacuo* to give [9]B(C₆F₅)₄ as a brown solid (70 mg, 90%). ¹H NMR (500 MHz, THF-d₈, 298 K): δ = 2.24 (m, 2H), 2.16 (m, 2H), 1.94 (m, 4H), 1.75 (m, 4H; under THF), 1.65 (m, 8H), 1.58 (s, 15H; Cp*), 1.10 (t, ³J_{H,H} = 7.2 Hz, 6H), 1.04 (t, ³J_{H,H} = 7.2 Hz, 6H). ¹³C{¹H} NMR (125.8 MHz, THF-d₈, 298 K): δ = 148.9 (dm, ¹J_{C,F} = 238 Hz; B(C₆F₅)₄), 137.9 (dm, ¹J_{C,F} = 238 Hz; B(C₆F₅)₄), 125.2 (br), 28.9 (m), 28.0 (m), 21.7 (m), 19.8, 18.8 (m), 15.9 (m), 9.93, B-C of B(C₆F₅)₄ not observed. ³¹P{¹H} NMR (202.5 MHz, THF-d₈, 298 K): δ = + 68.4. ¹¹B{¹H} NMR (160.5 MHz, CDCl₃, 298 K): δ = - 16.6 (B(C₆F₅)₄). ¹⁹F{¹H} NMR (470 MHz, THF-d₈, 298 K): δ = -132.6 (8F, F_{ortho}), -164.9 (t, ³J_{F,F} = 21 Hz; F_{para}), -168.4 (8F, F_{meta}).

Treatment of 4 with benzoic acids. In the glovebox, ~ 10 mg of [Cp*Co^I(P₂B^{Cy}₄)] (4) and a benzoic acid derivative (4 equivs.) were combined and dissolved in *ca.* 500 μL THF-d₈. The mixture was transferred to a J. Young NMR tube, removed from the glovebox, and immediately analyzed by NMR spectroscopy. These protonation experiments were performed in THF-d₈ and not acetonitrile due to insolubility of compound 4 in the latter.

Reaction of 4 with 4 equivs. PhCO₂H: NMR Characterization of [5]O₂CPh. ¹H NMR (500 MHz, THF-d₈, 298 K): δ = 11.27 (br, 1H; residual PhCO₂H), 8.01 (d, ³J_{H,H} = 7.5 Hz; H_o residual PhCO₂H/PhCO₂⁻ counteranion), 7.47 (t, ³J_{H,H} = 7.1 Hz; H_p for residual PhCO₂H/PhCO₂⁻ counteranion), 7.38 (t, ³J_{H,H} = 7.5 Hz; H_m residual PhCO₂H/PhCO₂⁻ counteranion), 1.87 (s, 15H; Cp*), -17.0 (t, ²J_{H,P} = 66.3 Hz; Co^{III}-H). ³¹P{¹H} NMR (202.5 MHz, THF-d₈, 298 K): δ = + 80.8 (d, ²J_{H,P} = 66.3 Hz).

Reaction of 4 with 4 equivs. 4-PyrCO₂H: NMR Characterization of [5]⁺. ¹H NMR (500 MHz, THF-d₈, 298 K): δ = 8.69 (br, 8H; H_o (to pyridine) of 4-PyrCO₂H/4-PyrCO₂⁻ counteranion), 8.06 (br, 8H; H_m (to pyridine) of 4-PyrCO₂H/4-PyrCO₂⁻ counteranion), 1.85 (s, 15H; Cp*), -17.1 (t, ²J_{H,P} = 66.1 Hz; Co^{III}-H), downfield-shifted 1H for residual carboxylic acid not observed. ³¹P{¹H} NMR (202.5 MHz, THF-d₈, 298 K): δ = + 78.0 (br). **Note:** 4-PyrCO₂H is poorly soluble in THF-d₈ or MeCN-d₃.

Reaction of 4 with 1 equiv. PhCO₂H: NMR Characterization of [5]O₂CPh. ¹H NMR (500 MHz, THF-d₈, 298 K): δ = 8.01 (d, ³J_{H,H} = 7.5 Hz, 2H; H_o), 7.22 (m, 3H; H_m + H_p), 1.87

(s, 15H; Cp*), -17.0 (t, $^2J_{\text{H,P}} = 66.3$ Hz; Co^{III}-H). $^{31}\text{P}\{^1\text{H}\}$ NMR (202.5 MHz, THF-d₈, 298 K): $\delta = +80.8$ (d, $^2J_{\text{H,P}} = 66.3$ Hz). ^1H NMR (500 MHz, C₆D₆, 298 K): $\delta = 8.65$ (d, $^3J_{\text{H,H}} = 7.5$ Hz, 2H; H_o), 7.32 (t, $^3J_{\text{H,H}} = 7.5$ Hz, 2H; H_m), 7.23 (t, $^3J_{\text{H,H}} = 7.3$ Hz, 1H; H_p), 1.51 (s, 15H; Cp*), -17.2 (t, $^2J_{\text{H,P}} = 66.3$ Hz; Co^{III}-H). $^{31}\text{P}\{^1\text{H}\}$ NMR (202.5 MHz, C₆D₆, 298 K): $\delta = +81.3$ (d, $^2J_{\text{H,P}} = 66.3$ Hz).

Treatment of BCy₂"OCT with benzoic acids. In the glovebox, ~ 40 mg of BCy₂"OCT and benzoic acid or 4-pyridylbenzoic acid (1 equiv.) were combined and dissolved in *ca.* 500 μL THF-d₈. The mixture was transferred to a J. Young NMR tube, removed from the glovebox, and immediately analyzed by NMR spectroscopy, which evidenced an adduct for 4-pyridylbenzoic acid and no reaction for benzoic acid.

Table S1. Summary of Data obtained for Cobalt Compounds

Compound	Name	Formula	Mw (g/mol)	δ_{H} (Cp*) (ppm)	δ_{P} (ppm)
[1]Cl	[Cp*Co ^{III} (tape)Cl]Cl	C ₂₄ H ₃₉ Cl ₂ P ₂ Co	519	1.45 (CDCl ₃)	65.3 (CDCl ₃)
[1]B(C ₆ F ₅) ₄	[Cp*Co ^{III} (tape)Cl]B(C ₆ F ₅) ₄	C ₄₈ H ₃₉ BClF ₂₀ P ₂ Co	1163	1.61 (CDCl ₃)	67.2 (CDCl ₃)
2	[Cp*Co ^I (tape)]	C ₂₄ H ₃₉ P ₂ Co	448	1.88 (tol-d ₈)	72.4 (tol-d ₈)
[3]B(C ₆ F ₅) ₄	[Cp*Co ^{III} (Cl)(P ₂ B ^{Cy} ₄)]B(C ₆ F ₅) ₄	C ₉₆ H ₁₃₁ B ₅ ClP ₂ F ₂₀ Co	1875	1.55 (CDCl ₃)	66.4 (CDCl ₃)
4	[Cp*Co ^I (P ₂ B ^{Cy} ₄)]	C ₇₂ H ₁₃₁ B ₄ P ₂ Co	1161	2.04 (tol-d ₈)	82.5 (tol-d ₈)
[5]BPh ₄	[Cp*Co ^{III} (H)(P ₂ B ^{Cy} ₄)]BPh ₄ [Cp*Co ^{III} (H)(P ₂ B ^{Cy} ₄)(DMAP)] ₄	C ₉₆ H ₁₅₂ B ₅ P ₂ Co	1481	1.83 (THF-d ₈)	80.0 (THF-d ₈) ^a
[6]BPh ₄]BPh ₄	C ₁₂₄ H ₁₉₂ B ₅ P ₂ N ₈ Co	1969	1.90 (THF-d ₈)	78.7 (THF-d ₈) ^b
7	[Cp*Co ^I (dnppe)]	C ₂₄ H ₄₇ P ₂ Co	456	1.79 (THF-d ₈)	84.2 (THF-d ₈)
[8]BPh ₄	[Cp*Co ^{III} (H)(dnppe)]BPh ₄	C ₄₈ H ₆₈ BP ₂ Co	776	1.76 (THF-d ₈)	81.4 (THF-d ₈) ^c
[9]B(C ₆ F ₅) ₄	[Cp*Co ^{III} (dnppe)Cl]B(C ₆ F ₅) ₄	C ₄₈ H ₄₇ BClP ₂ F ₂₀ Co	1171	1.58 (THF-d ₈)	68.4 (THF-d ₈)

^a Doublet with ²J_{H,P} = 67.6 Hz (THF-d₈). ^b Doublet with ²J_{H,P} = 68.4 Hz (THF-d₈). ^c Doublet with ²J_{H,P} = 67.6 Hz (THF-d₈).

Figure S1. [1]Cl, ^1H NMR, CDCl_3 , 500 MHz, 298 K

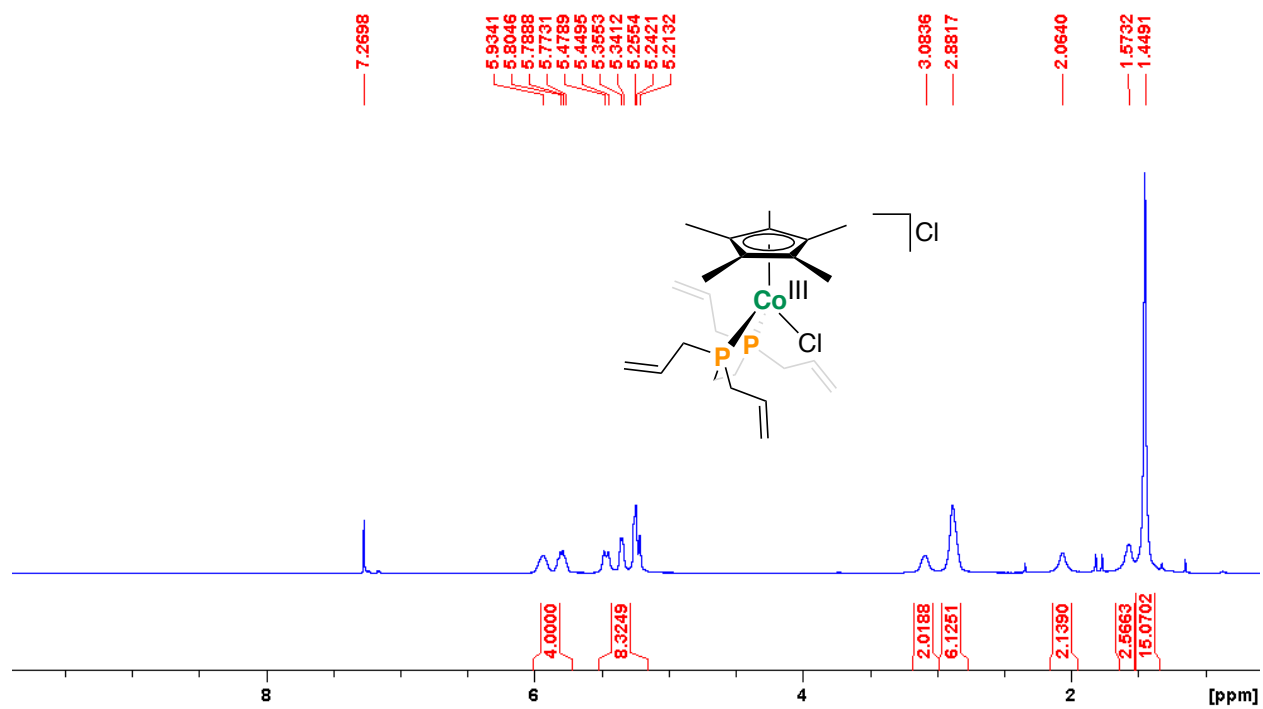


Figure S2. [1]Cl, $^{31}\text{P}\{^1\text{H}\}$ NMR, CDCl_3 , 203 MHz, 298 K

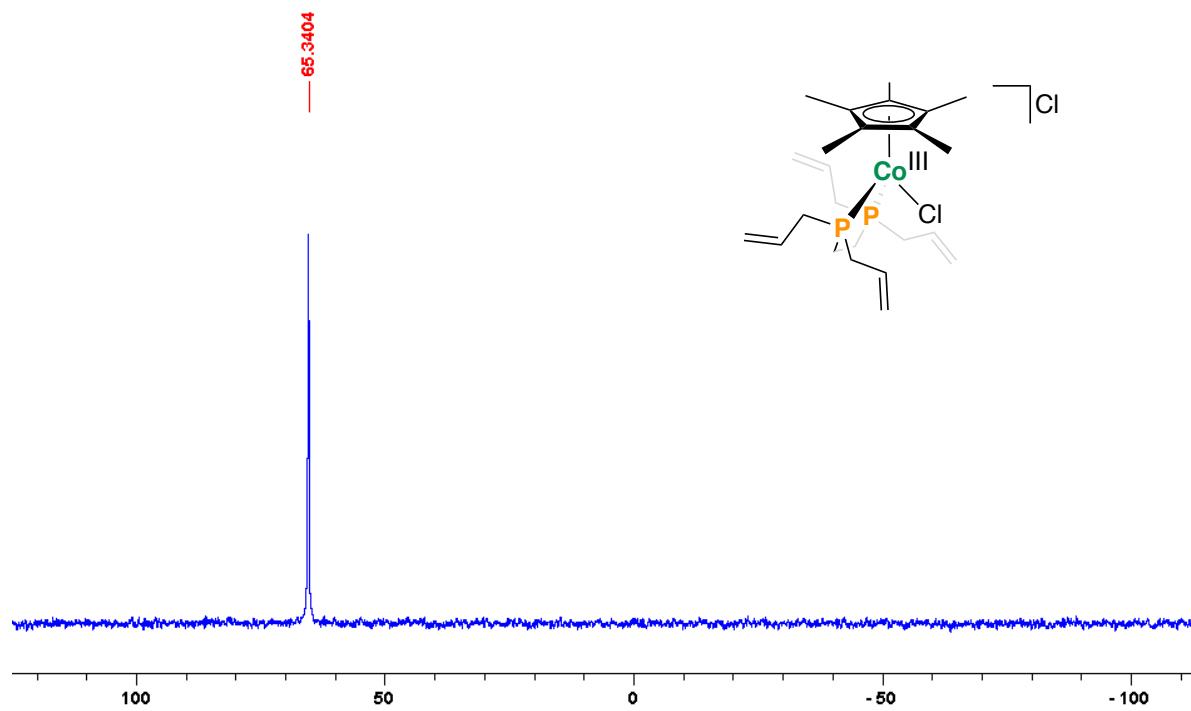


Figure S5. $[1]B(C_6F_5)_4$, $^{31}P\{^1H\}$ NMR, $CDCl_3$, 203 MHz, 298 K

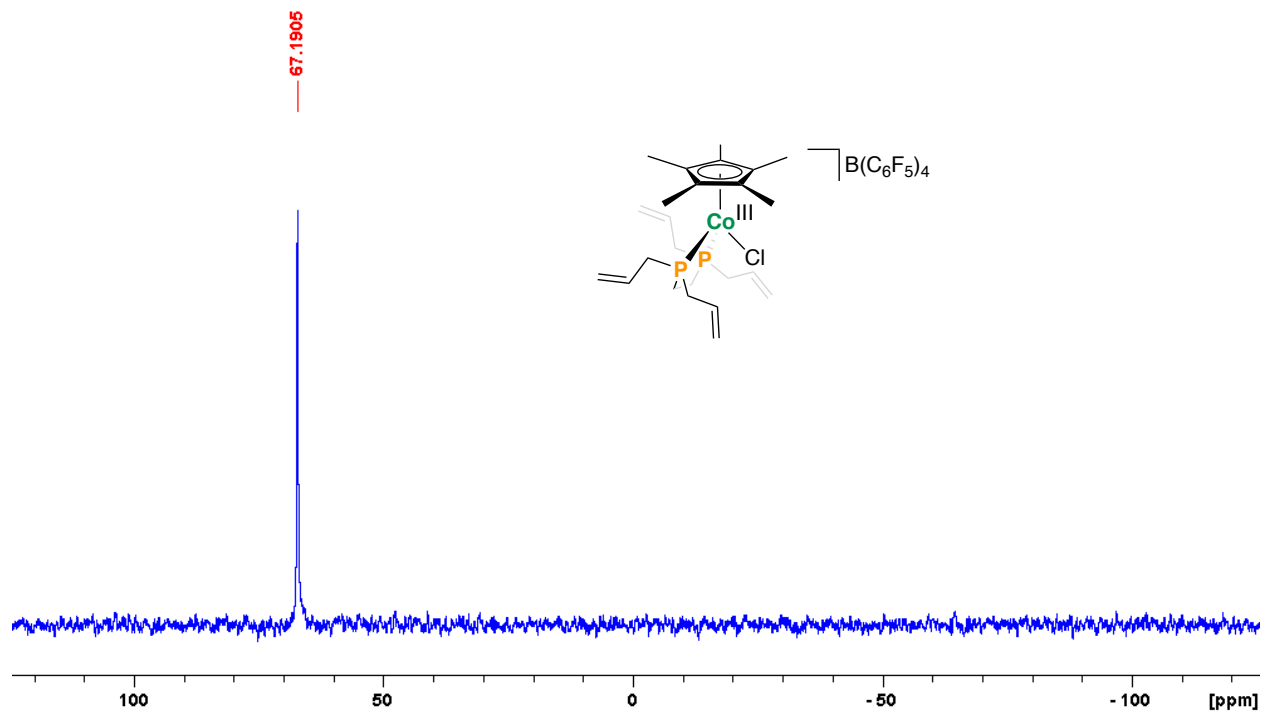


Figure S6. $[1]B(C_6F_5)_4$, $^{11}B\{^1H\}$ NMR, $CDCl_3$, 160.5 MHz, 298 K

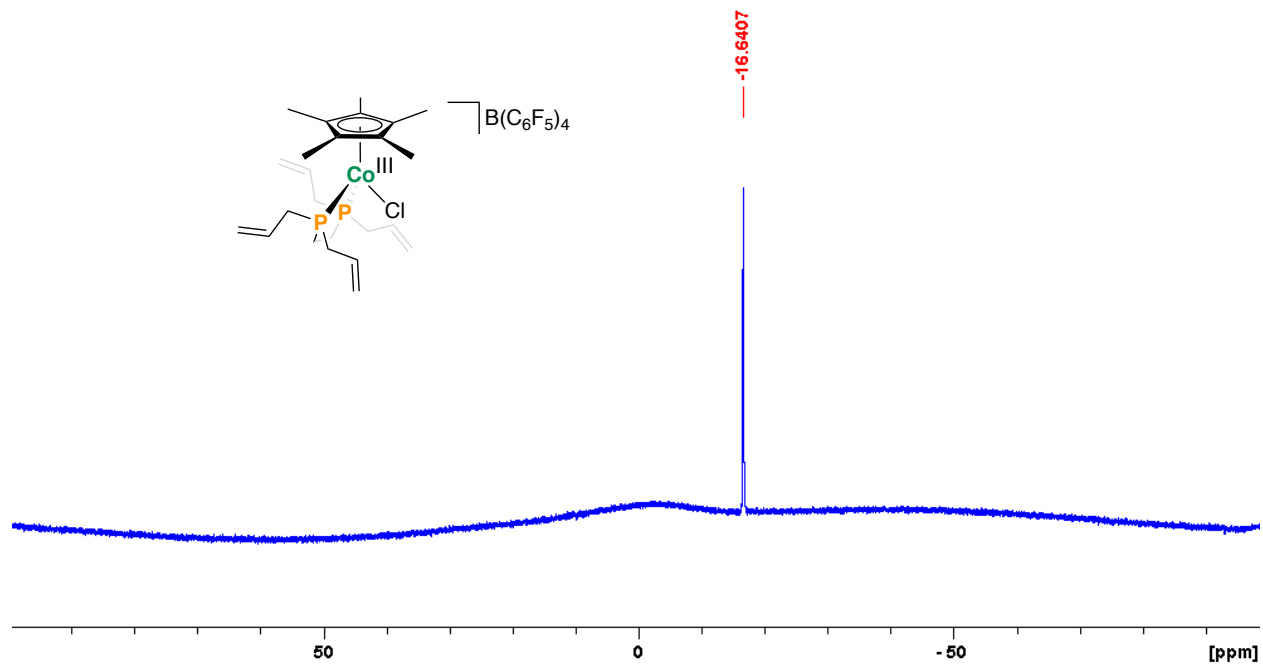


Figure S7. [1]B(C₆F₅)₄, ¹⁹F{¹H} NMR, CDCl₃, 470 MHz, 298 K

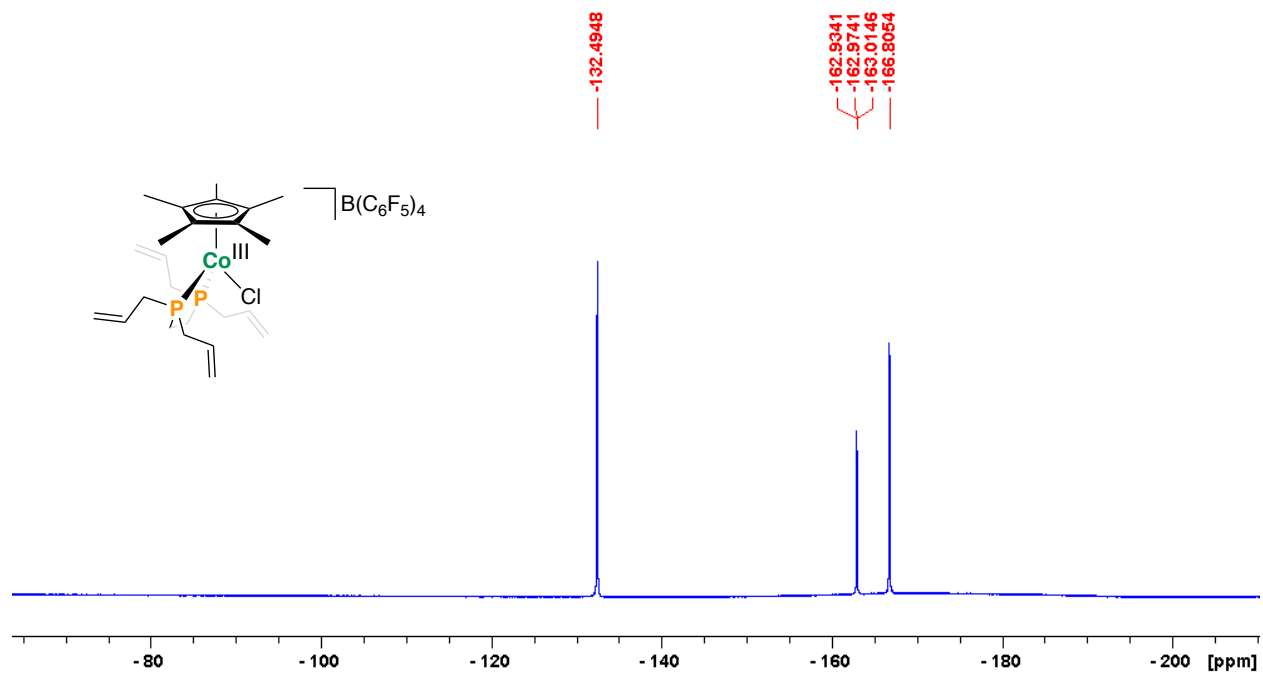


Figure S8. [1]B(C₆F₅)₄, ¹³C{¹H} NMR, CDCl₃, 125 MHz, 298 K

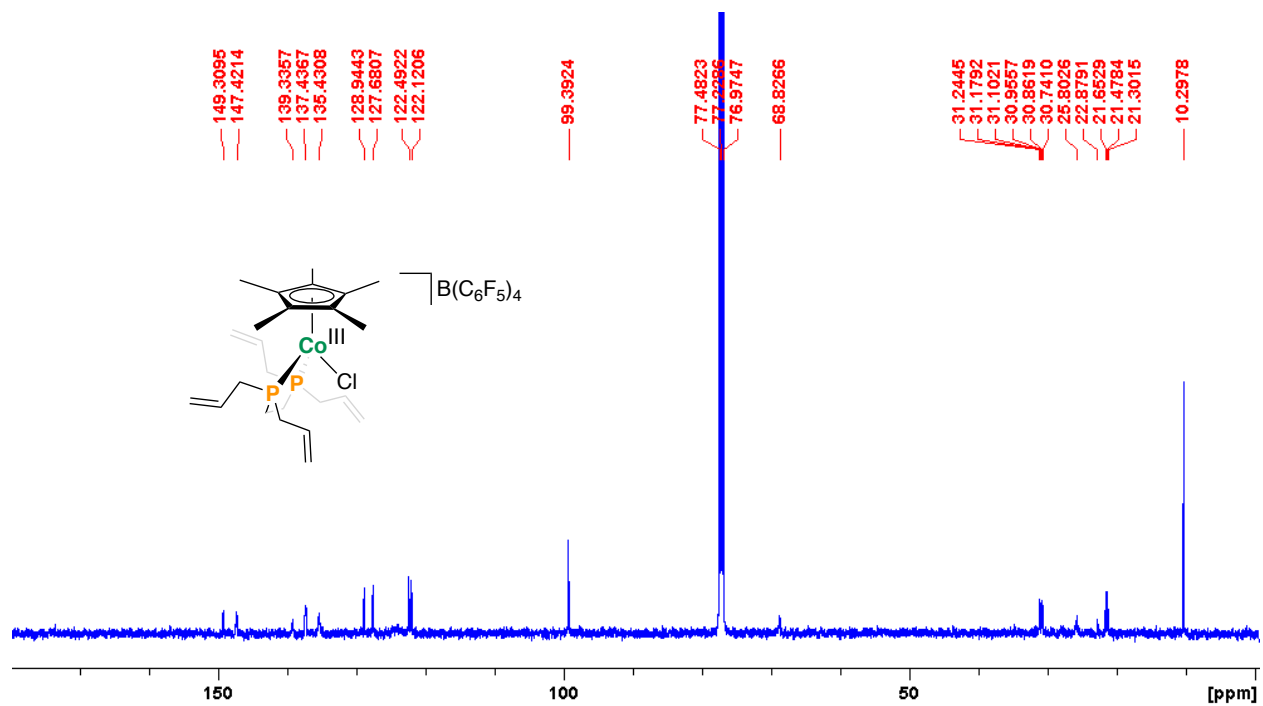


Figure S9. 2, ^1H NMR, tol-d_8 , 500 MHz, 298 K

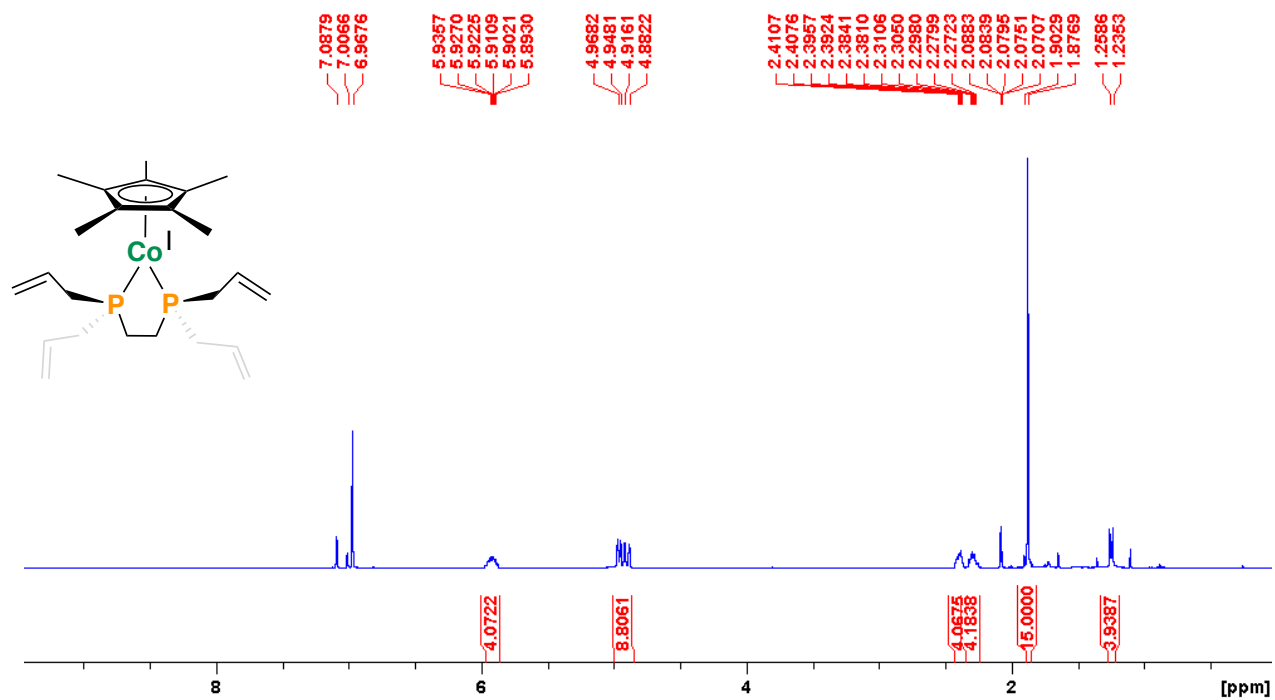


Figure S10. 2, $^{31}\text{P}\{^1\text{H}\}$ NMR, tol-d_8 , 203 MHz, 298 K

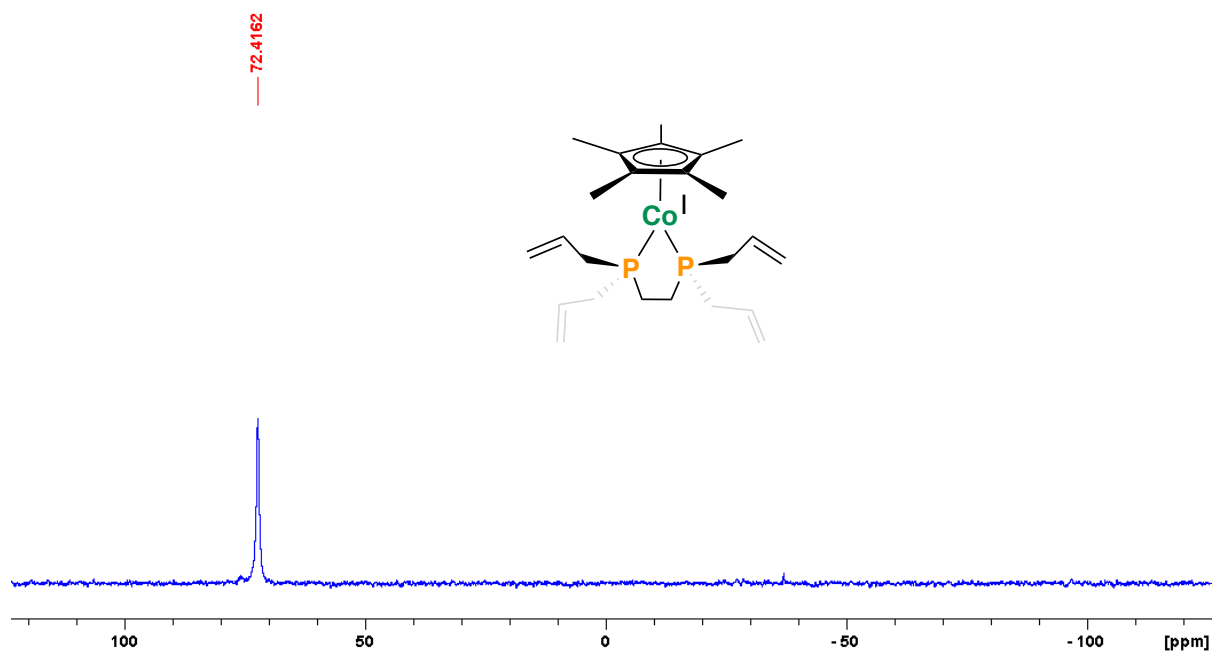


Figure S11. 2, $^{13}\text{C}\{^1\text{H}\}$ NMR, tol-d_8 , 125 MHz, 298 K

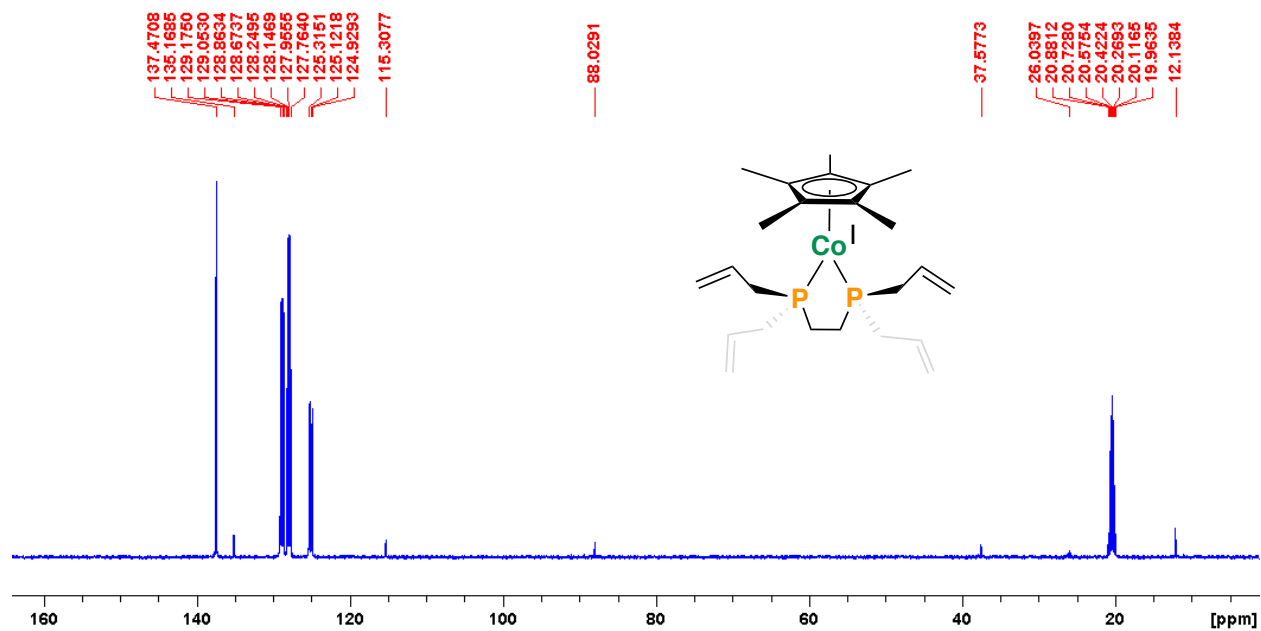


Figure S12. $[\text{3}]\text{B}(\text{C}_6\text{F}_5)_4$, ^1H NMR, CDCl_3 , 500 MHz, 298 K (residual THF at 3.77 and 1.85 ppm)

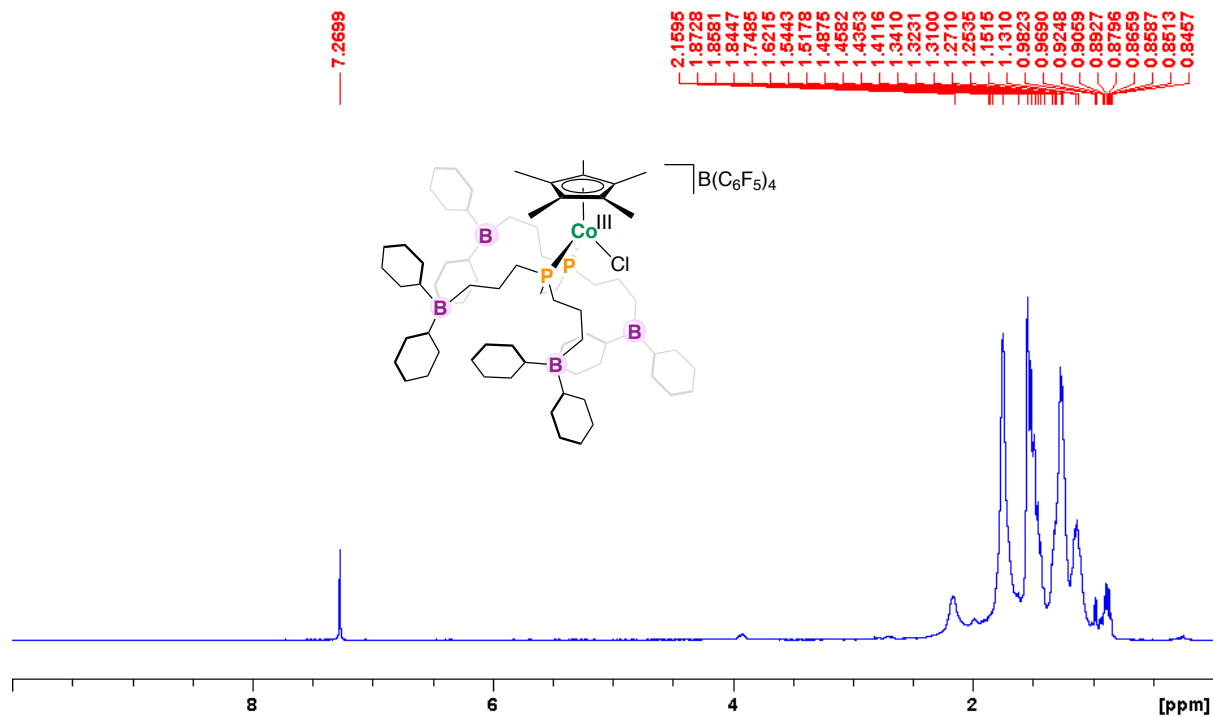


Figure S13. $[3]B(C_6F_5)_4$, $^{31}P\{^1H\}$ NMR, $CDCl_3$, 203 MHz, 298 K

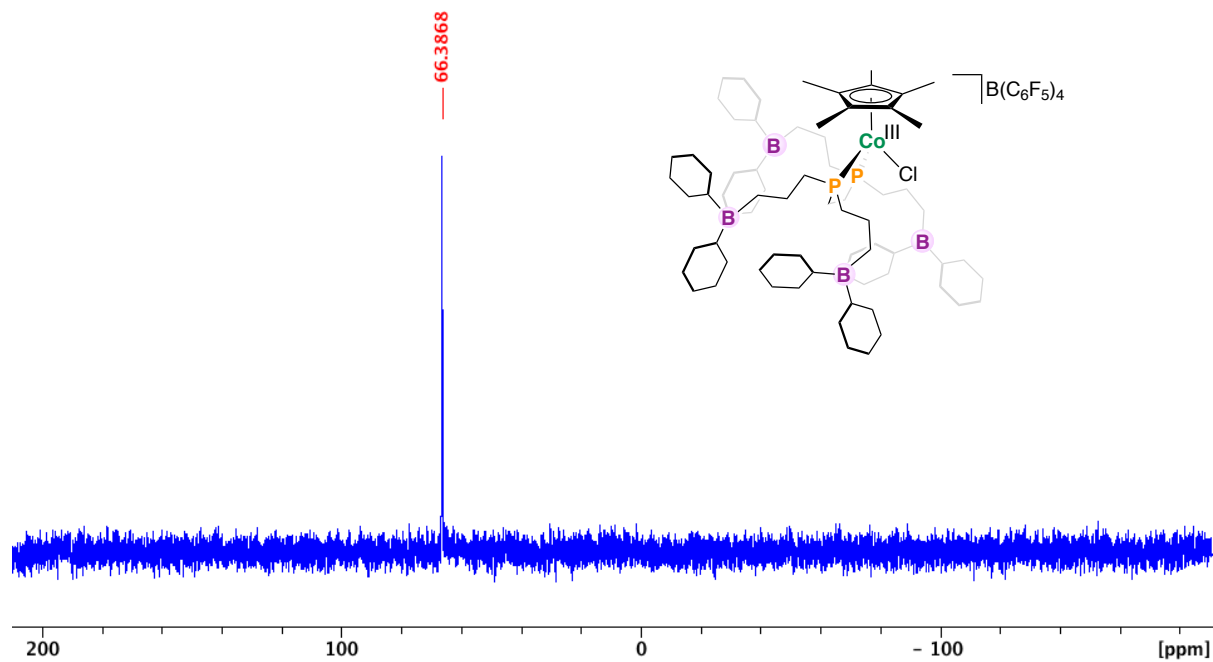


Figure S14. $[3]B(C_6F_5)_4$, $^{11}B\{^1H\}$ NMR, $CDCl_3$, 160.5 MHz, 298 K

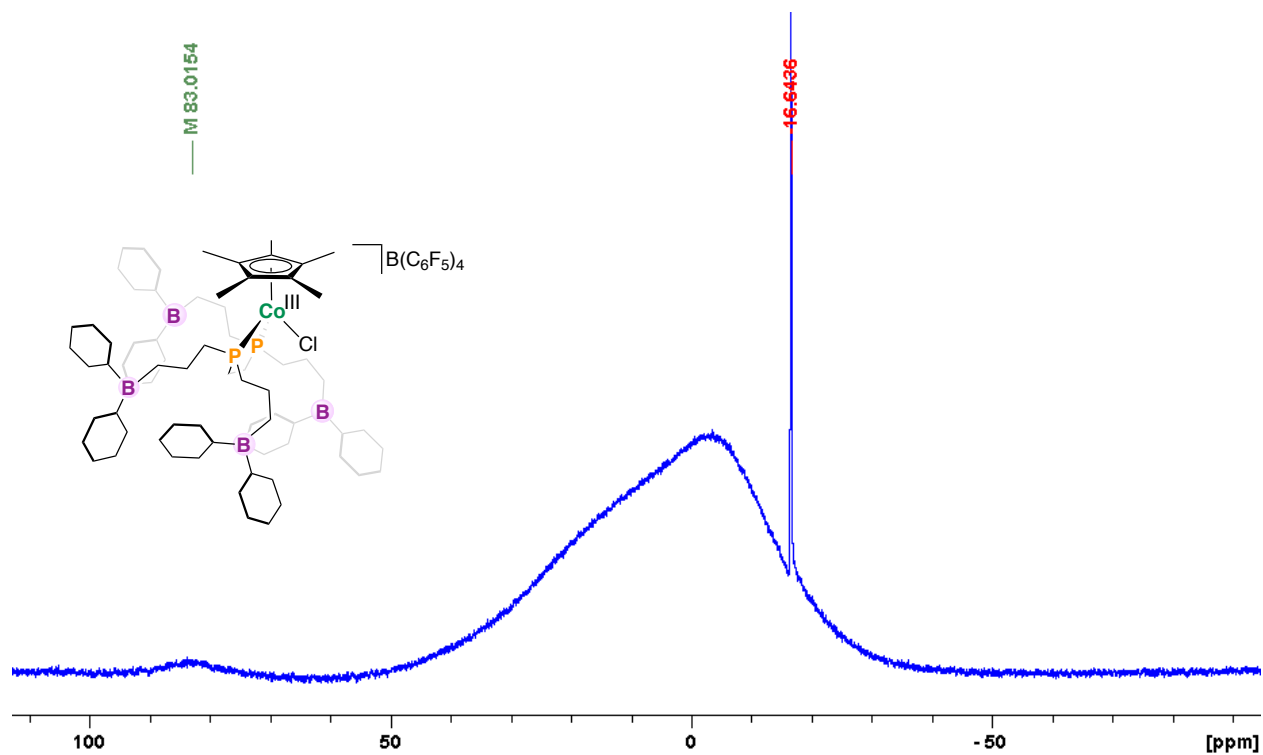


Figure S15. $[3]B(C_6F_5)_4$, $^{11}B\{^1H\}$ NMR, THF- d_8 , 160.5 MHz.

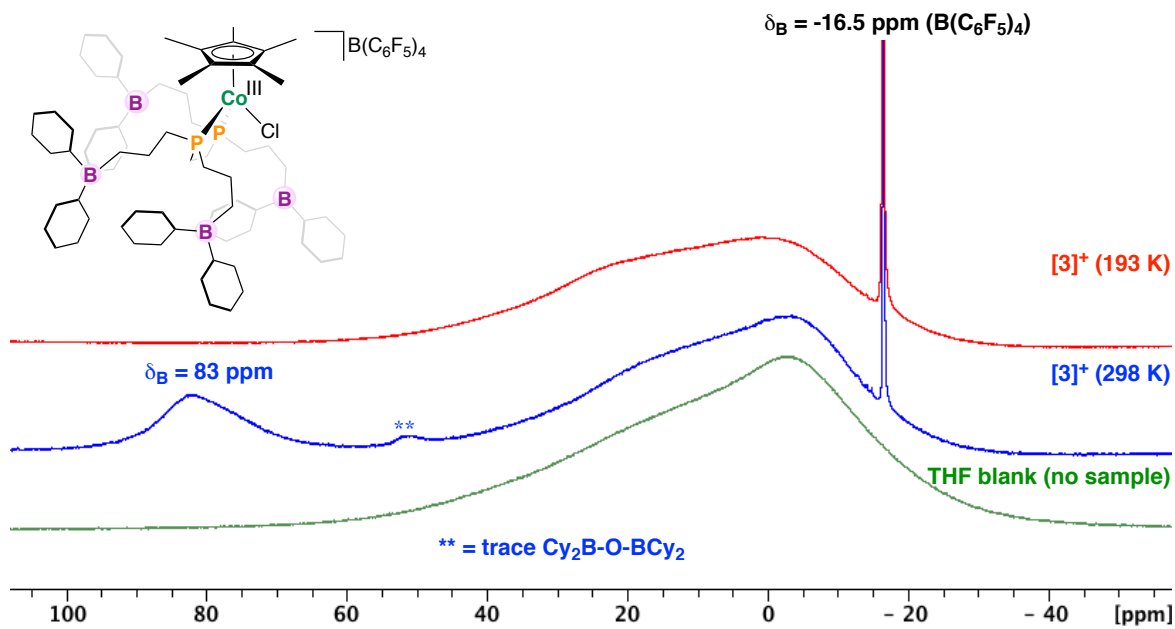


Figure S16. $[3]B(C_6F_5)_4$, $^{19}F\{^1H\}$ NMR, $CDCl_3$, 470 MHz, 298 K

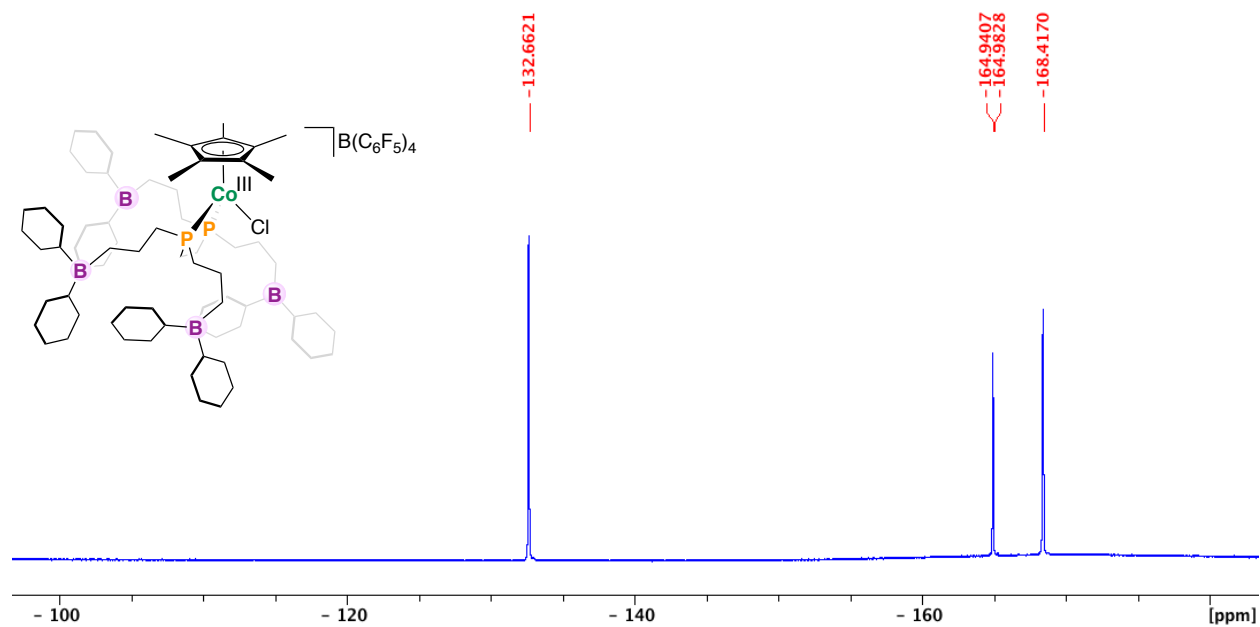


Figure S17. $[3]B(C_6F_5)_4$, $^{13}C\{^1H\}$ NMR, $CDCl_3$, 125 MHz, 298 K

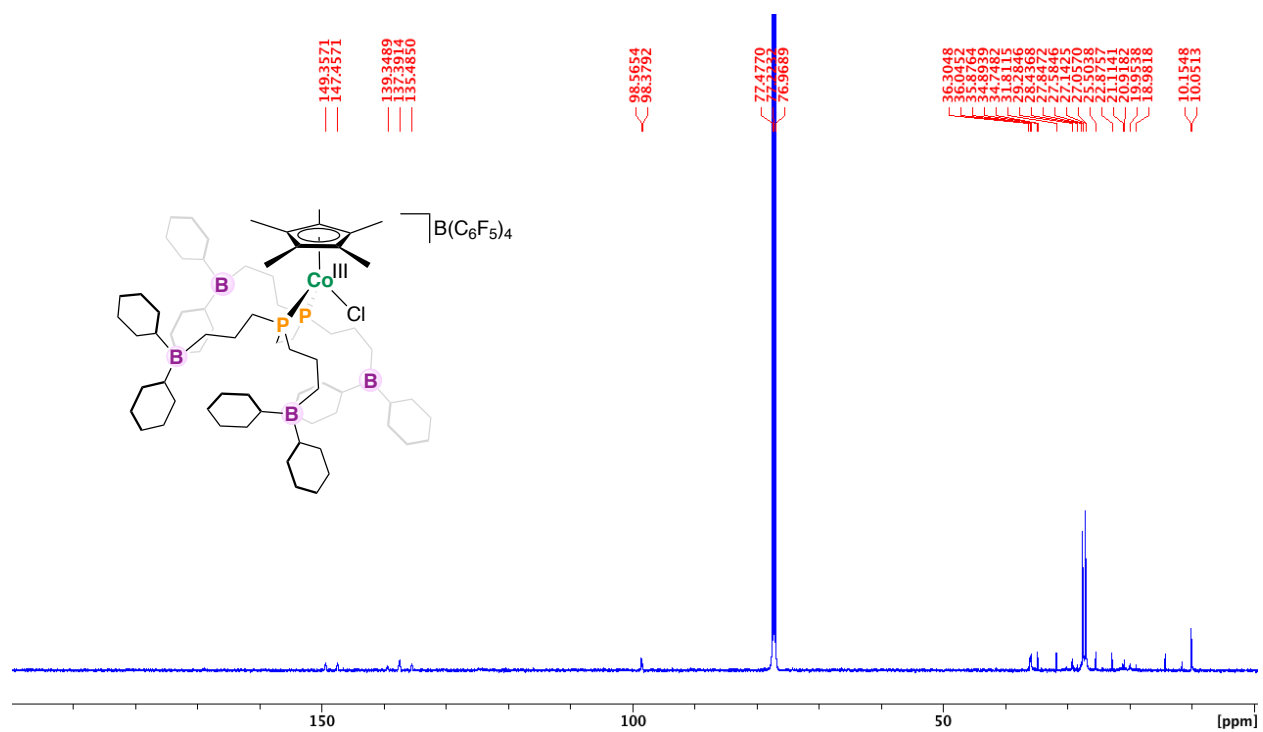


Figure S18. 4 , 1H NMR, $tol-d_8$, 500 MHz, 298 K

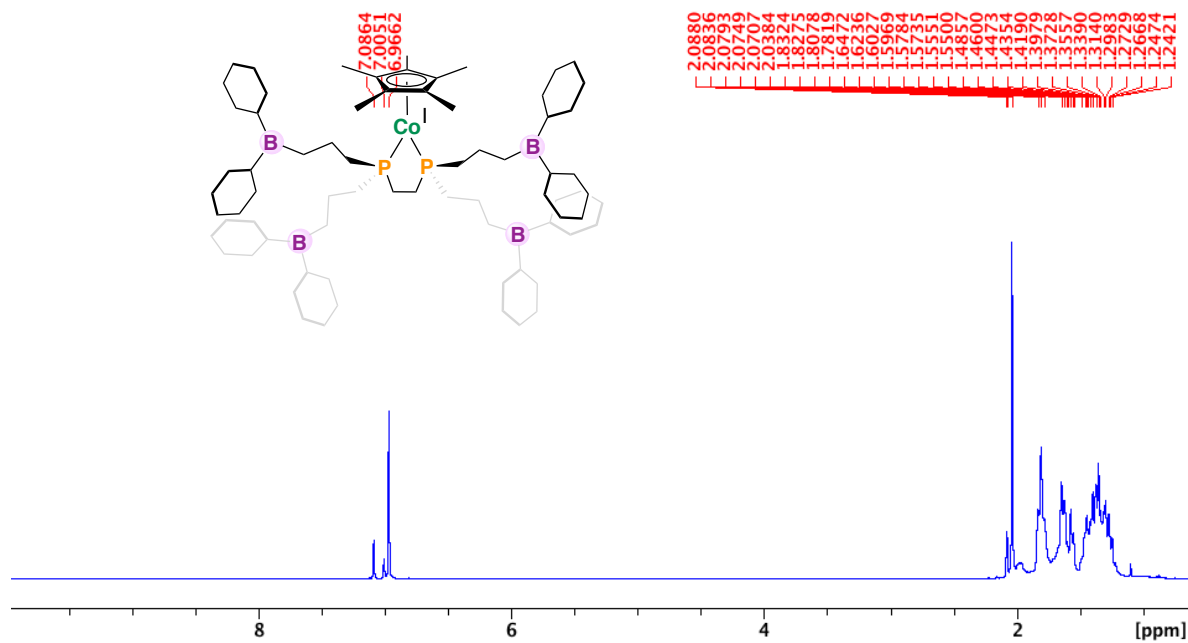


Figure S19. 4, $^{31}\text{P}\{^1\text{H}\}$ NMR, tol-d_8 , 203 MHz, 298 K

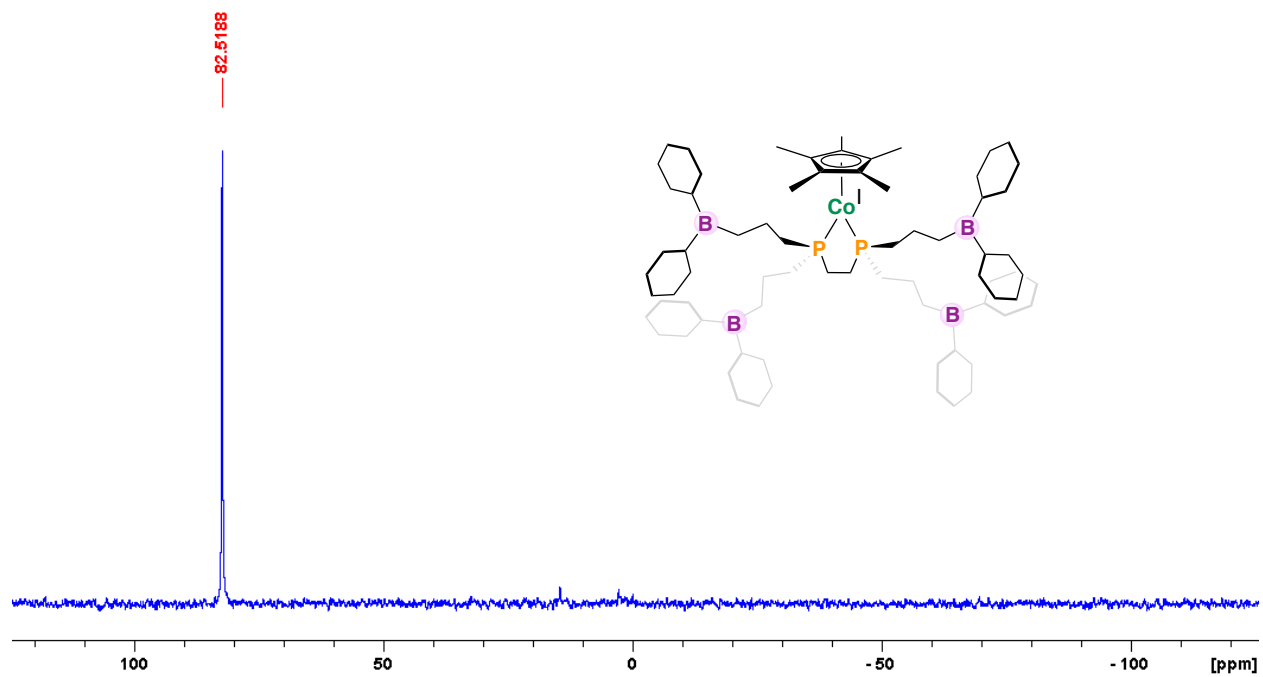


Figure S20. 4, $^{11}\text{B}\{^1\text{H}\}$ NMR, C_6D_6 , 160.5 MHz, 298 K

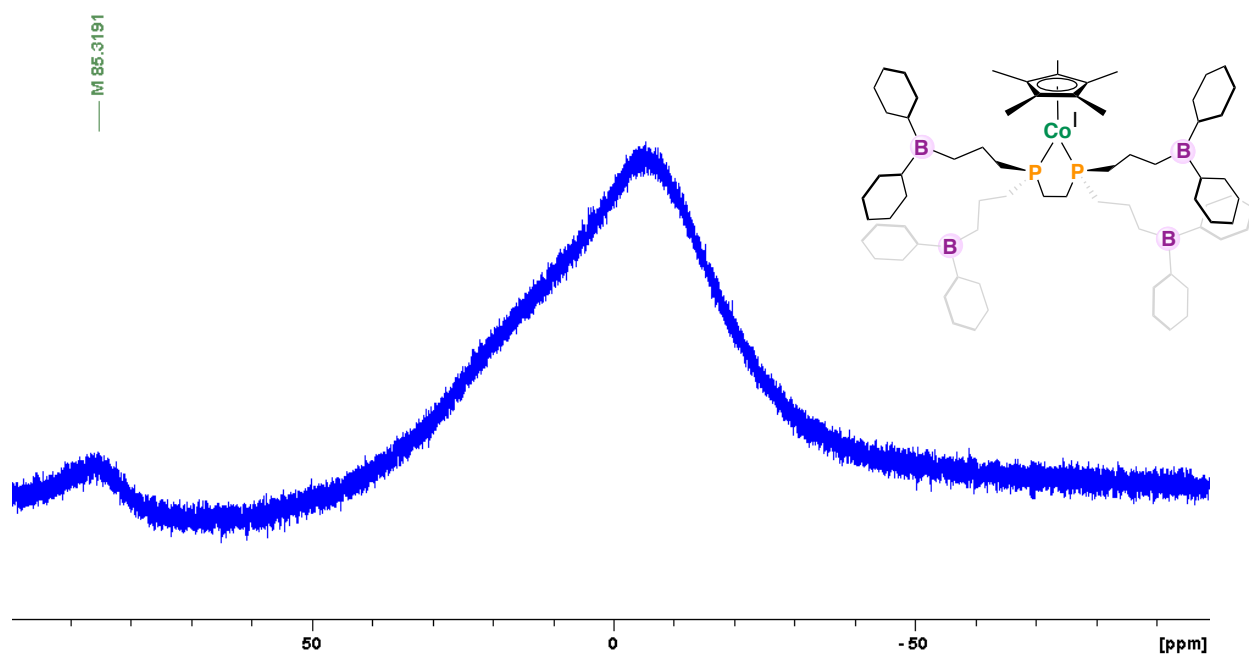


Figure S21. 4, $^{11}\text{B}\{^1\text{H}\}$ NMR, THF- d_8 , 160.5 MHz.

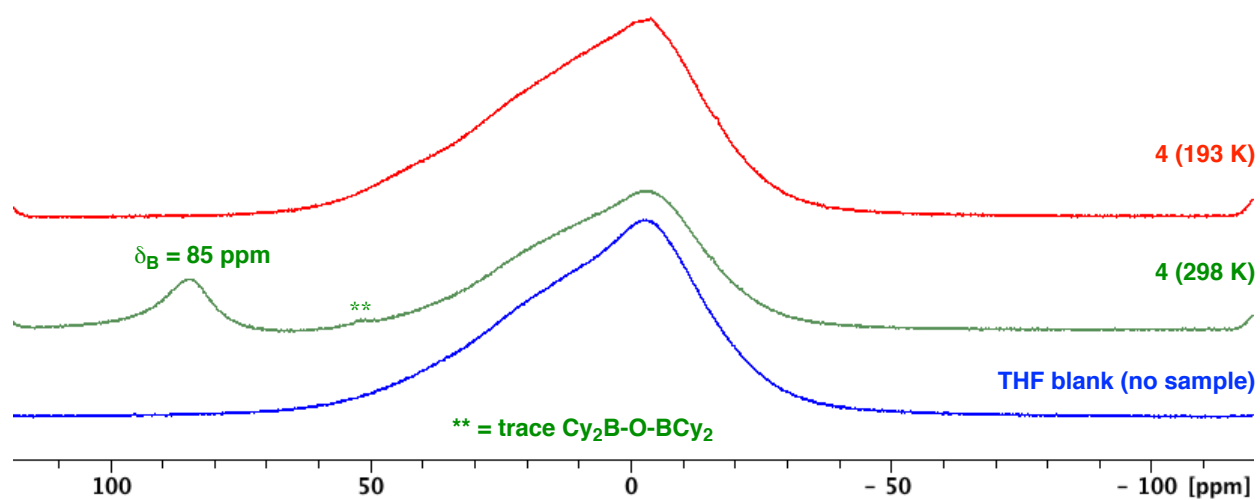


Figure S22. 4, $^{13}\text{C}\{^1\text{H}\}$ NMR, C_6D_6 , 125 MHz, 298 K

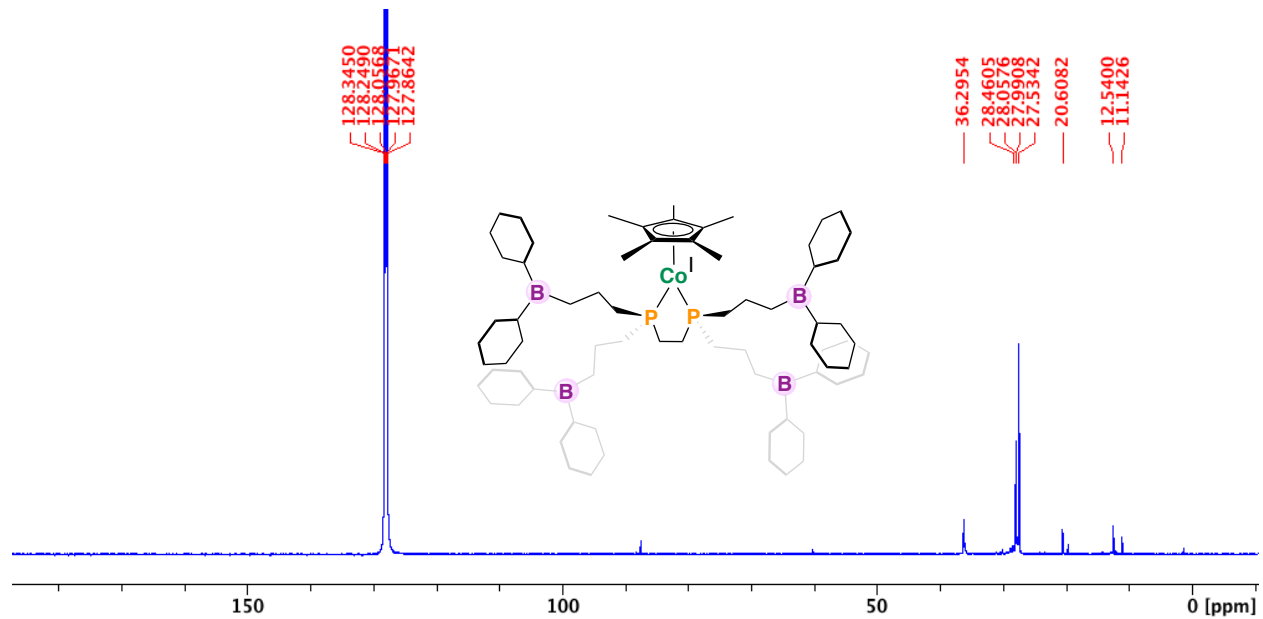


Figure S23. [5]BPh₄, ¹H NMR, THF-d₈, 500 MHz, 298 K (inset shows Co^{III}-H signal at δ_H = -16.8 ppm)

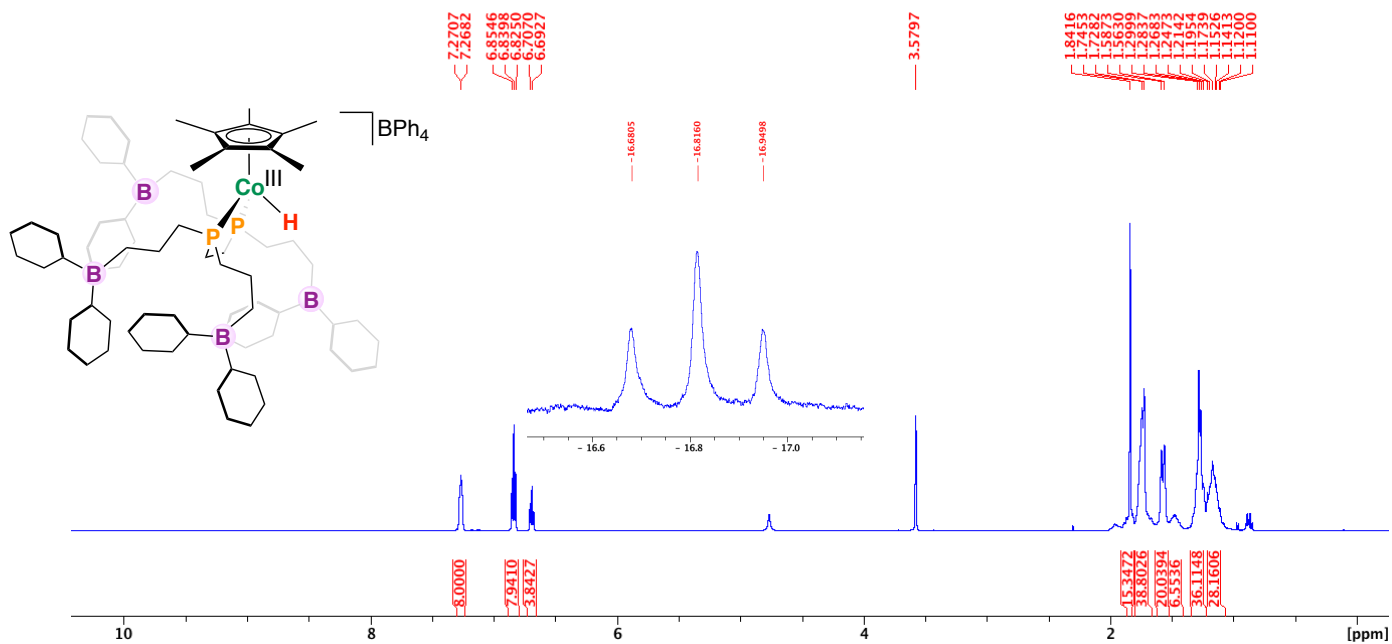


Figure S24. [5]BPh₄, ³¹P{¹H} NMR, THF-d₈, 203 MHz, 298 K

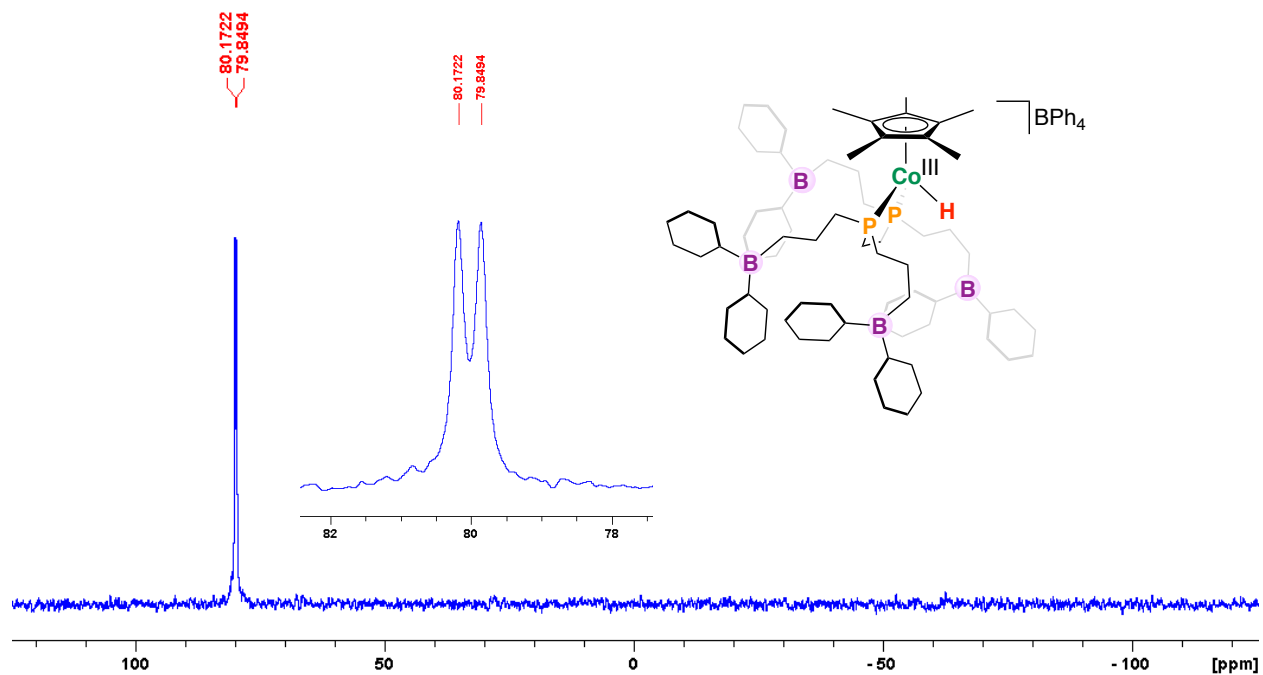


Figure S25. [5]BPh₄, ¹¹B{¹H} NMR, THF-d₈, 160.5 MHz, 298 K.

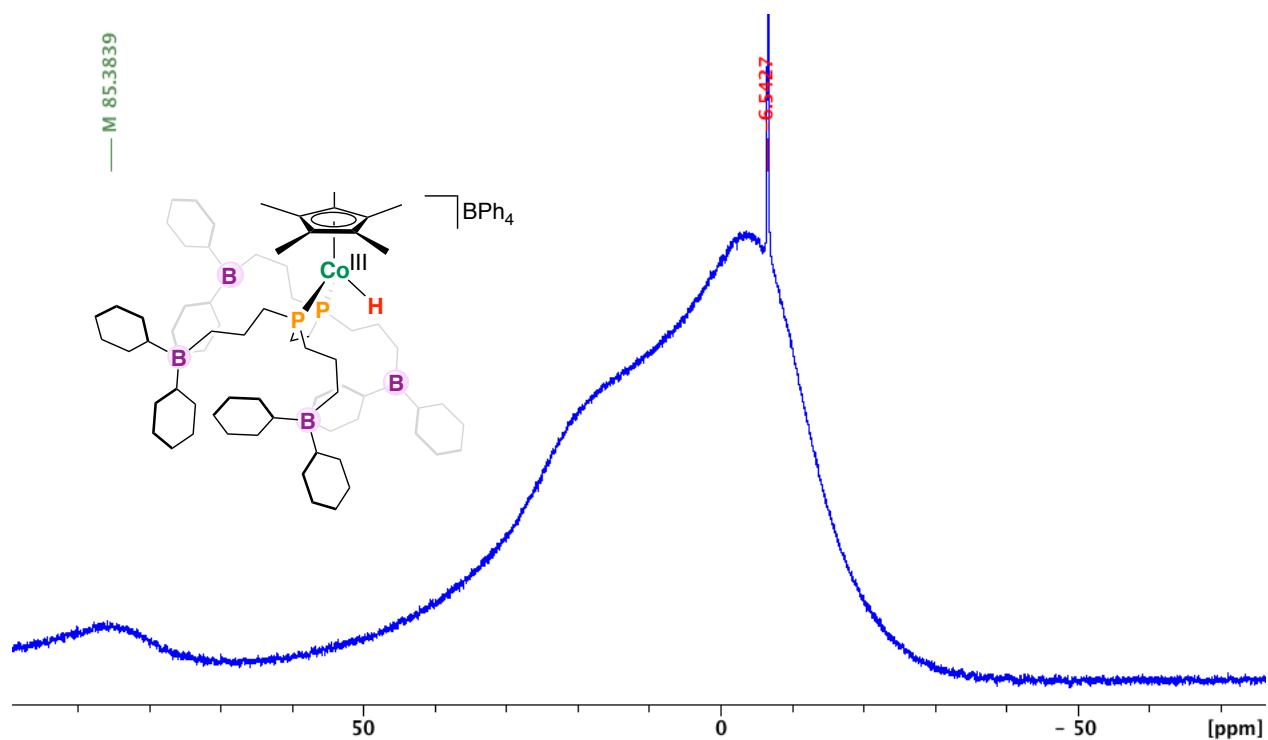


Figure S26. [5]BPh₄, Variable Temperature ¹¹B{¹H} NMR, THF-d₈, 160.5 MHz.

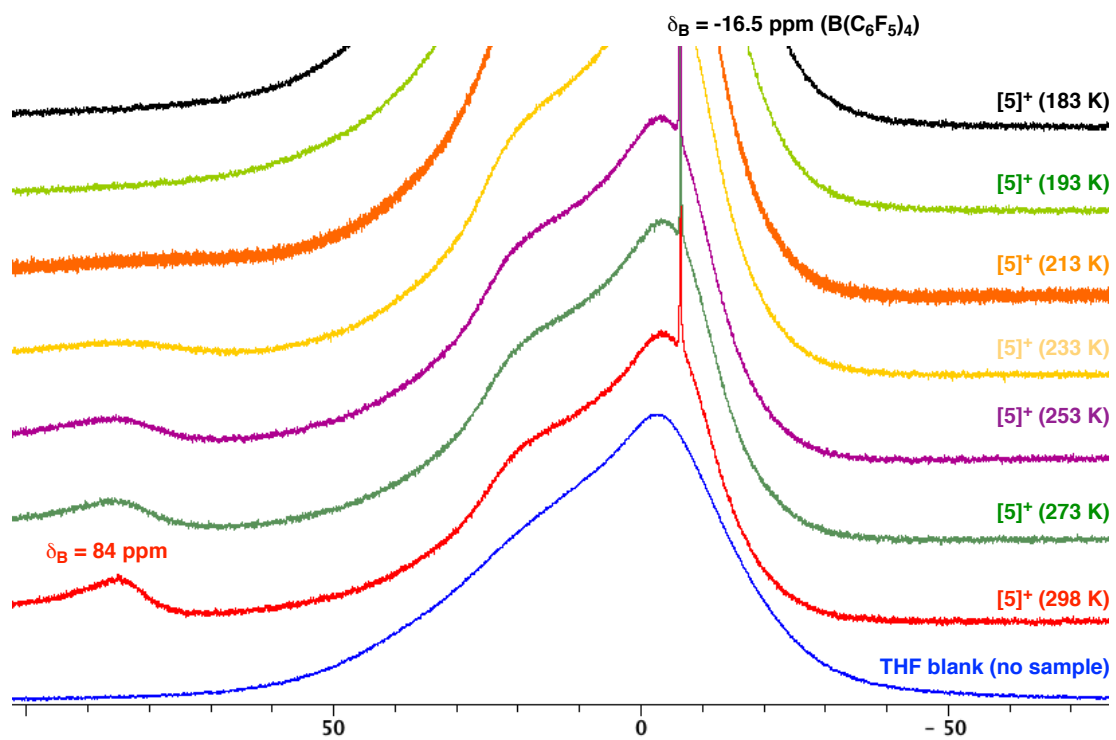


Figure S27. [5]BPh₄, ¹³C{¹H} NMR, THF-d₈, 125 MHz, 298 K

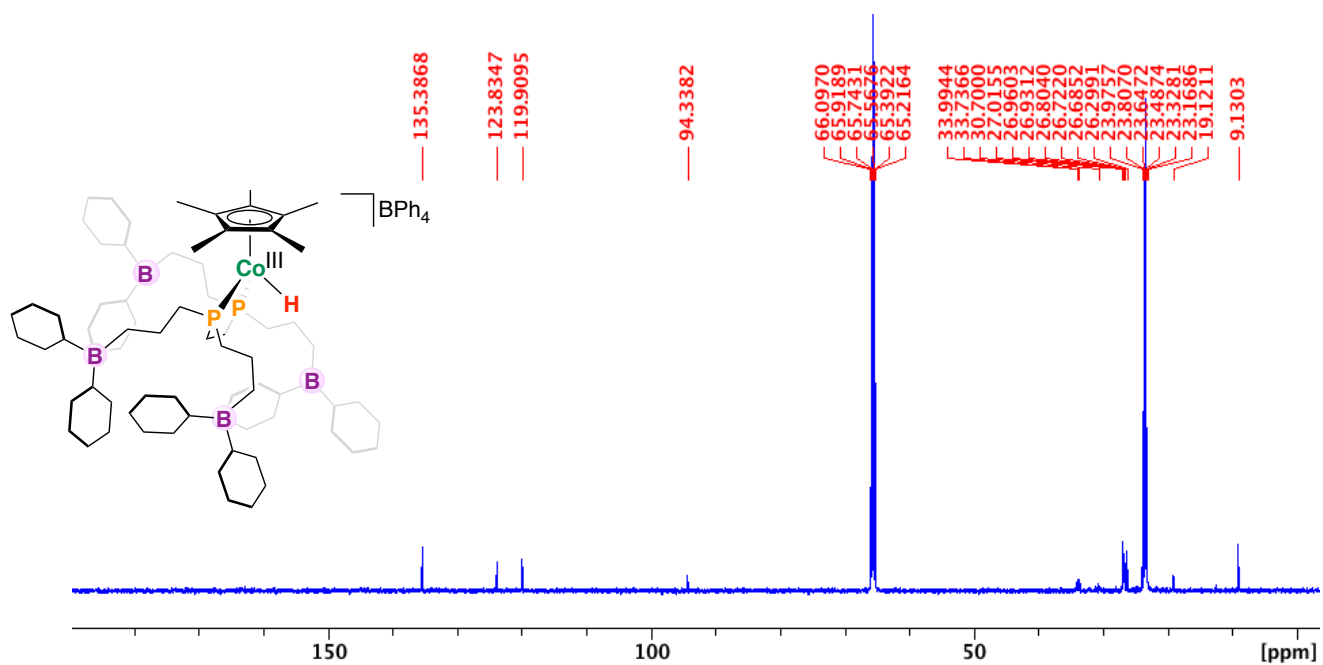


Figure S28. [5]BPh₄, Variable Temperature ¹H NMR, THF-d₈, 500 MHz.

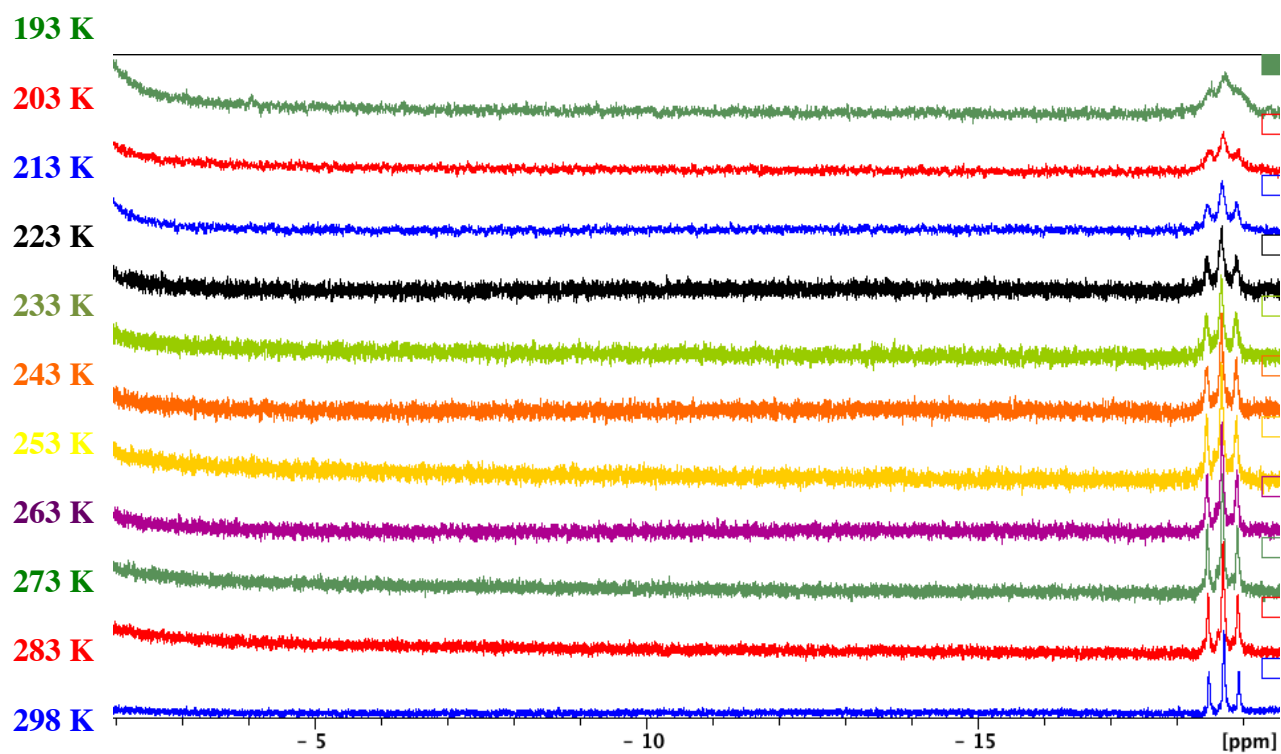


Figure S29. [5]BPh₄, Variable Temperature ³¹P{¹H} NMR, THF-d₈, 203 MHz.

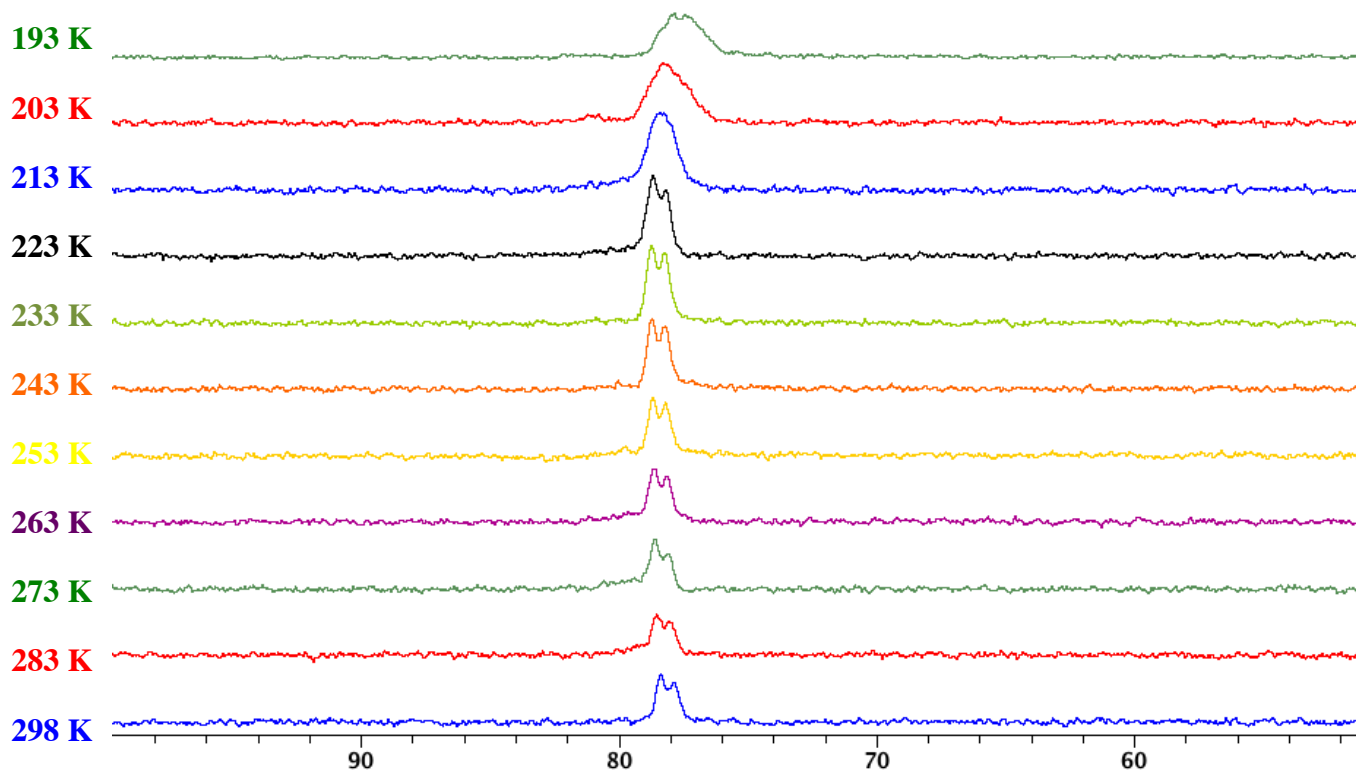


Figure S30. [6]BPh₄, ¹H NMR, THF-d₈, 500 MHz, 298 K

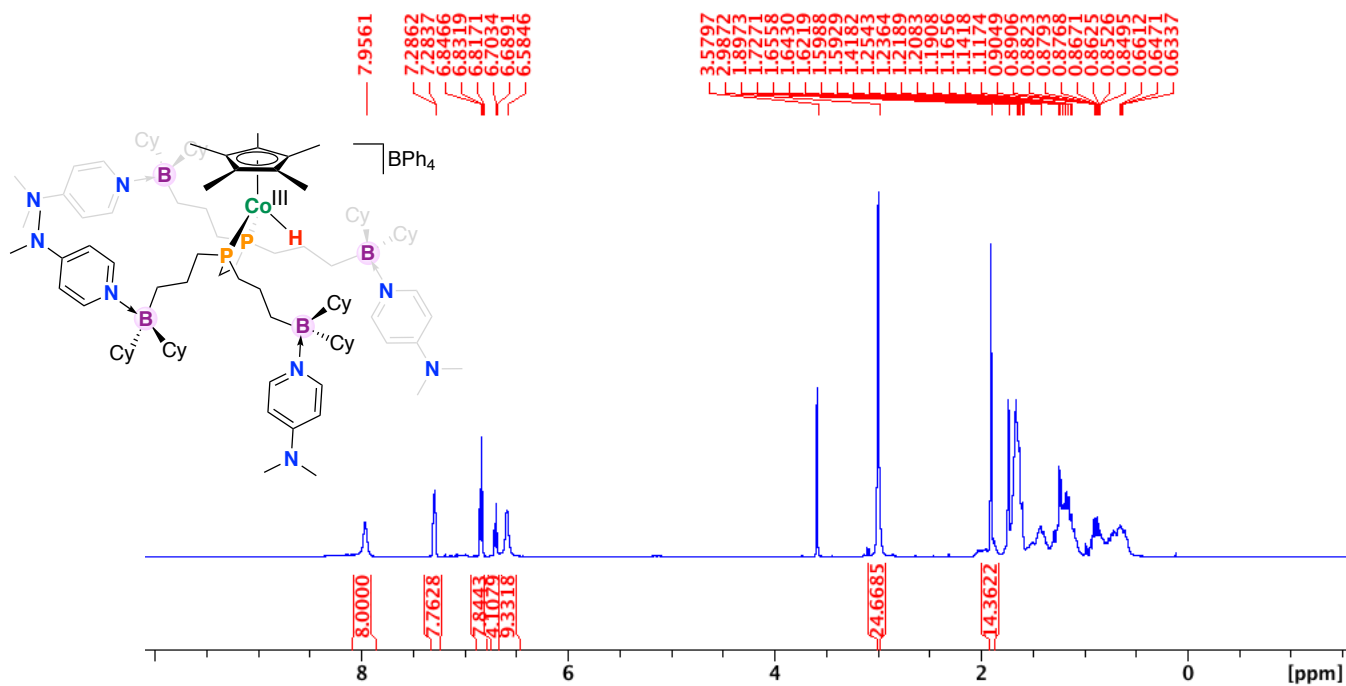


Figure S31. [6]BPh₄, a) ¹H NMR and b) ¹H{³¹P} NMR, THF-d₈, 500 MHz, 298 K

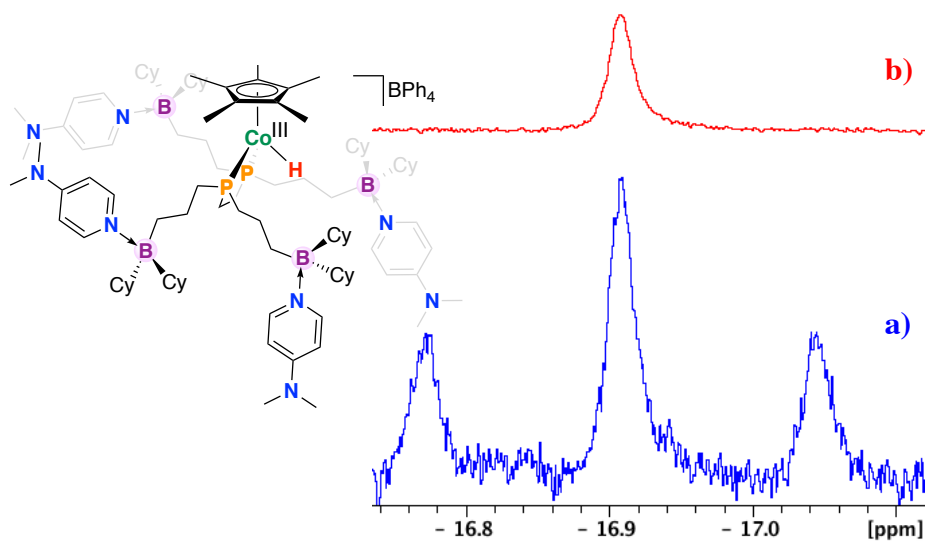


Figure S32. [6]BPh₄, ³¹P{¹H} NMR, THF-d₈, 203 MHz, 298 K

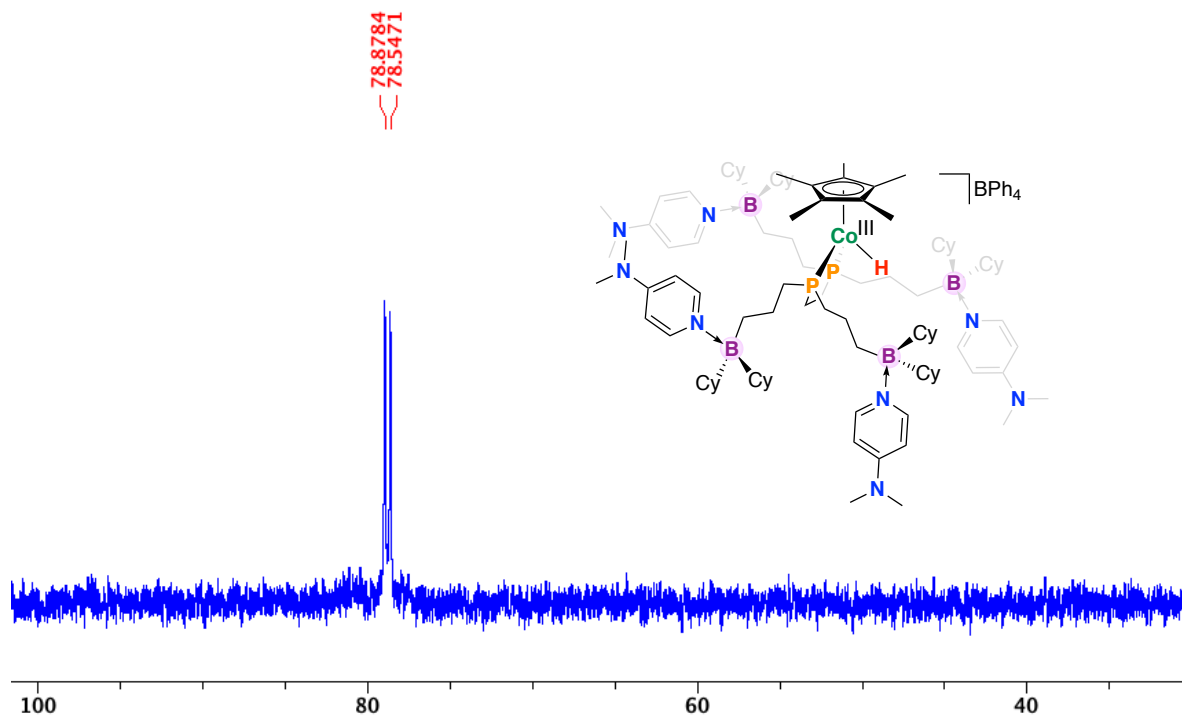


Figure S33. [6]BPh₄, ¹¹B{¹H} NMR, THF-d₈, 160.5 MHz.

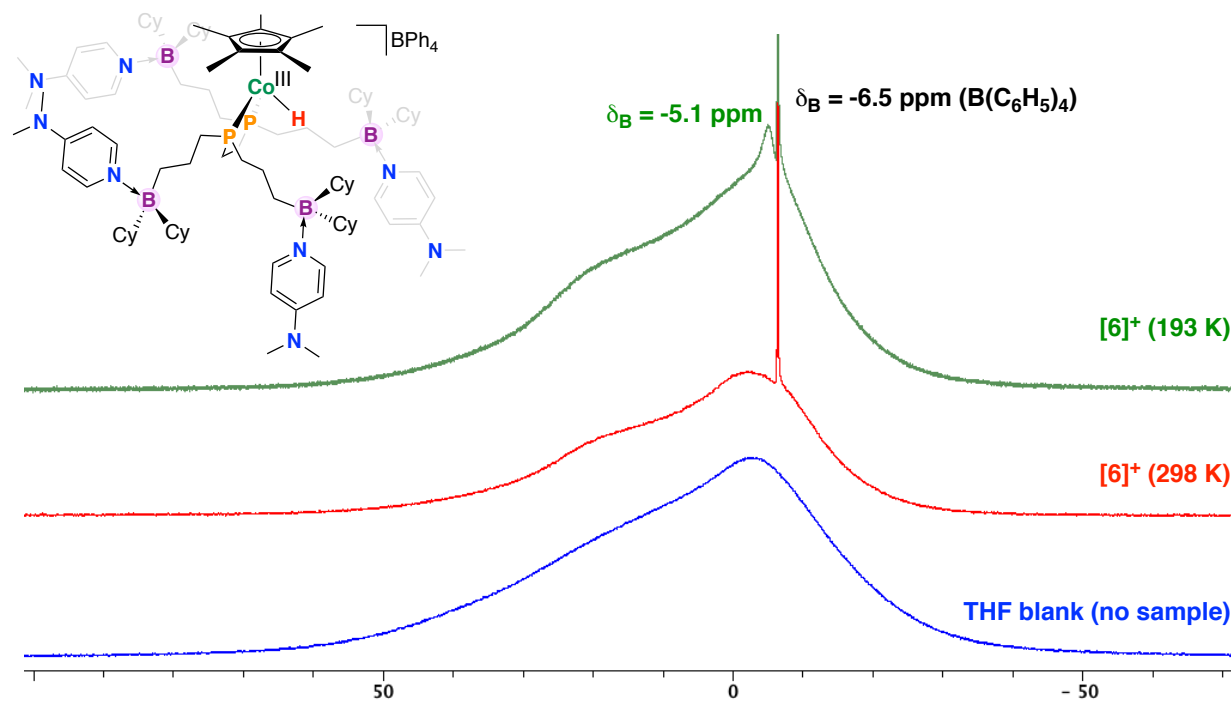


Figure S34. 7, ¹H NMR, THF-d₈, 500 MHz, 298 K

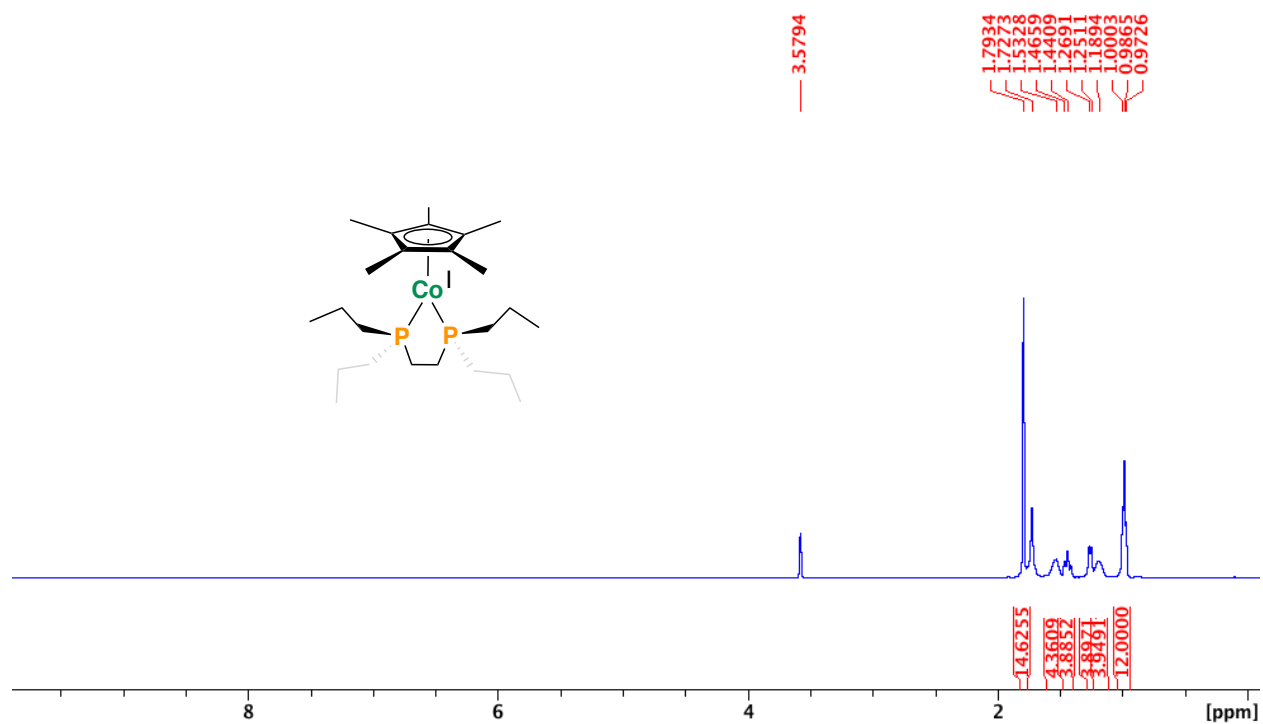


Figure S35. 7, $^{31}\text{P}\{^1\text{H}\}$ NMR, THF- d_8 , 203 MHz, 298 K

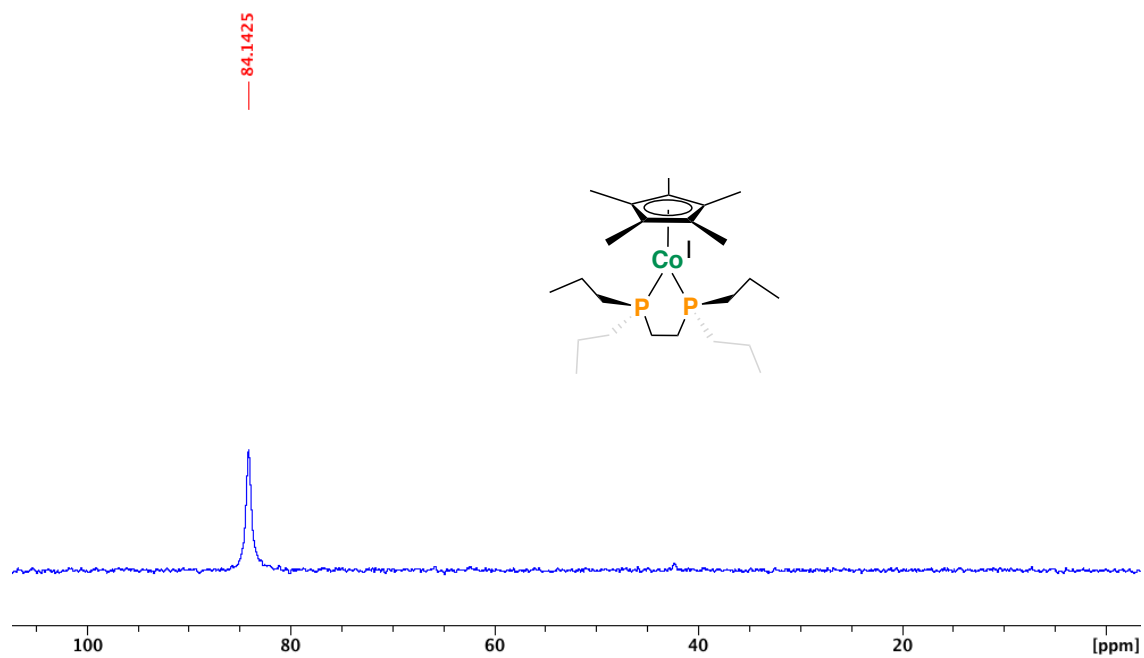


Figure S36. [5]BPh $_4$, $^{13}\text{C}\{^1\text{H}\}$ NMR, THF- d_8 , 125 MHz, 298 K

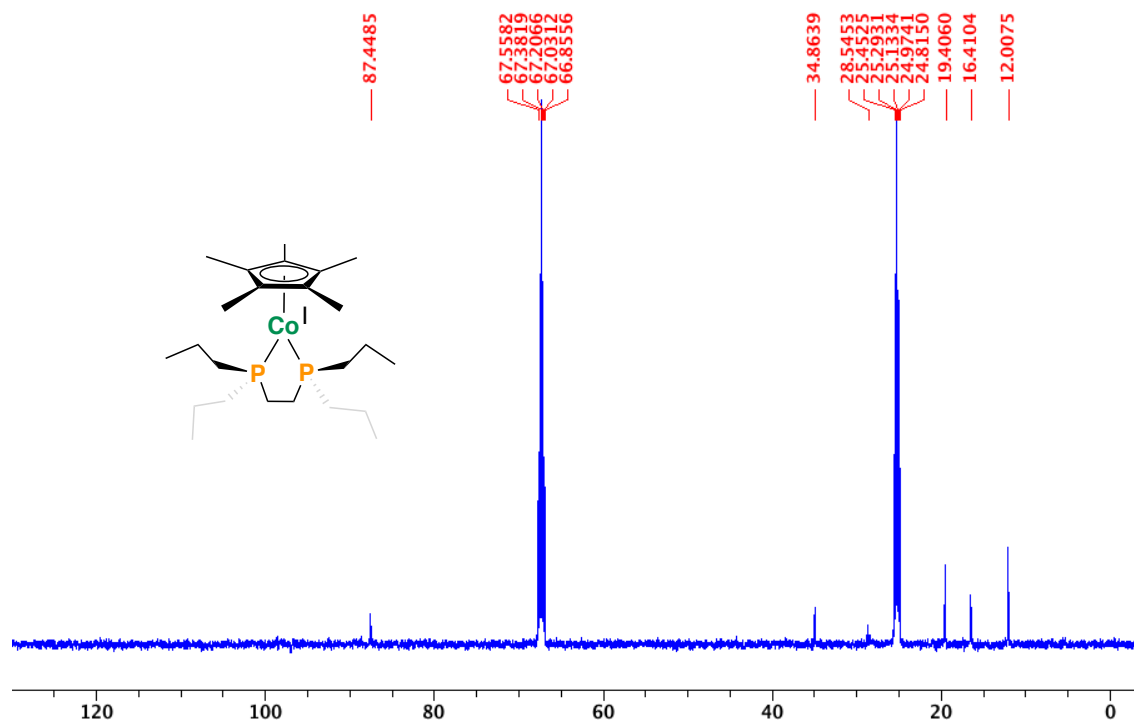


Figure S37. [8]BPh₄, ¹H NMR, THF-d₈, 500 MHz, 298 K (inset shows hydride resonance)

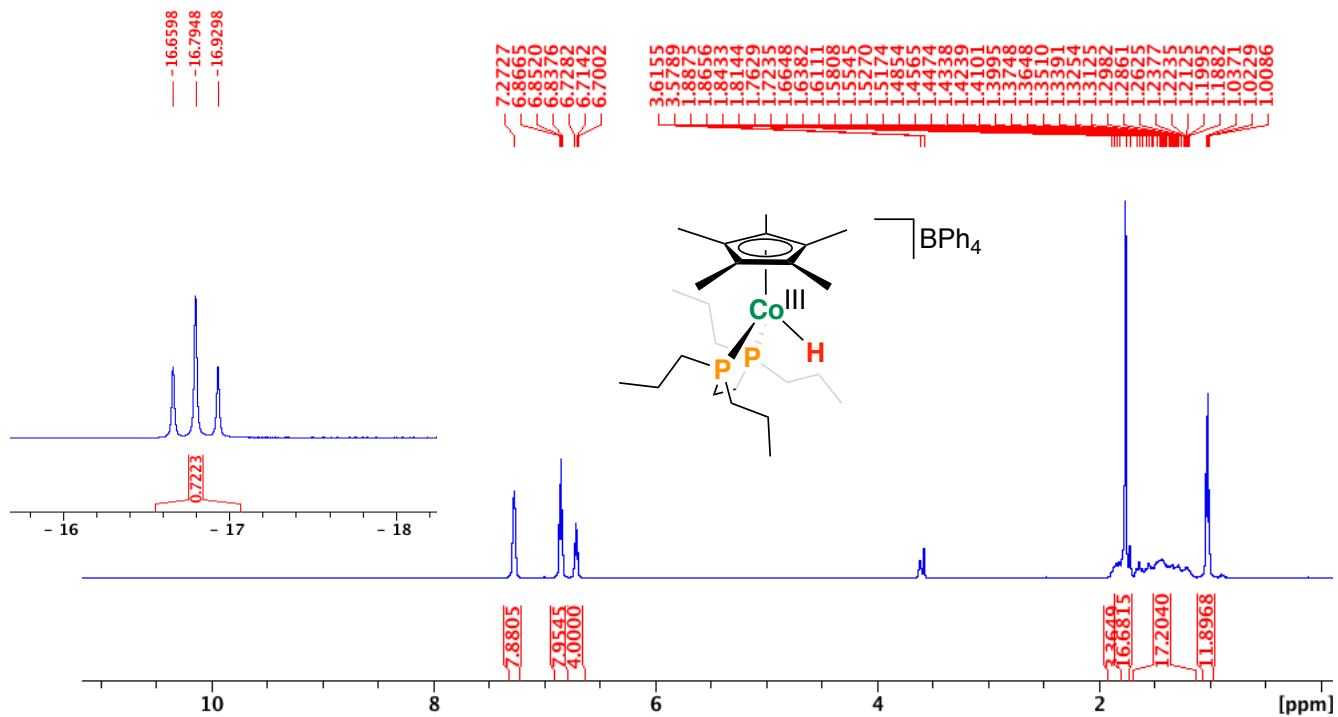


Figure S38. [8]BPh₄, a) ¹H NMR and b) ¹H{³¹P} NMR, THF-d₈, 500 MHz, 298 K

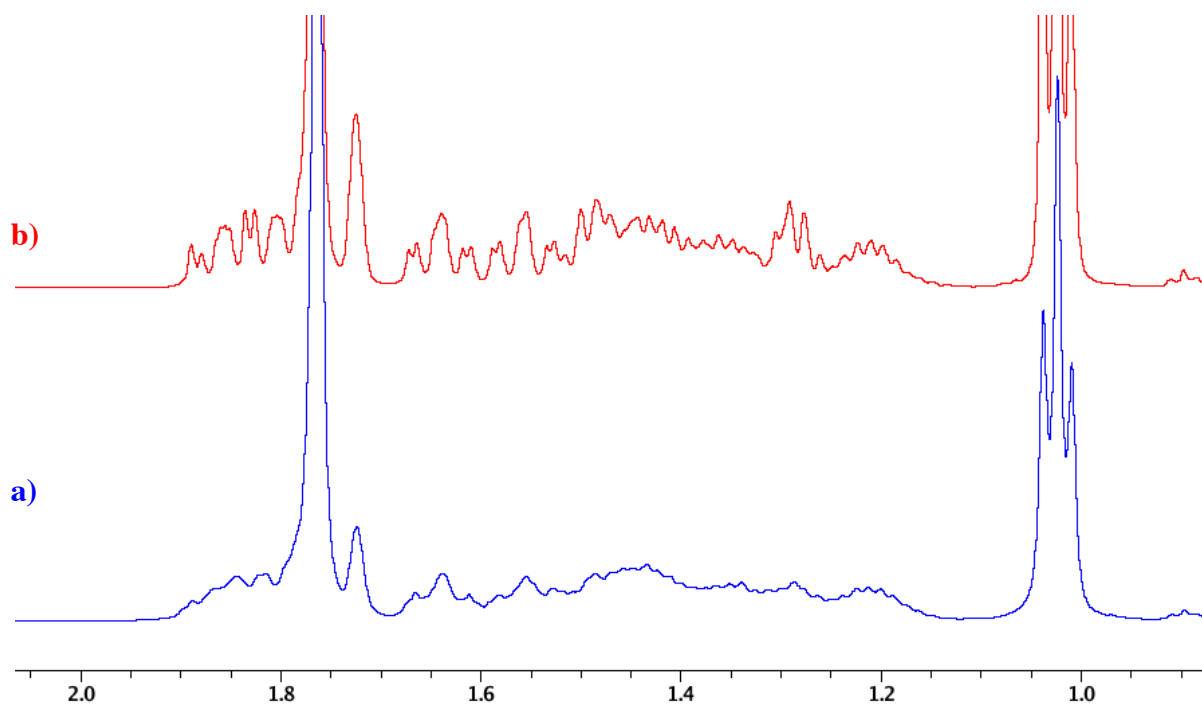


Figure S39. [8]BPh₄, ³¹P{¹H} NMR, THF-d₈, 203 MHz, 298 K

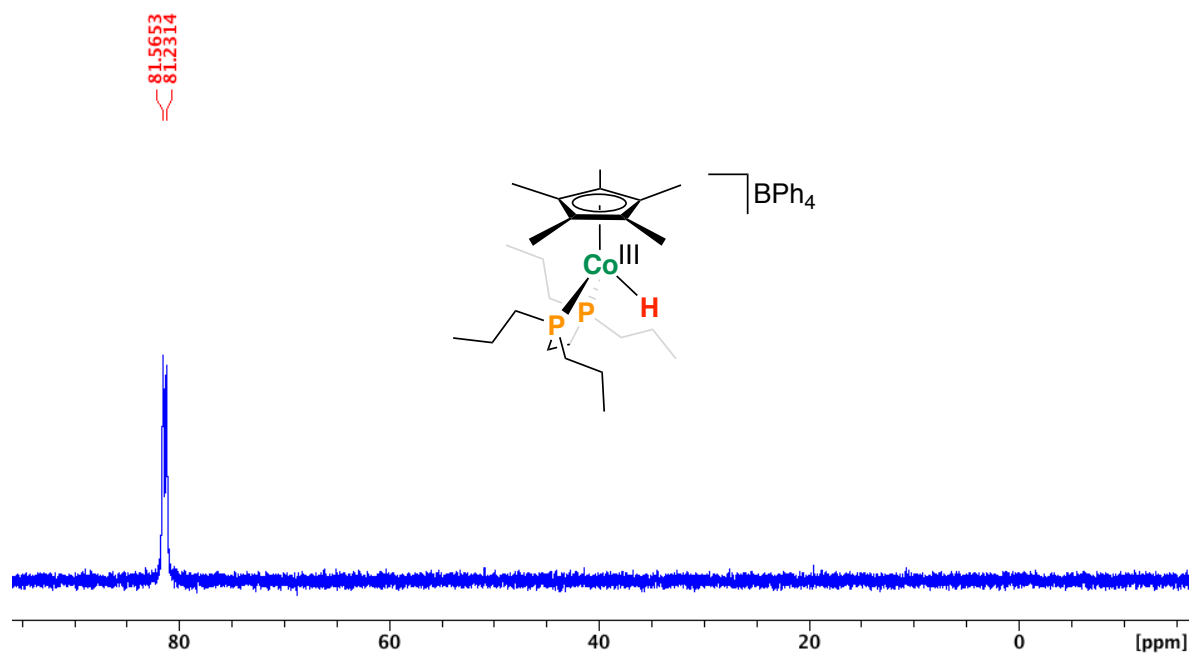


Figure S40. [8]BPh₄, ¹¹B{¹H} NMR, THF-d₈, 160.5 MHz, 298 K.

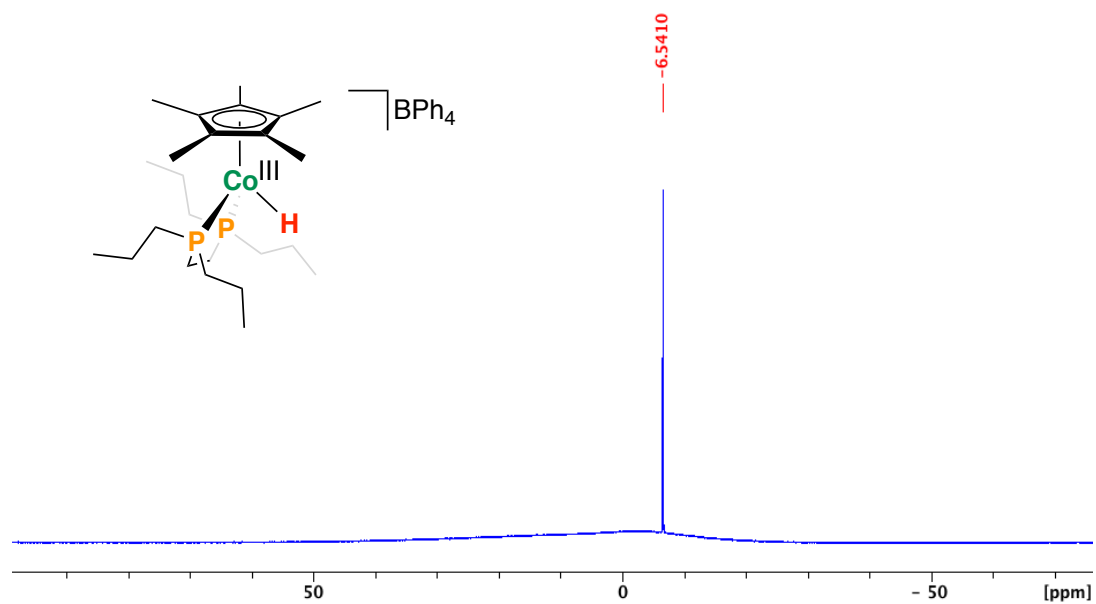


Figure S41. [8]BPh₄, ¹³C{¹H} NMR, THF-d₈, 125 MHz, 298 K

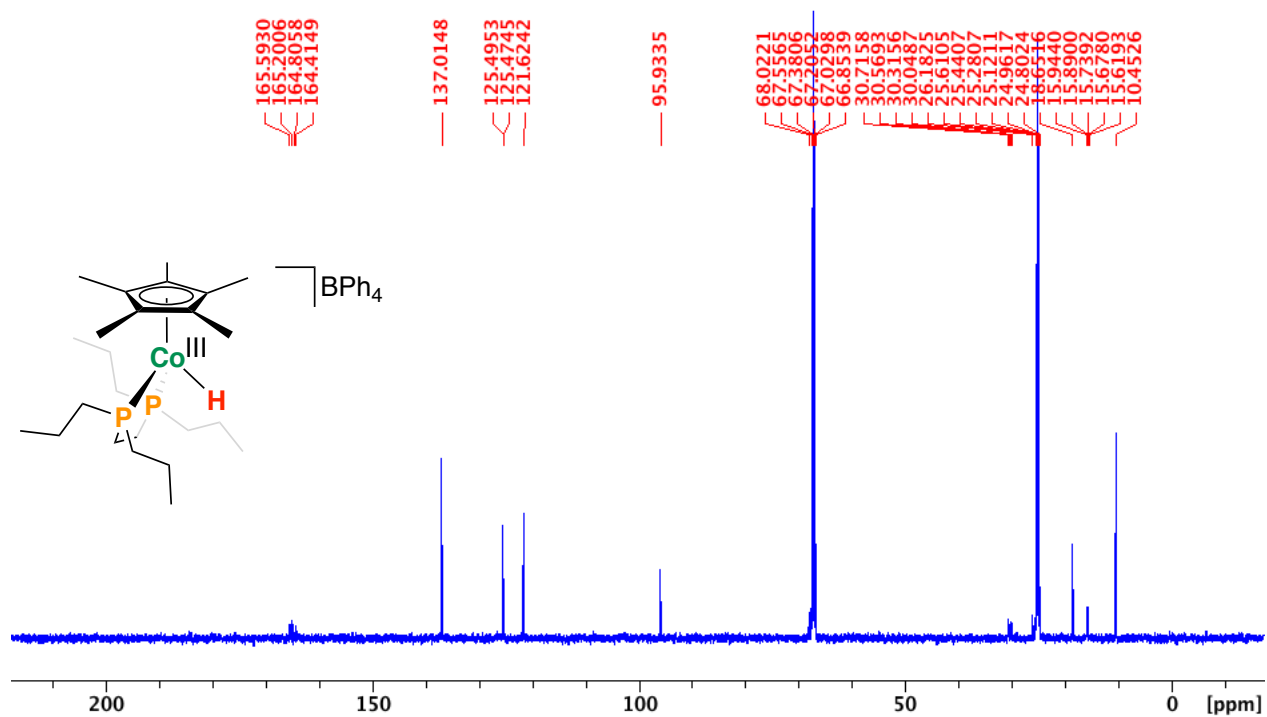


Figure S42. [9]B(C₆F₅)₄, ¹H NMR, THF-d₈, 500 MHz, 298 K

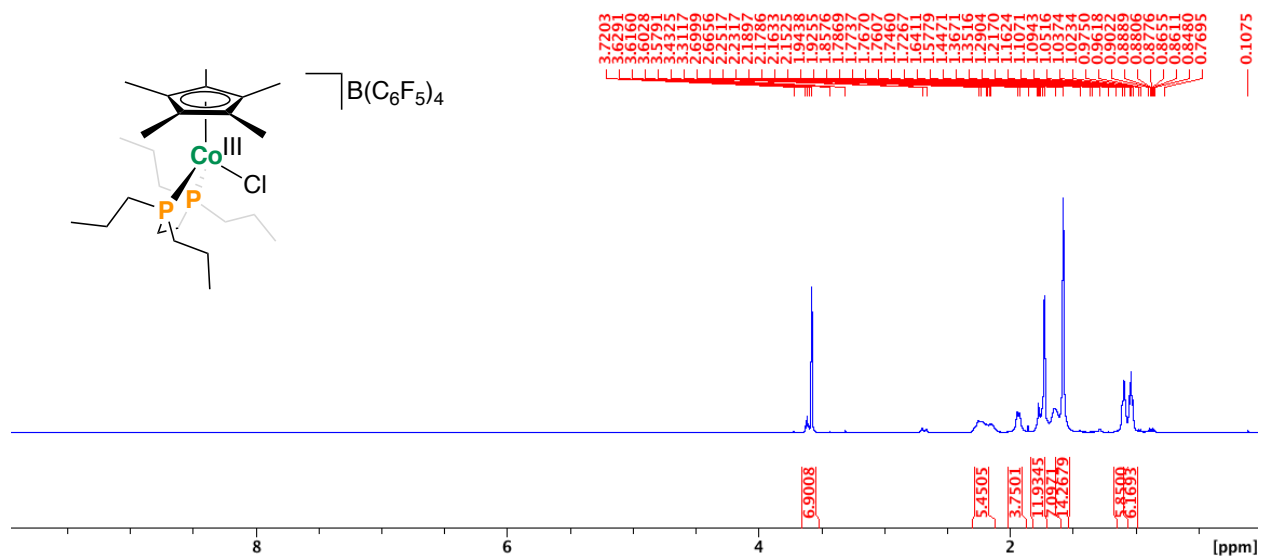


Figure S43. $[9]B(C_6F_5)_4$, $^{31}P\{^1H\}$ NMR, THF- d_8 , 203 MHz, 298 K

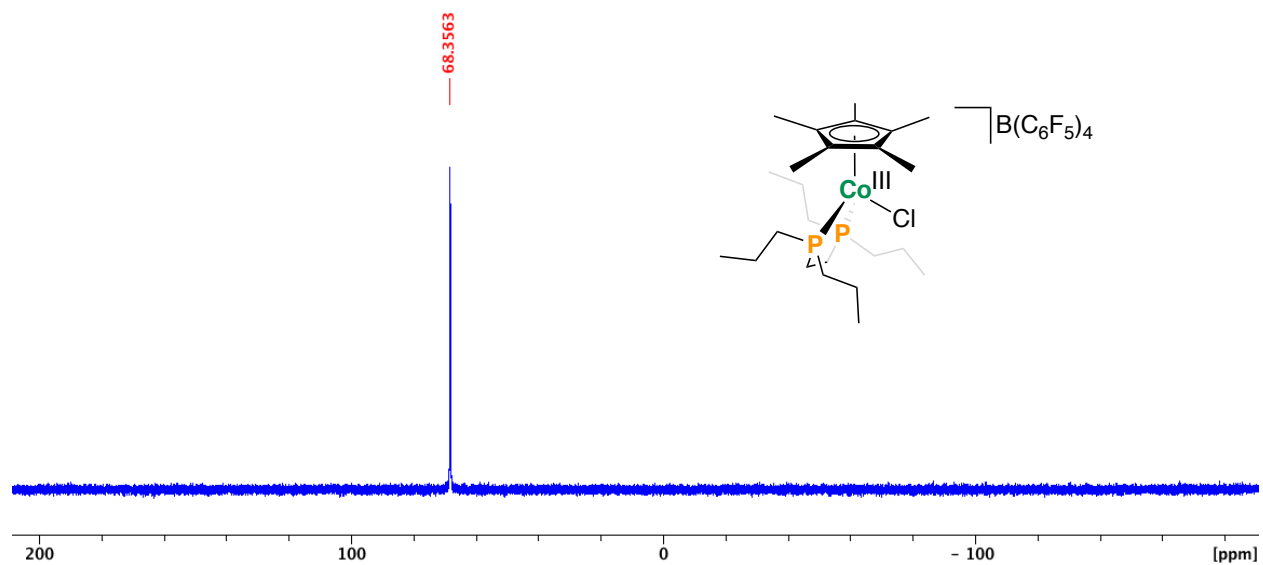


Figure S44. $[9]B(C_6F_5)_4$, $^{11}B\{^1H\}$ NMR, THF- d_8 , 160.5 MHz, 298 K.

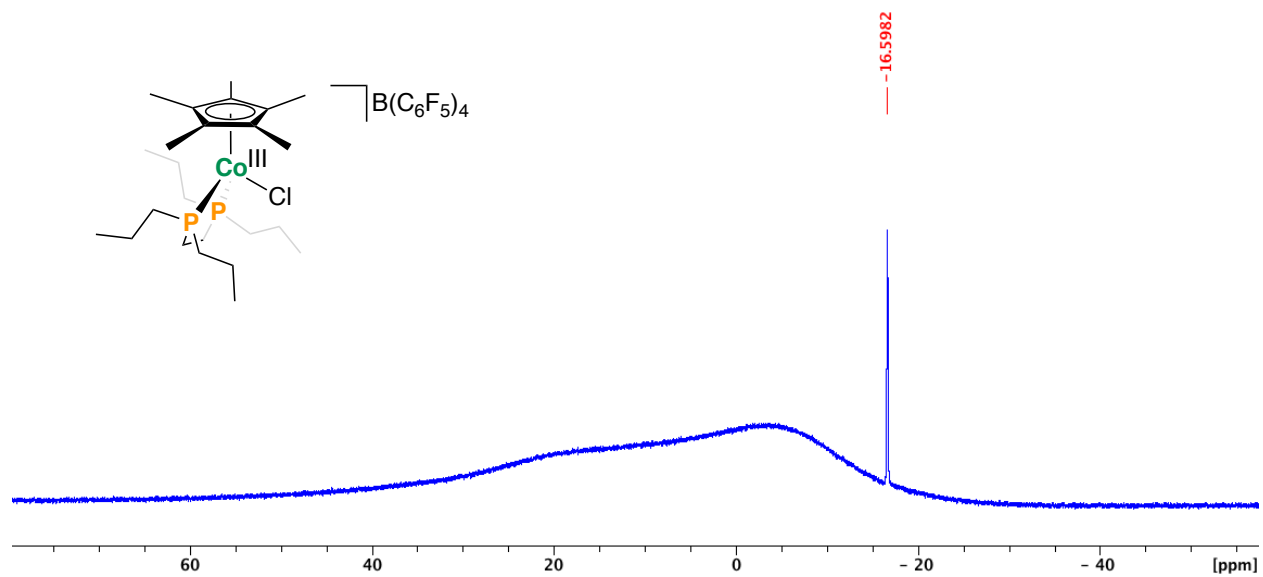


Figure S47. Crude ^1H NMR for treatment of **4** with **a)** benzoic acid and **b)** 4-pyridylbenzoic acid, THF- d_8 , 500 MHz, 298 K.

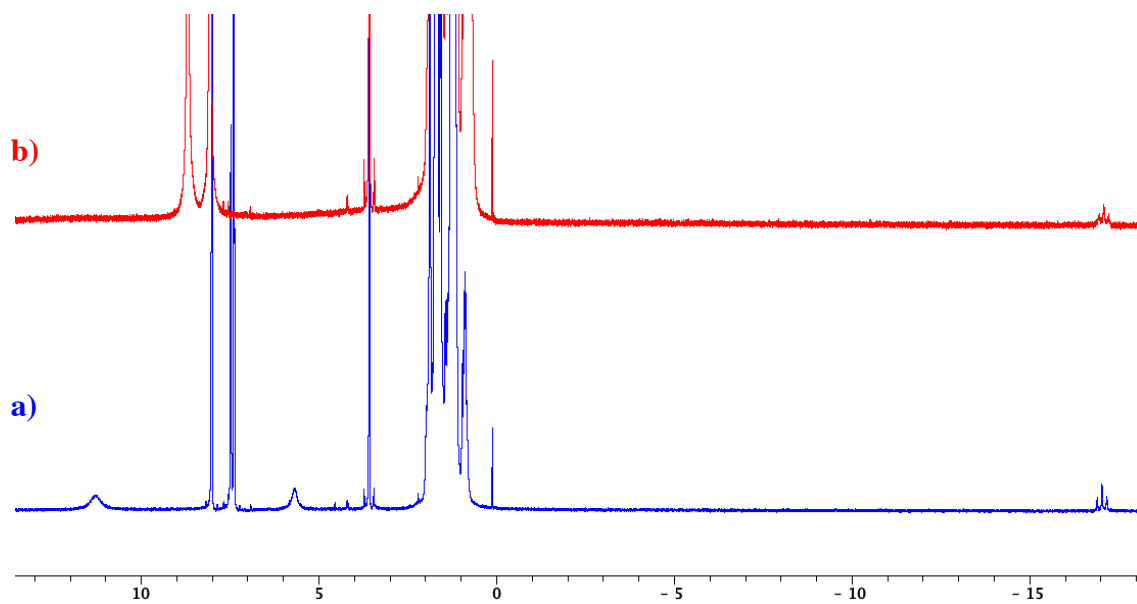


Figure S48. Crude ^1H NMR (expansion) for treatment of **4** with 4 equivalents of **a)** benzoic acid or **b)** 4-pyridylbenzoic acid, THF- d_8 , 500 MHz, 298 K.

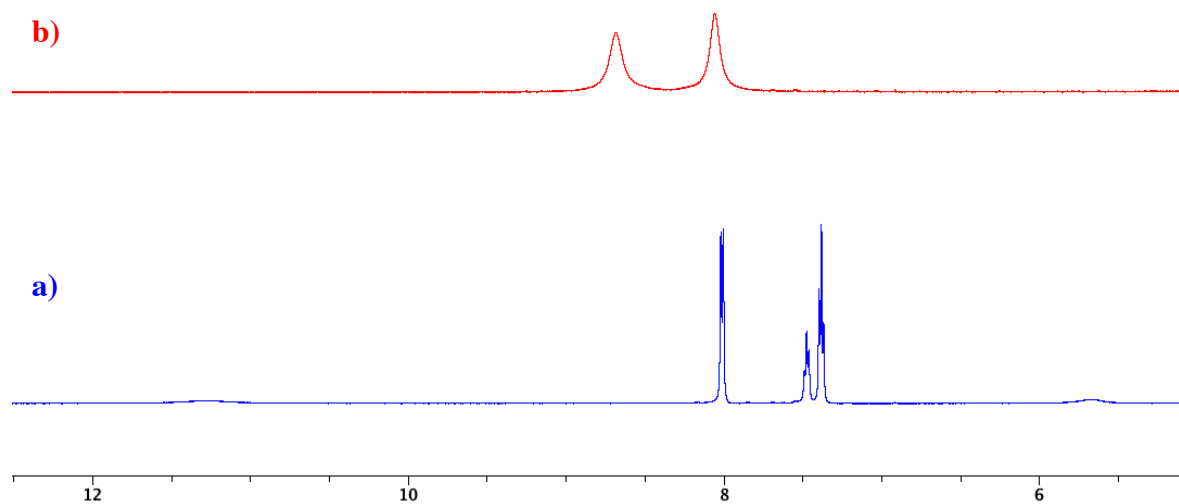


Figure S49. Crude ^1H NMR (expansion) for treatment of **4** with 4 equivalents of **a)** benzoic acid or **b)** 4-pyridylbenzoic acid, THF- d_8 , 500 MHz, 298 K.

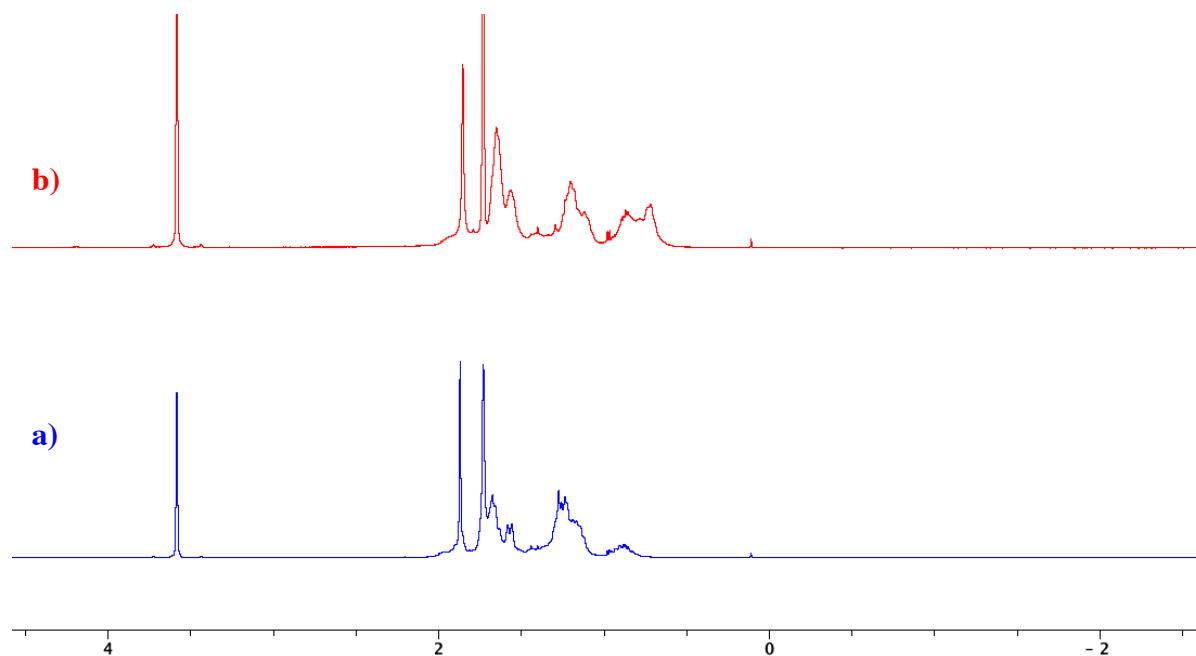


Figure S50. Crude ^1H NMR (expansion) for treatment of **4** with 4 equivalents of **a)** benzoic acid or **b)** 4-pyridylbenzoic acid, THF- d_8 , 500 MHz, 298 K.

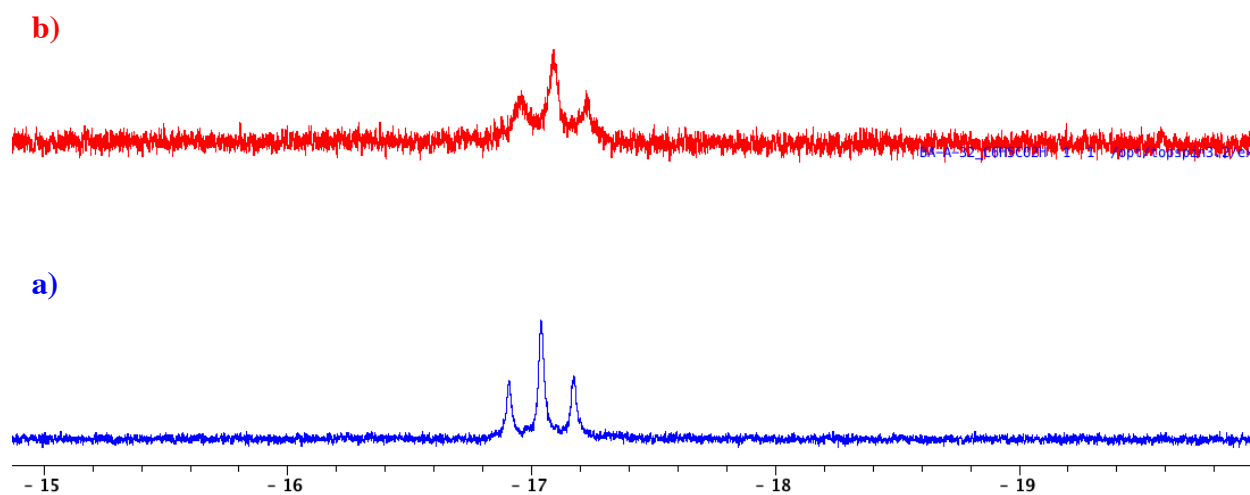


Figure S51. ^1H NMR comparison **a)** treatment of **4** with 4-pyridylbenzoic acid and **b)** a saturated 4-pyridylbenzoic solution, THF- d_8 , 500 MHz, 298 K.

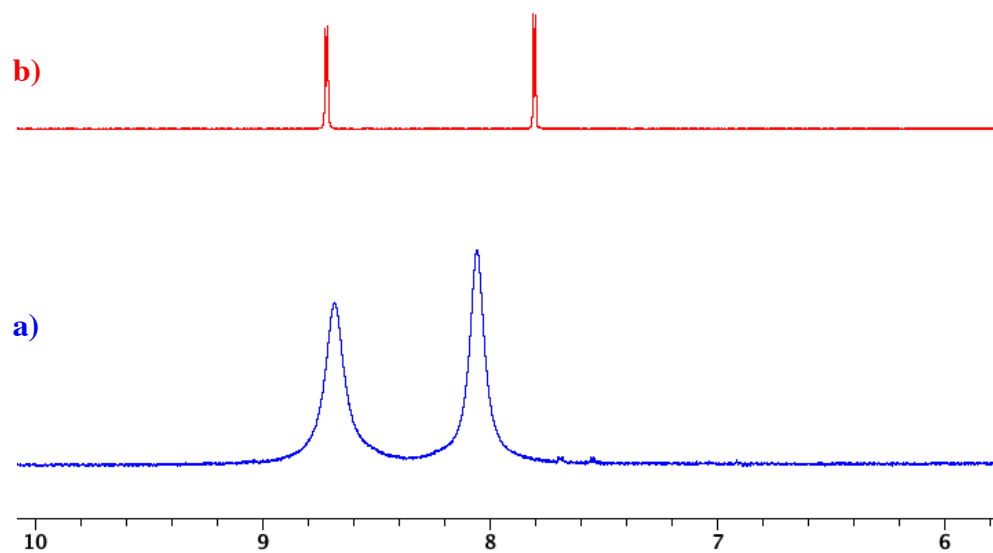


Figure S52. Crude ^{31}P NMR for treatment of **4** with 4 equivalents of **a)** benzoic acid or **b)** 4-pyridylbenzoic acid, THF- d_8 , 203 MHz, 298 K.

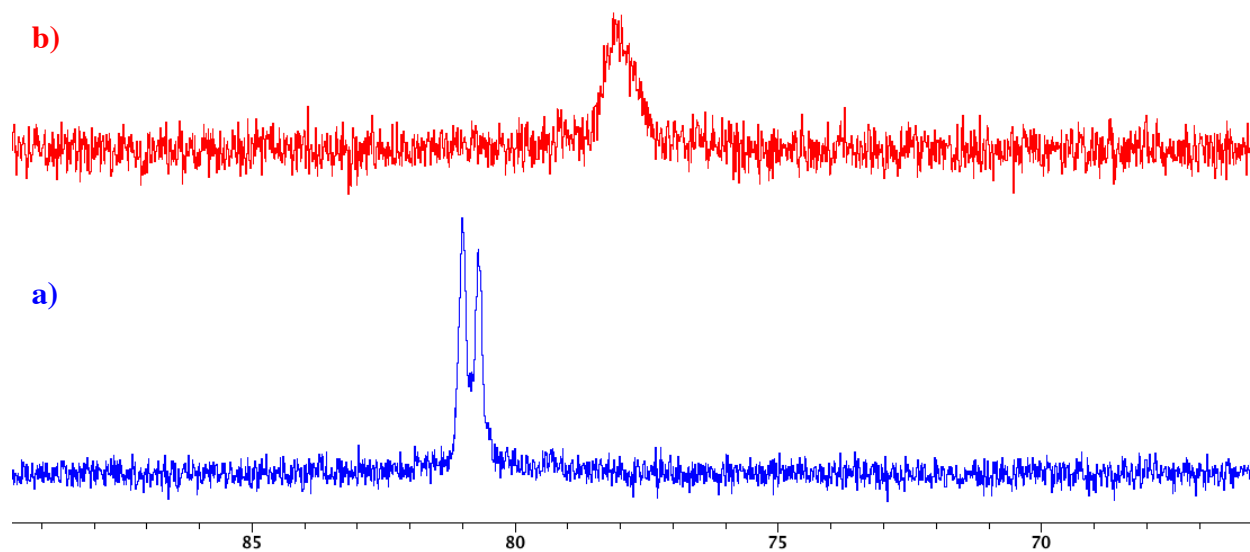


Figure S53. $^{11}\text{B}\{^1\text{H}\}$ NMR, THF- d_8 , 160.5 MHz, 298 K of **a)** $\text{BCy}_2^{\text{n}}\text{Oct}$ + 1 equiv. BzOH (showing no reaction) and **b)** $\text{BCy}_2^{\text{n}}\text{Oct}$ + 1 equiv. 4-pyridylbenzoic acid (showing adduct formation at $\delta_{\text{B}} = 6$ ppm). **Signal at $\delta_{\text{p}} = 50$ ppm due to trace $\text{Cy}_2\text{B-O-BCy}_2$.

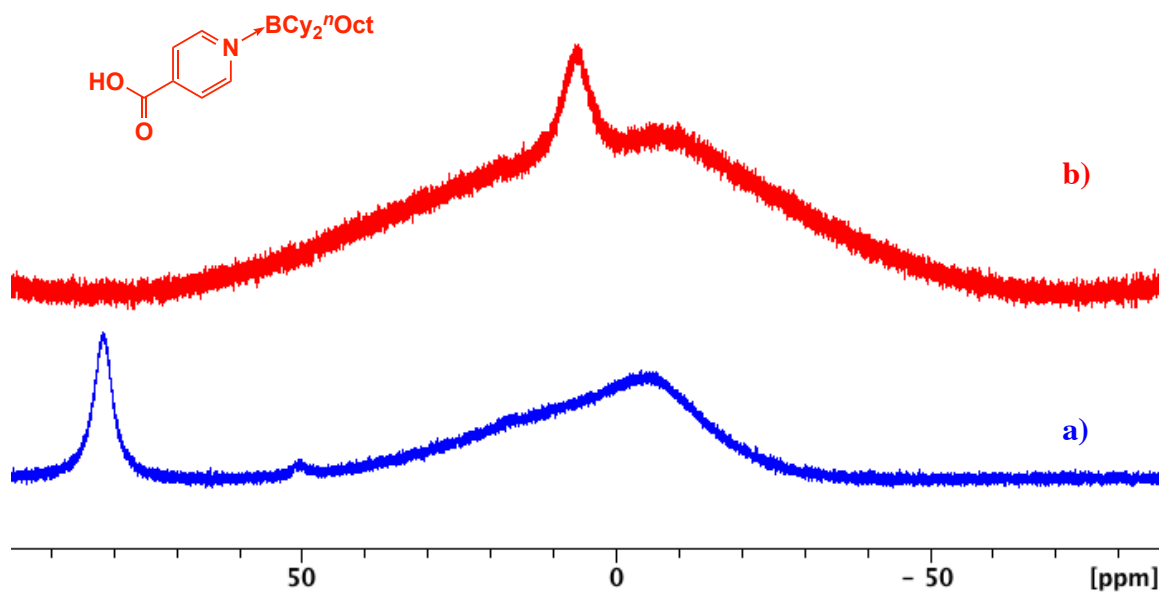


Figure S54. ^{31}P NMR for treatment of 7 with 4-pyridylbenzoic acid, THF- d_8 , 203 MHz, 298 K.

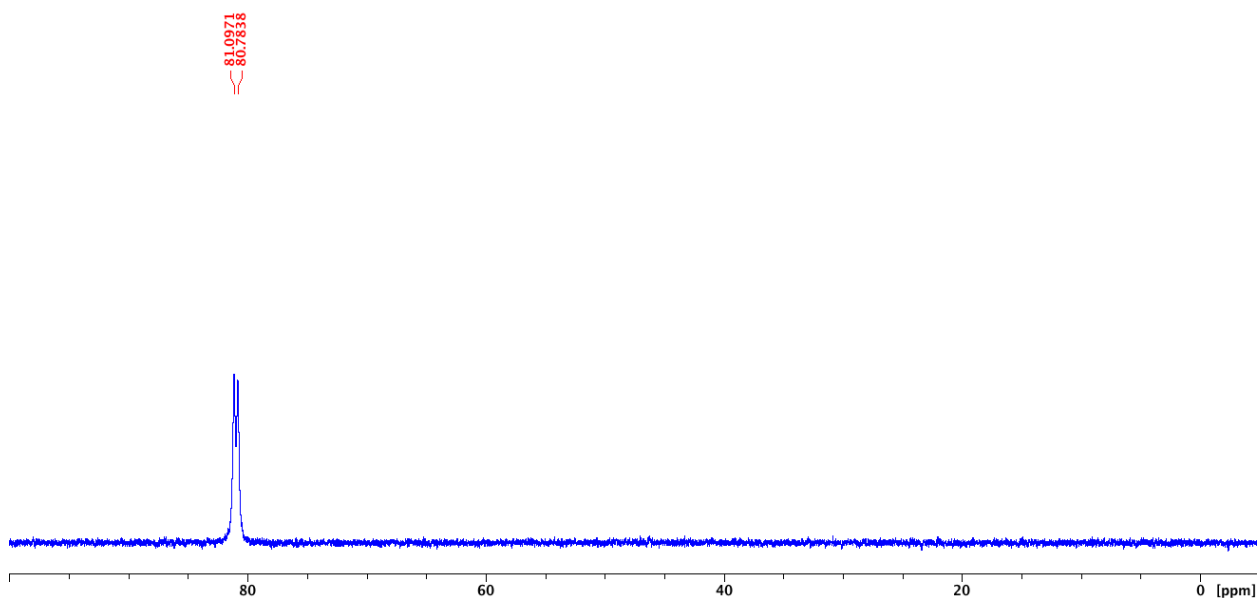


Figure S55. [5]O₂CPh, ¹H NMR, THF-d₈, 500 MHz, 298 K.

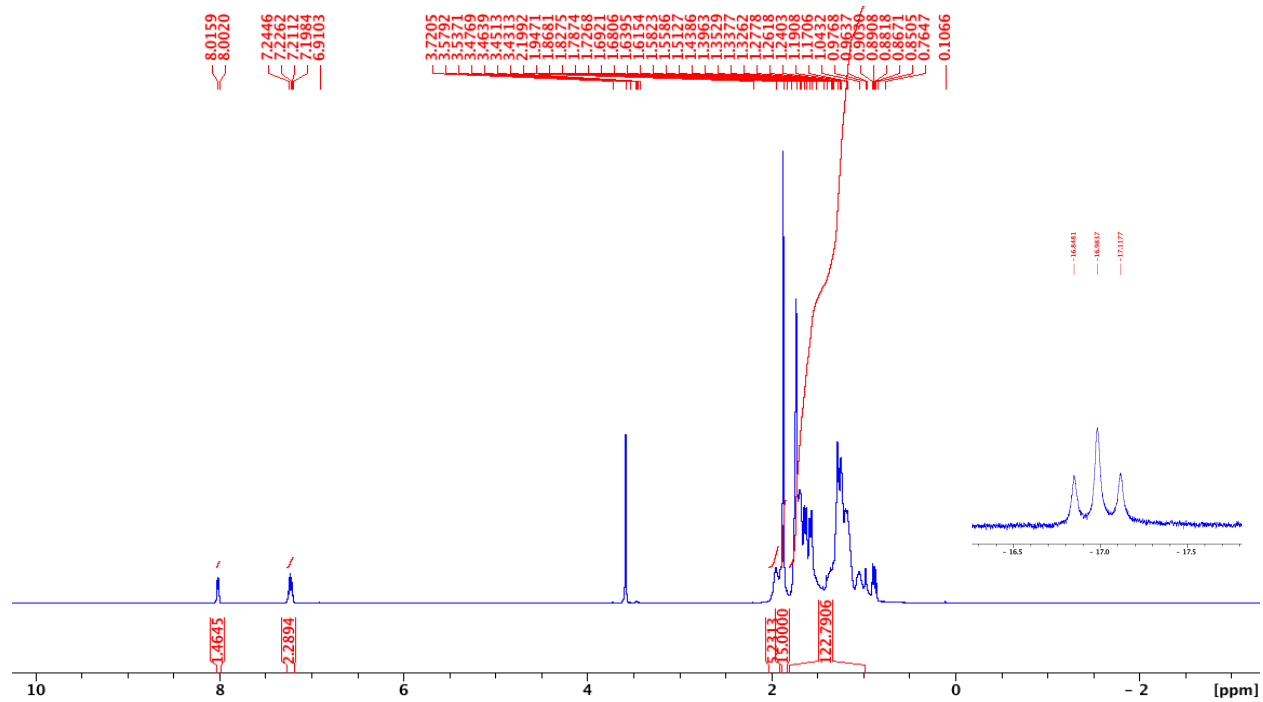


Figure S56. [5]O₂CPh, ³¹P NMR, THF-d₈, 203 MHz, 298 K.

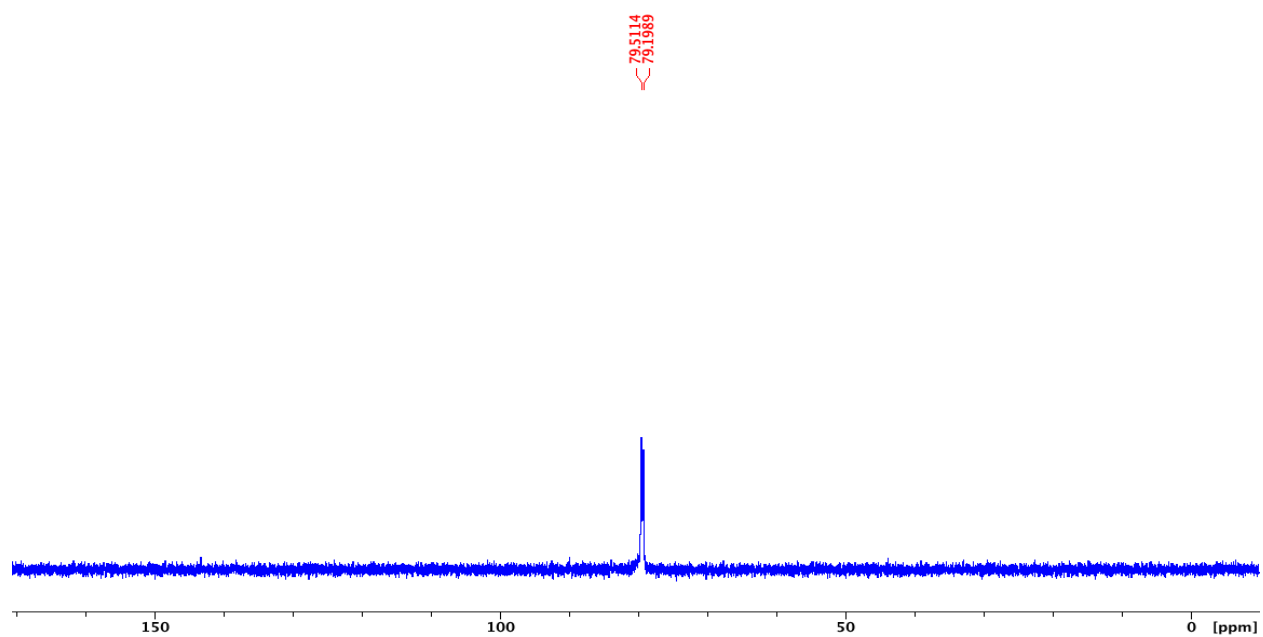


Figure S57. ^1H NMR, 500 MHz, 298 K of **a)** [5]O₂CPh in C₆D₆, **b)** [5]O₂CPh in THF-d₈.

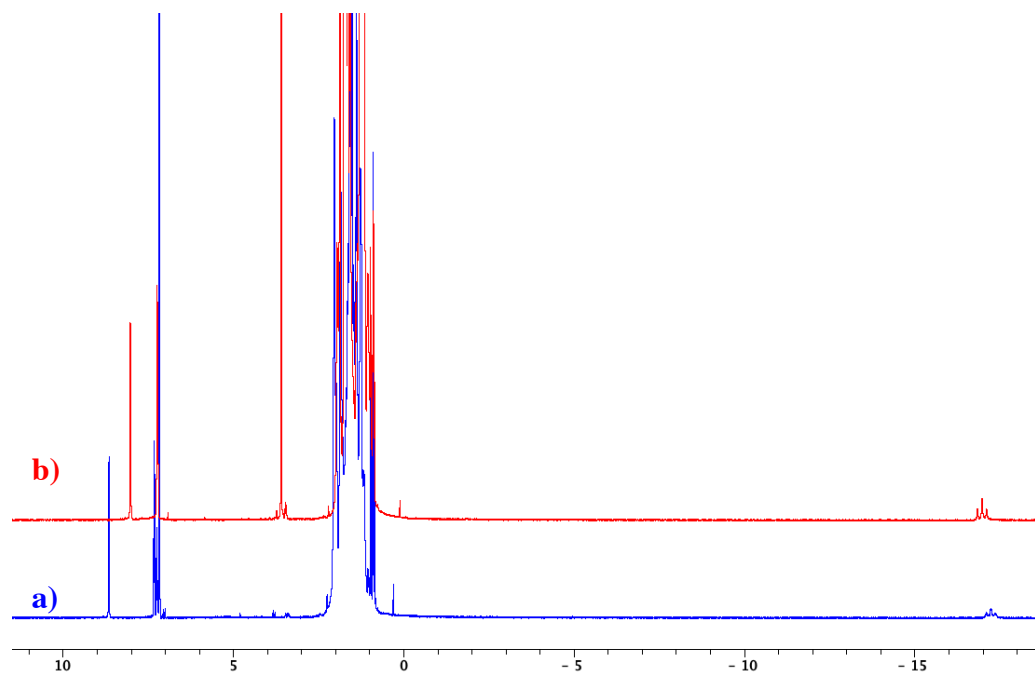


Figure S58. ^1H NMR, 500 MHz, 298 K of **a)** [5]O₂CPh in C₆D₆, **b)** [5]O₂CPh in THF-d₈ showing aromatic region.

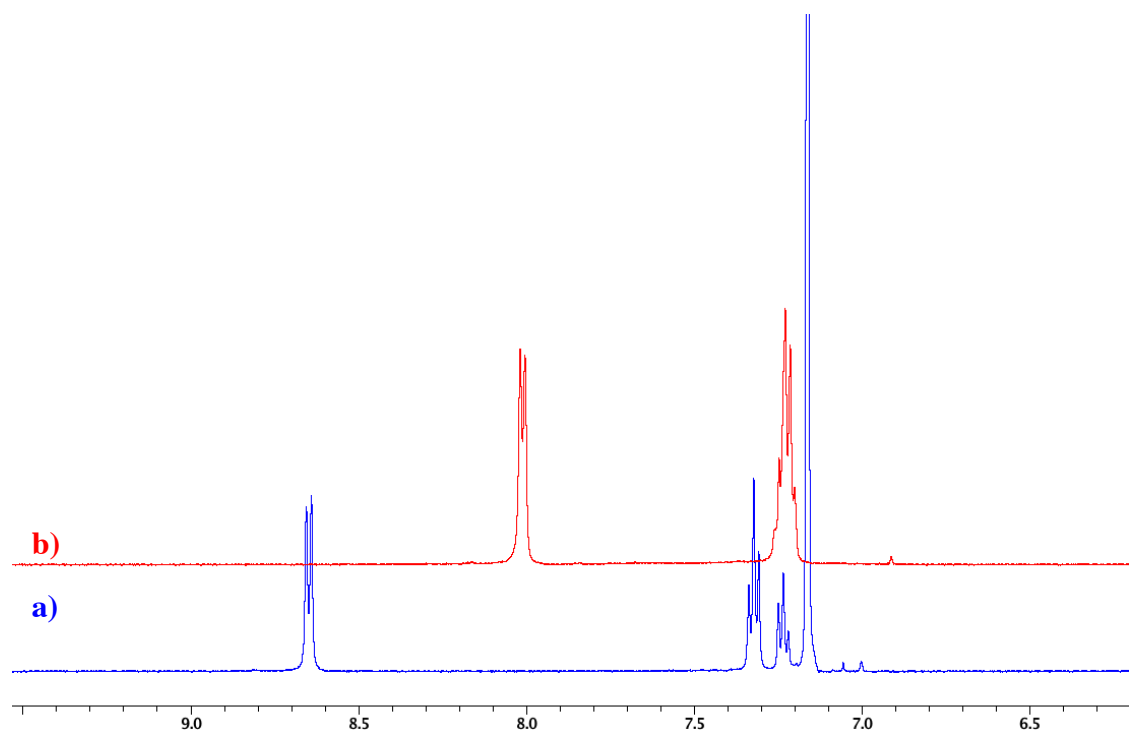


Figure S59. ^1H NMR, 500 MHz, 298 K of **a)** $[\text{5}]\text{O}_2\text{CPh}$ in C_6D_6 , **b)** $[\text{5}]\text{O}_2\text{CPh}$ in THF-d_8 and **c)** $[\text{5}]\text{BPh}_4$ in THF-d_8 .

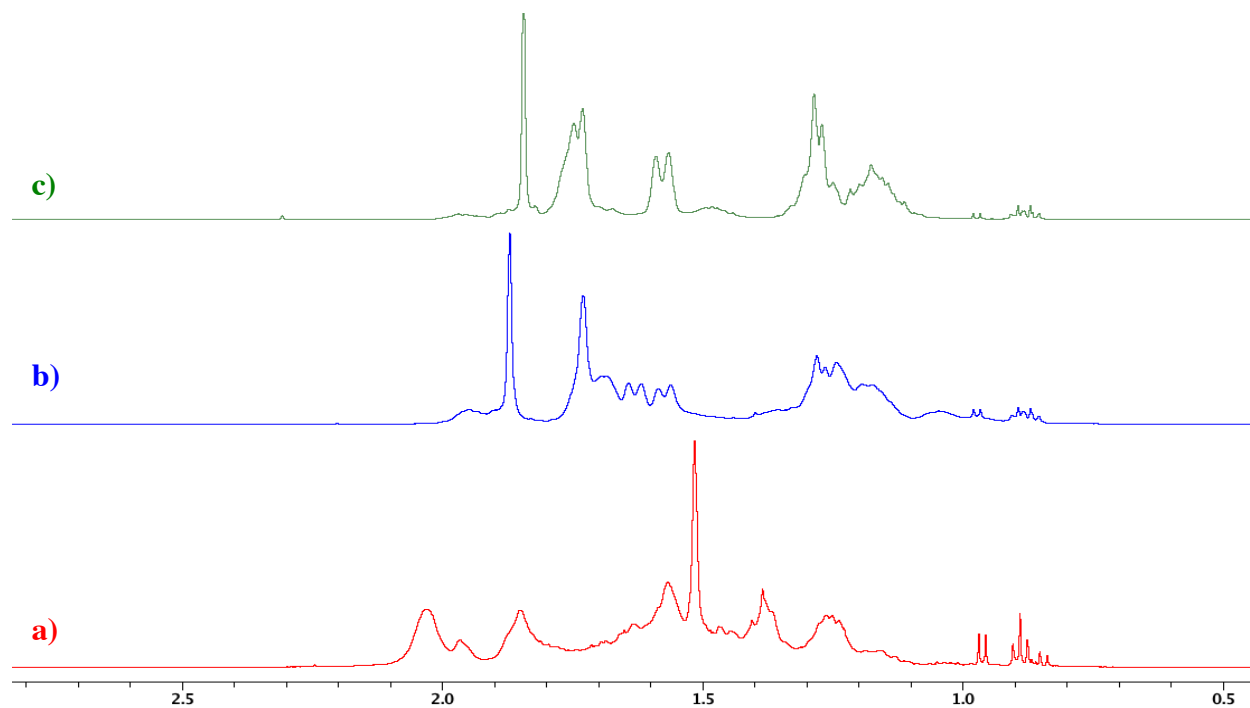


Figure S60. Benzoic acid, ^1H NMR, 500 MHz, 298 K in **a)** C_6D_6 and **b)** THF-d_8 . Note: $\text{K}[\text{O}_2\text{CPh}]$ and $\text{Na}[\text{O}_2\text{CPh}]$ are insoluble in C_6D_6 and THF-d_8 .

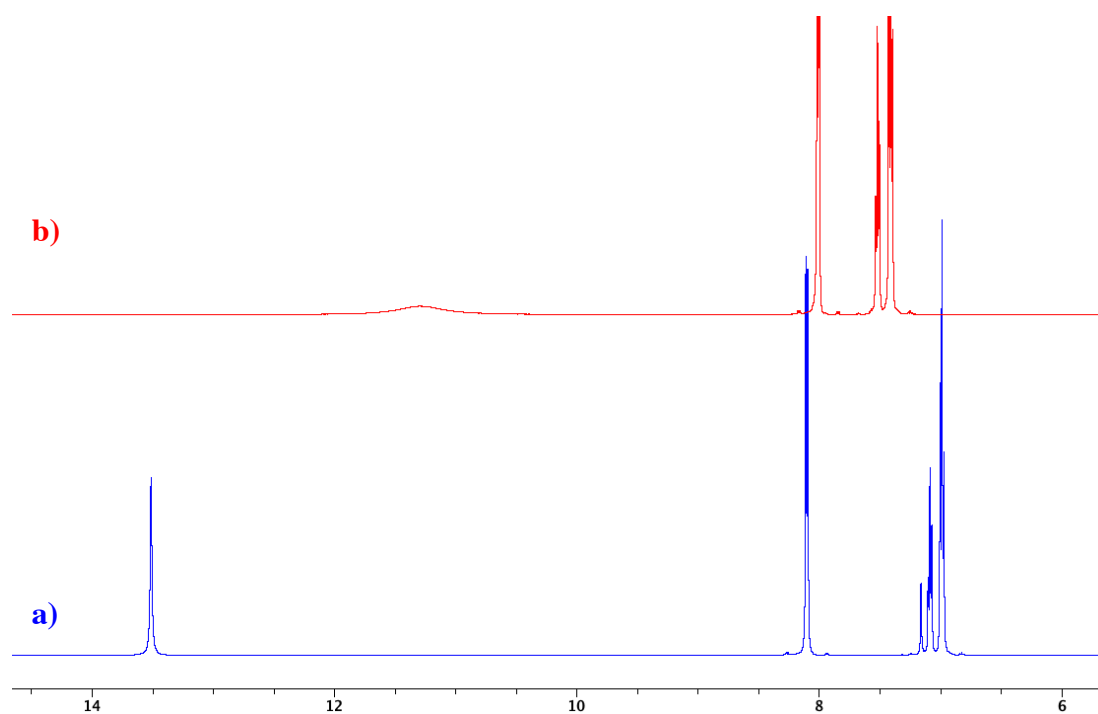


Figure S61. [5]O₂CPh, Variable Temperature ¹H NMR, THF-d₈, 500 MHz.

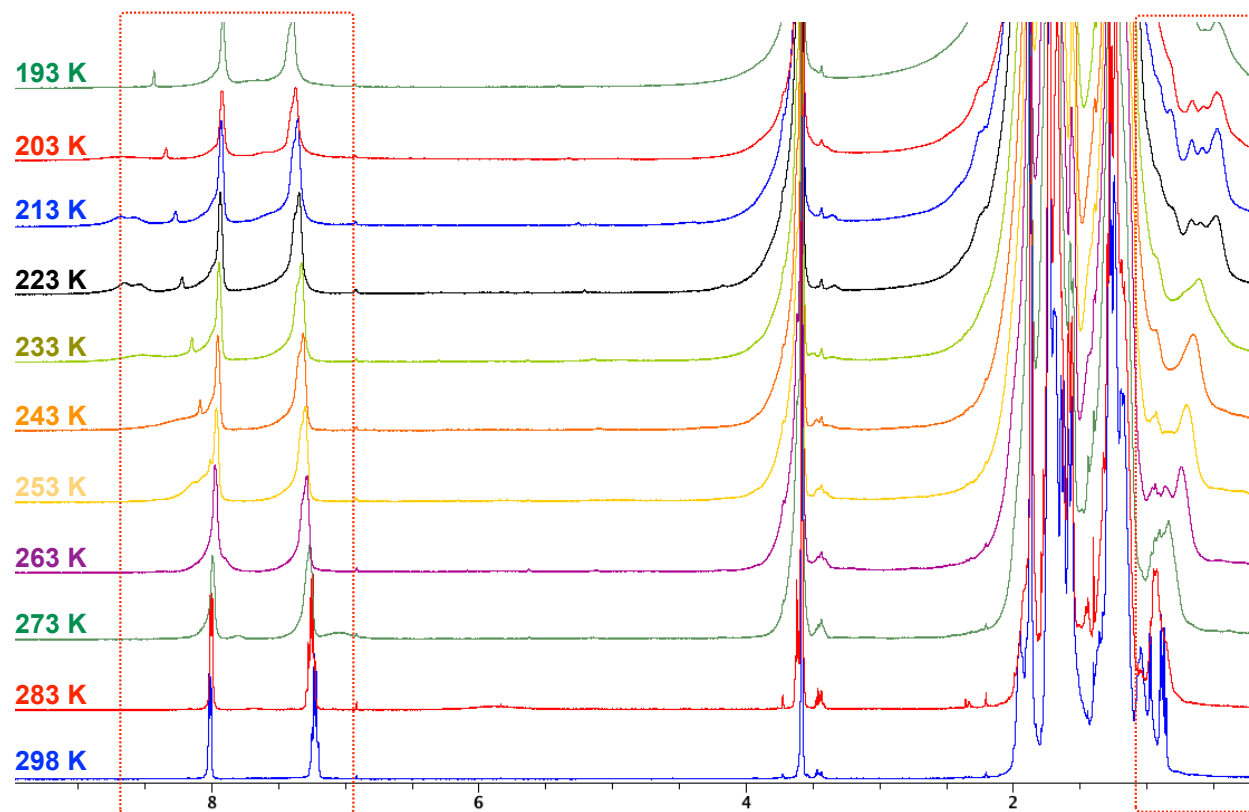


Figure S62. [5]O₂CPh, Variable Temperature ¹H NMR, THF-d₈, 500 MHz (hydride region).

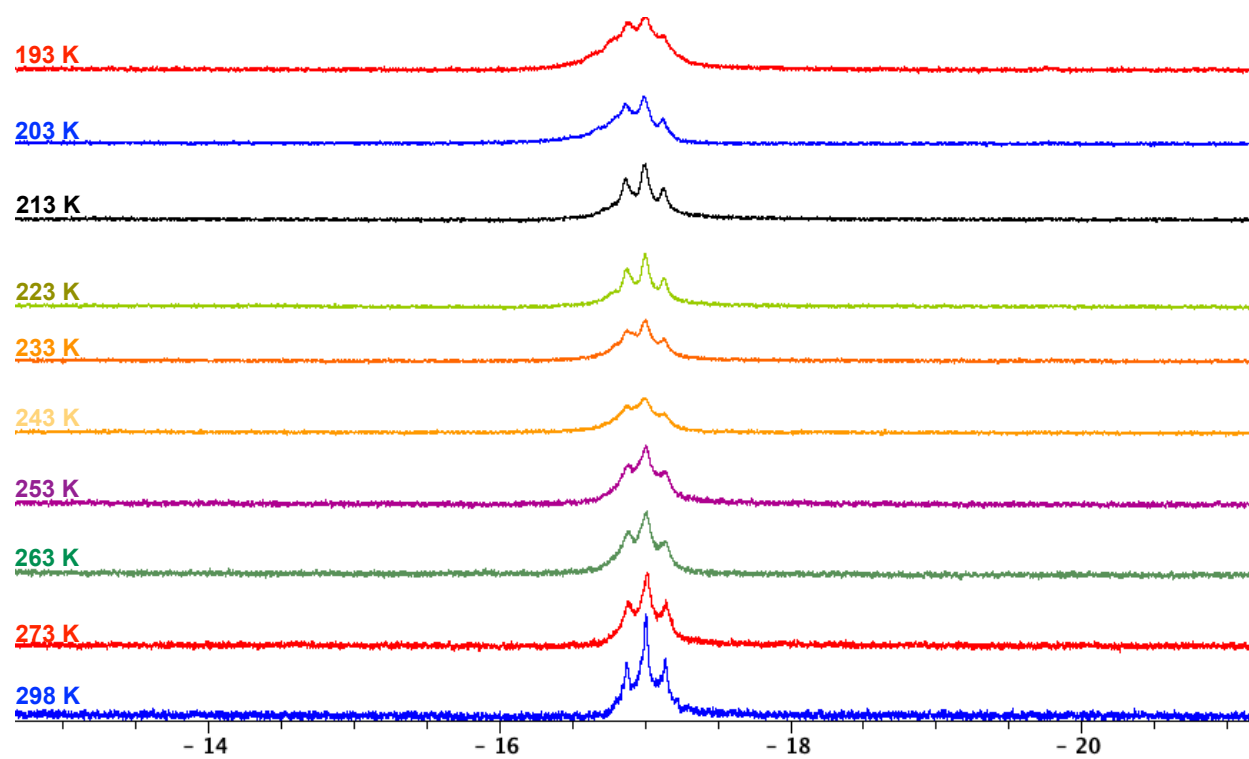


Figure S63. [5]O₂CPh, Variable Temperature ³¹P{¹H} NMR, THF-d₈, 203 MHz.

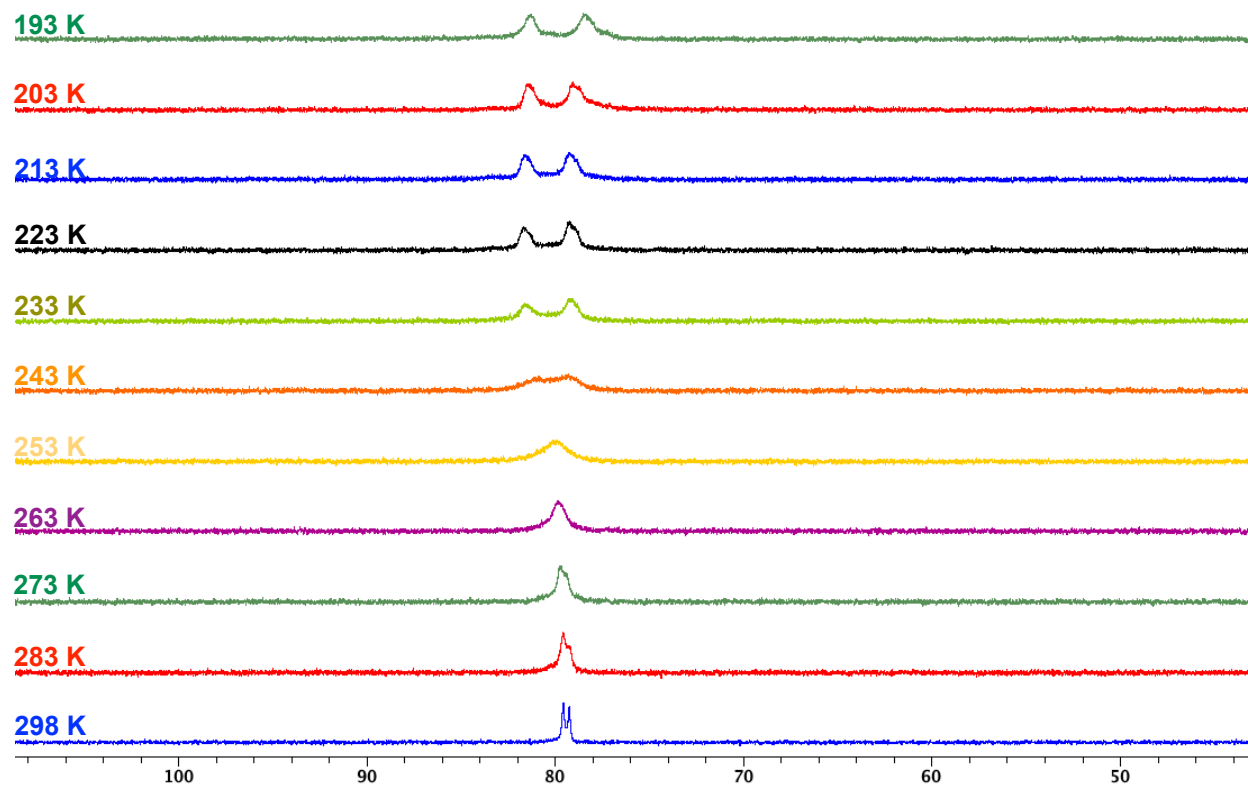


Figure S64. Treatment of **a)** **4** with 4 equivalents of benzoic acid after 4 h showing cyclohexane formation at $\delta_{\text{H}} = 1.40$ ppm and **b)** **4** with 1 equivalent of benzoic acid, ¹H NMR, THF-d₈, 500 MHz.

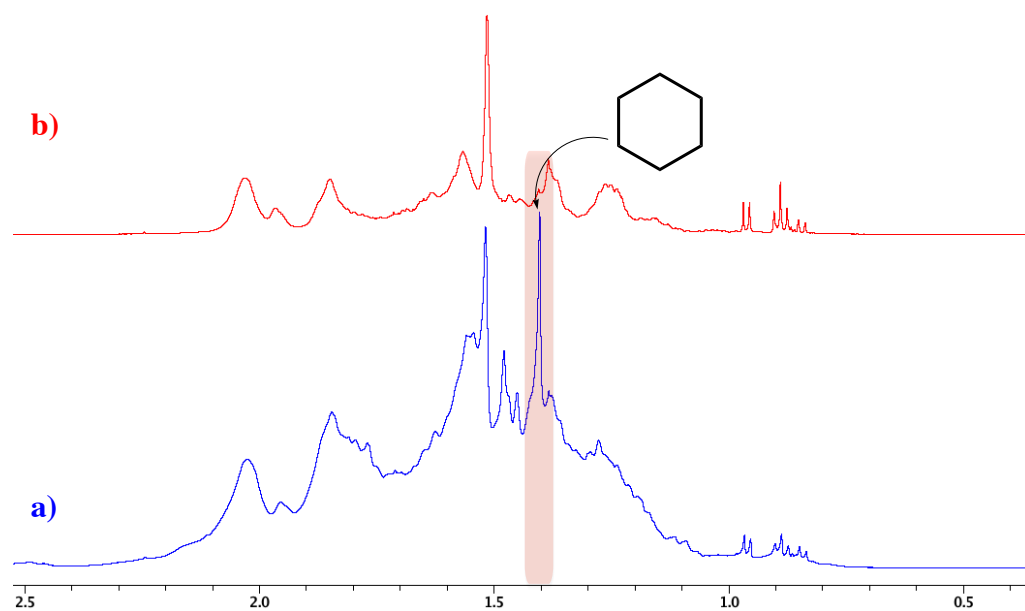


Figure S65. [5]⁺, FT-IR (NaCl plate) spectrum, 298 K, ($\nu(\text{Co}-\text{H}) = 1937 \text{ cm}^{-1}$)

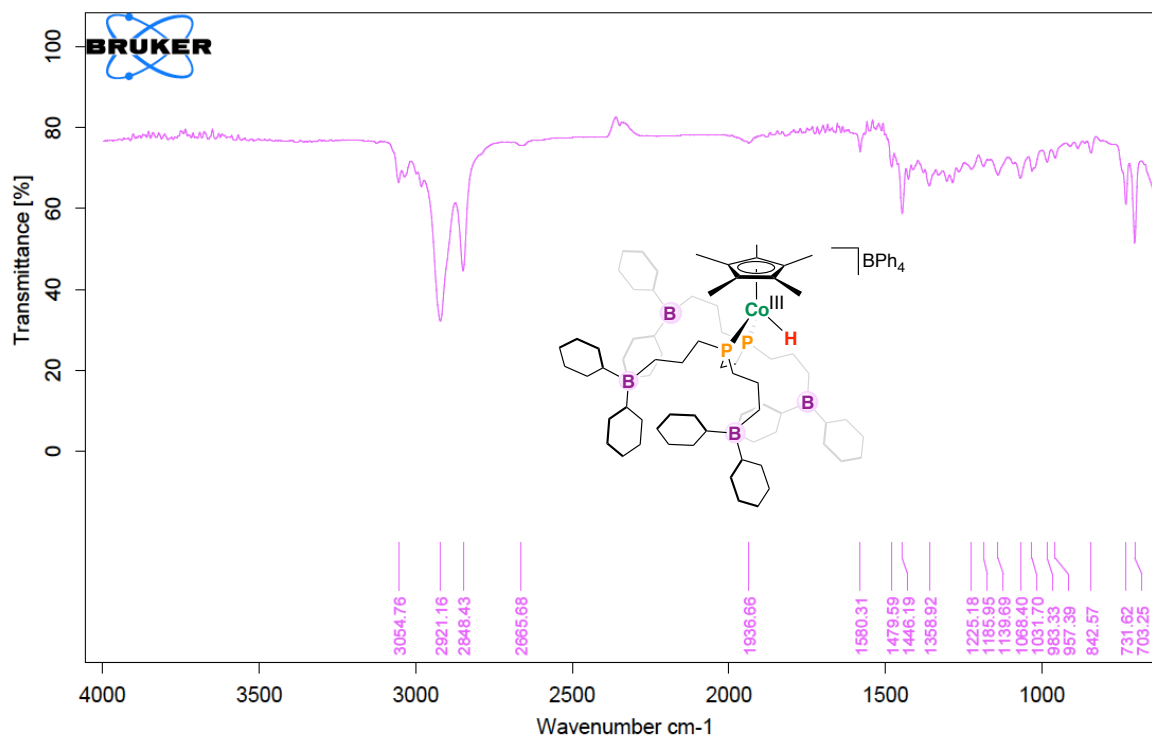


Figure S66. [6]⁺, FT-IR (NaCl plate) spectrum, 298 K, ($\nu(\text{Co}-\text{H}) = 1937 \text{ cm}^{-1}$)

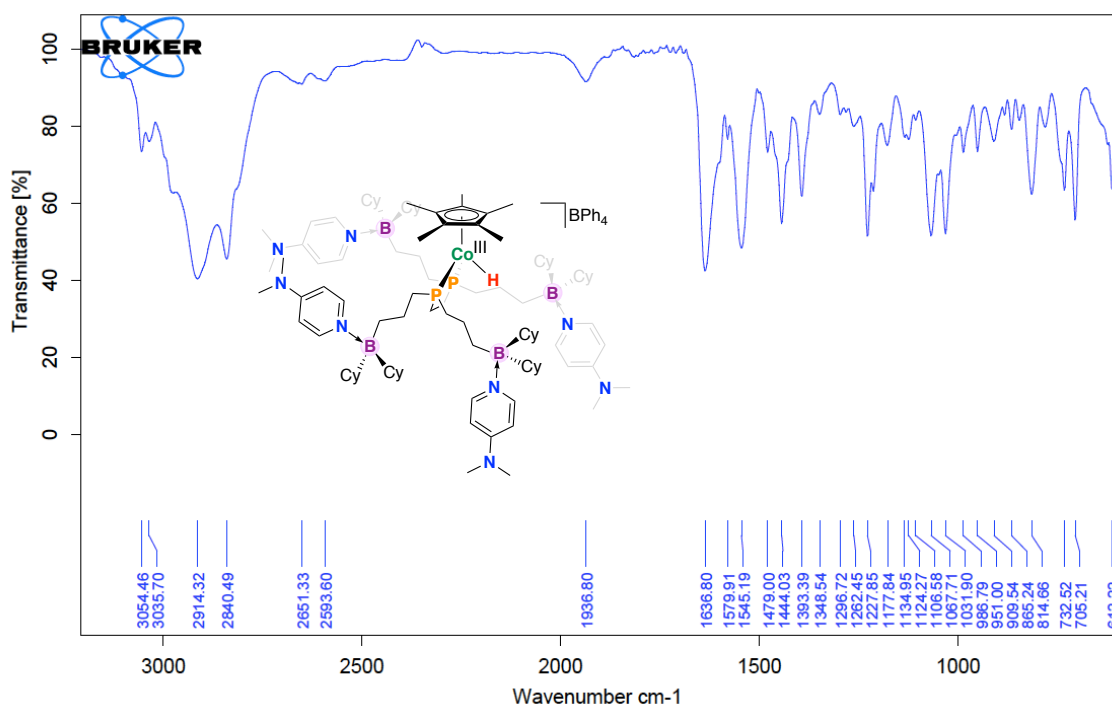


Figure S67. [8]⁺, FT-IR ATR spectrum, 298 K, thin film ($\nu(\text{Co}-\text{H}) = 1939 \text{ cm}^{-1}$)

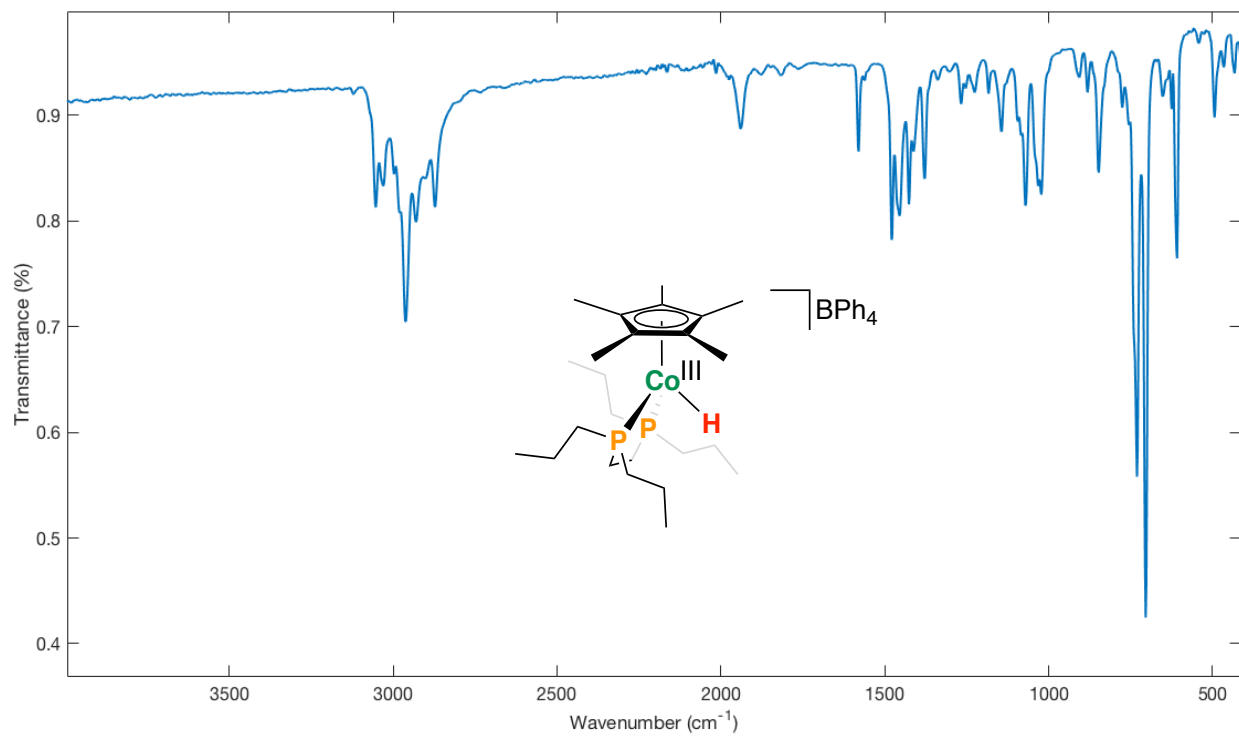


Table S2. Relevant Electrochemical Data

Compound	E_{pc}/V	E_{pa}/V	$\Delta E/V^*$	$E_{1/2}/V$
2 in THF	-1.30	-1.09	0.21	-1.21
	N/A	-0.09	N/A	N/A
2 + 5 equivs. MeCN	-1.29	-1.14	0.15	-1.21
	-0.85	-0.62	0.23	-0.74
[3] ⁺ in THF	-1.40	-1.23	0.17	-1.32
[3] ⁺ in MeCN	-1.41	N/A	N/A	N/A
4	-1.40	-1.14	0.26	-1.31
4 + 5 equivs. MeCN	-1.47	-1.22	0.25	-1.31
	N/A	-0.59	N/A	N/A
[5] ⁺	-1.41	N/A	N/A	N/A
[8] ⁺ 5 equivs. MeCN	-1.32	-1.24	0.08	-1.28
	N/A	-0.61	N/A	N/A
[9] ⁺ in THF	-1.39	-1.23	0.16	-1.31
[9] ⁺ in MeCN	-1.43	-1.35	0.08	-1.39
	-1.13	-1.03	0.1	-1.08

* ΔE was 0.17 V for Fc/Fc⁺ in THF and 0.085 V in MeCN.

Figure S68. Cyclic voltammogram depicting the scan-rate dependence for $[3]^+$ (2 mM analyte, 0.25 M $[N^rBu_4]PF_6$).

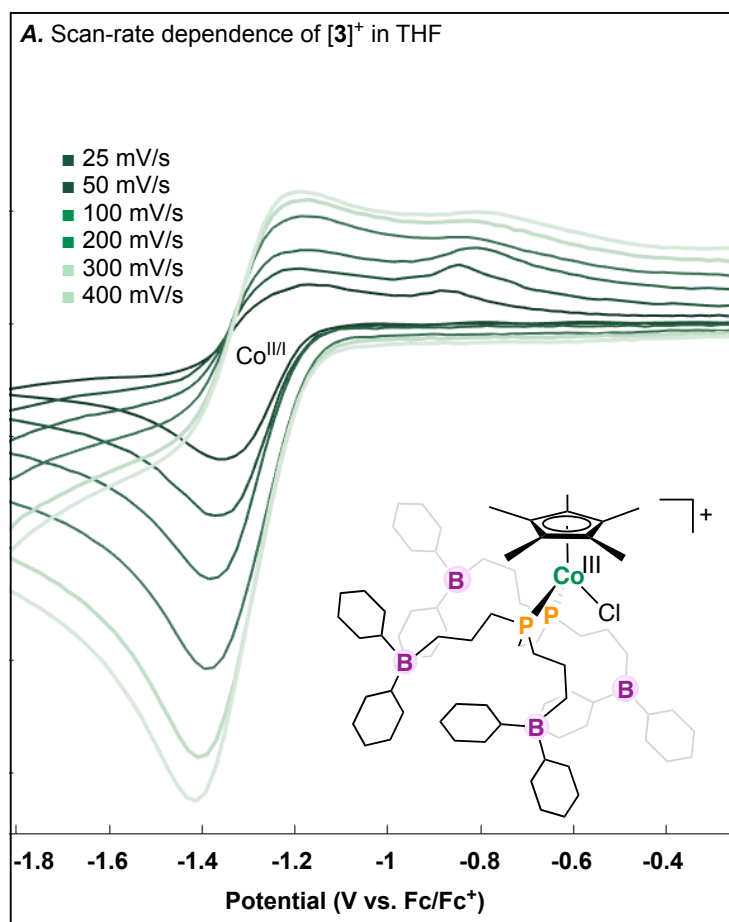


Figure S69. Cyclic voltammograms depicting the scan-rate dependence for [9]⁺ (2 mM analyte, 0.25 M [NⁿBu₄]PF₆).

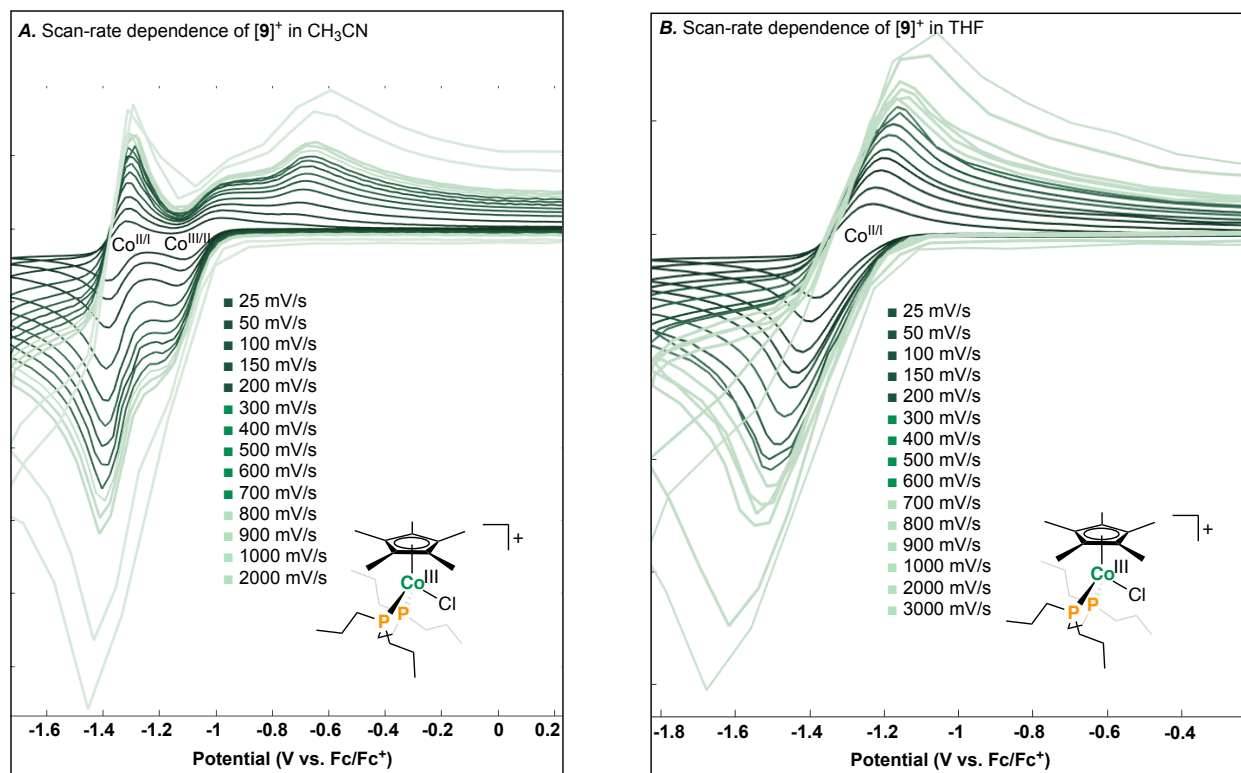


Figure S70. Cyclic voltammograms depicting [5]⁺ (dotted green line) and [6]⁺ (solid orange line) (THF, 2 mM analyte, 0.25 M [NⁿBu₄]PF₆). $\nu = 200$ mV/s.

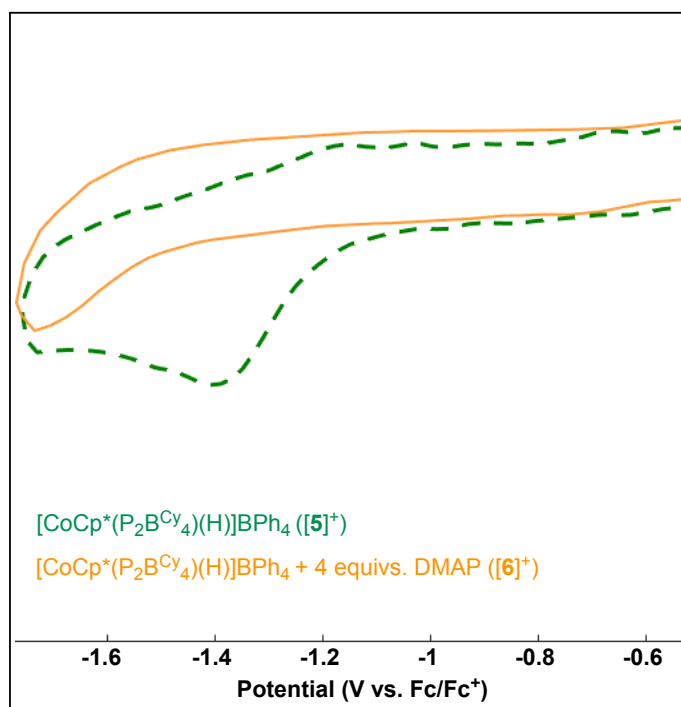
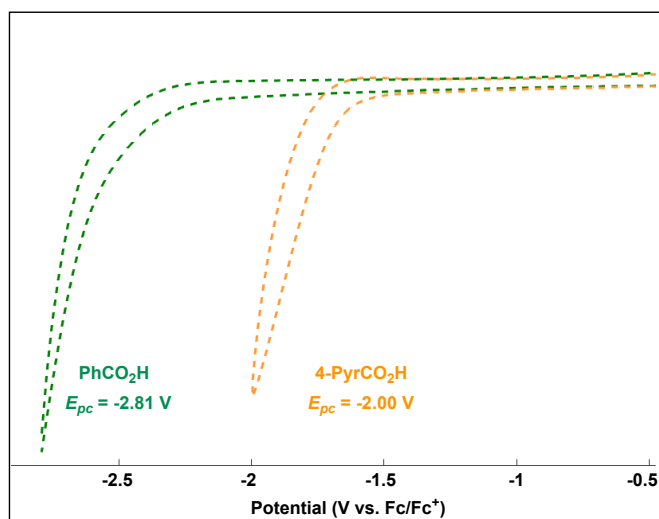


Figure S71. Cyclic voltammograms depicting reductions of benzoic acid (green) and 4-pyridylbenzoic acid (orange) (THF, 2 mM analyte, 0.25 M [NⁿBu₄]PF₆). $\nu = 200$ mV/s.³



³ For a summary of organic redox potentials, see: Roth, H. G.; Romero, N. A.; Nicewicz, D. A. *Synlett* **2016**, 27, 714.

Crystallographic details:

Single crystal X-ray diffraction (scXRD) data for [5]⁺ was collected at the Canadian Macromolecular Crystallography Facility CMCF-BM beamline at the Canadian Light Source.⁴ CMCF-BM is a bending magnet beamline equipped with a Si(111) double crystal monochromator, Pilatus 6M detector, and MD2 microdiffractometer equipped with a Mini Kappa Goniometer. Data for [5]⁺ was collected at 0.675 Å at the CMCF-BM at 100 K.

Cell refinement and data reduction were performed using XDS.⁵ An empirical absorption correction, based on the multiple measurements of equivalent reflections and merging of data was performed using SADABS.⁶ Data conversion from XDS to SADABS file format was performed using XDS2SAD.⁷ Space group was confirmed by XPREP.⁸

The initial model and difference Fourier map for [5]⁺ was obtained with SHELXL-2018.⁹ The crystal structure of [5]⁺ was solved by a combination of direct-methods and real-space refinement. The real-space refinement was performed using COOT.¹⁰ Direct methods refinement was performed with SHELXL-2018⁸ using conjugate-gradient refinement (CGLS) in the initial stages and then by full-matrix least-squares and difference Fourier techniques at the final stages.

All non-hydrogen atoms were refined with anisotropic displacement parameters. Hydrogen atoms, except for the [Co]-H unit in [5]⁺, were placed at calculated positions and refined using a riding model. The [Co]-H unit was not extracted from Fourier electron density map. The compound crystallizes as multicomponent non-merohedral twin. As a result, the structure contains two additional molecules of the compound in a different orientation with about 25% occupancy. Attempts were made to detwin the data and collect other crystals, but none of these attempts yielded a better result. Only heavy atoms of the secondary domain have been assigned in the structure. The unassigned electronic density of lighter atoms of the secondary twinning domain contributes negatively to the refinement parameters but their assignment is complicated by numerous structural overlaps.

⁴ P. Grochulski, M. N. Fodje, J. Gorin, S. L. Labiuk, and R. Berg, *J. Synchrotron Rad.* **2011**, *18*, 681.

⁵ W. Kabsch, *J. Appl. Cryst.* **1993**, *26*, 795.

⁶ L. Krause, R. Herbst-Irmer, G. M. Sheldrick, and D. Stalke, *J. Appl. Cryst.* **2015**, *48*, 3-10.

⁷ XDS2SAD, G. M. Sheldrick, 2008, University of Gottingen, Germany.

⁸ a) XPREP, **2014**, Bruker AXS Inc., Madison, Wisconsin, USA. b) XPREP Version 2008, G. M. Sheldrick, 2008 Bruker AXS Inc., Madison, Wisconsin, USA.

⁹ a) G. M. Sheldrick, SHELXS97, University of Gottingen, Germany 1997; b) G. M. Sheldrick, *Acta Cryst. A* **2008**, *64*, 112; c) G. M. Sheldrick, *Acta Cryst. C* **2015**, *71*, 3.

¹⁰ P. Emsley, B. Lohkamp, W. G. Scott, and K. Cowtan, *Acta Cryst. A* **2010**, *D66*, 486.

The publication materials were prepared using LinXTL¹¹ and Mercury¹² programs. Routine checkCIF and structure factor analyses were performed using Platon.¹³

CCDC 2068546 contains the supplementary crystallographic data for this paper. These data can be obtained free of charge from The Cambridge Crystallographic Data Centre *via* www.ccdc.cam.ac.uk/data_request/cif.

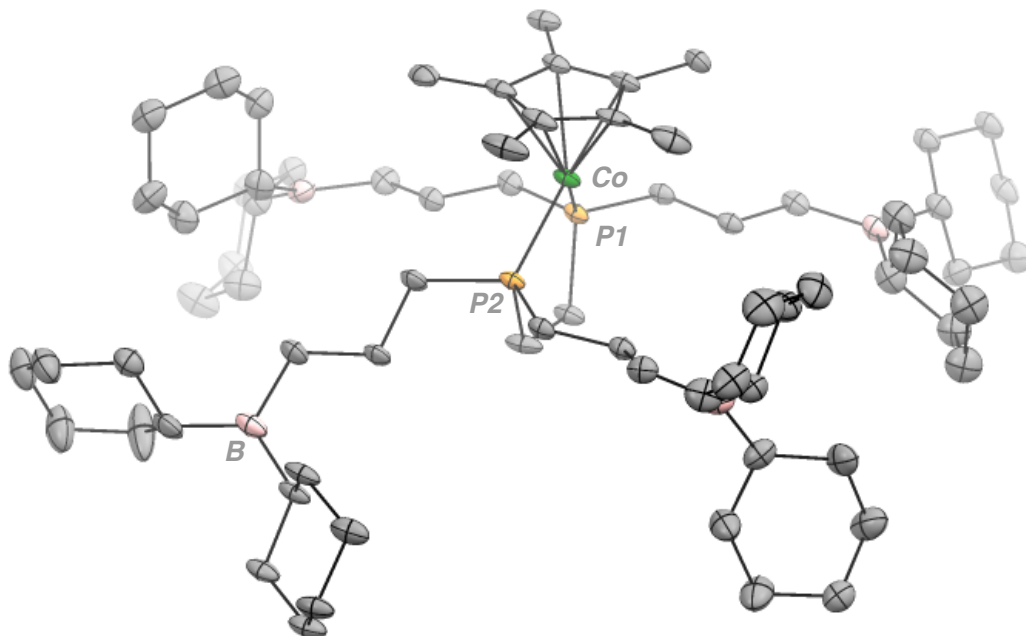


Figure S72. Crystal structure of [Cp*Co(P₂B^{Cy}₄)(H)]BPh₄ ([5]BPh₄). Hydrogens and BPh₄ counterion omitted for clarity, ellipsoids shown at 20% probability. This structure suffers from a high R1-value and provides a heavy-atom connectivity map only.

¹¹ LinXTL, D. M. Spasyuk, 2009, University of Montreal, Canada. <http://sourceforge.net/projects/linxtl/>

¹² C. F. Macrae, I. Sovago, S. J. Cottrell, P. T. A. Galek, P. McCabe, E. Pidcock, M. Platings, G. P. Shields, J. S. Stevens, M. Towler and P. A. Wood, *J. Appl. Cryst.* 2020, 53, 226.

¹³ A. L. Spek, *Acta Cryst.* 2009, D65, 148.

Table S3. Crystallographic data for [5]BPh₄.

Compound	[5]BPh ₄
Empirical formula	C ₇₆₈ H ₁₂₀₈ B ₄₀ Co ₁₀ P ₂₀
Formula weight	12082.37
Temperature/K	100
Crystal system	Monoclinic
Space group	<i>P2₁/c</i>
a/Å	22.927(5)
b/Å	25.816(5)
c/Å	34.235(7)
α/°	90
β/°	96.68(3)
γ/°	90
V/Å ³	20126(7)
Z	1
r/ g/cm ⁻³	0.997
m/ mm ⁻¹	0.251
F(000)	6586.0
Crystal size/ mm ³	0.1 × 0.05 × 0.05
Radiation	synchrotron (λ = 0.675)
2θ range for datacollection/°	1.698 to 47.38
	-27 ≤ h ≤ 27, -30 ≤ k ≤ 30, -38 ≤
Index ranges	l ≤ 40
Reflections Collected	109622
Independent Reflections	35184 [R _{int} = 0.1134, R _{sigma} = 0.1085]
Data/restraints/parameters	35184/6265/1867
Goodness-of-fit on F ²	1.541
R [I>=2θ (I)] (R ₁ , wR ₂)	R ₁ = 0.1811, wR ₂ = 0.4454
R (all data) (R ₁ , wR ₂)	R ₁ = 0.2507, wR ₂ = 0.4964
Largest diff. peak/hole / (e Å ⁻³)	3.82/-0.95

$$R_1 = \frac{\sum ||F_o| - |F_c||}{\sum |F_o|}; wR_2 = [\frac{\sum (w(F_o^2 - F_c^2)^2)}{\sum w(F_o^2)^2}]^{1/2}$$

Computational Chemistry:

All calculations were performed using version 4.2.1 of the ORCA computational package¹⁴ and were run on the Cedar cluster at Simon Fraser University, maintained by Compute Canada.

Geometry optimizations (for Co containing complexes) and the potential energy surface (PES) scan were performed using the TPSS functional with D3(BJ)¹⁵ dispersion correction. The def2-TZVP basis set was used on Co and the def2-SVP¹⁶ basis set on all other atoms. Frequency calculations were performed on all optimized geometries to confirm that each was a true minimum indicated by the absence of imaginary frequencies. The geometries from the PES scan were used as printed. The RI approximation was used to enhance computational efficiency, with an auxiliary basis set *def2/J*¹⁷. *TIGHTOPT* methods were employed. Convergence criteria were met using *Grid4* and *FinalGrid6* integral grid sizes. An .xyz file containing pertinent geometries can be found in the supporting information.

For the carboxylic acid / carboxylate systems discussed in **Scheme 6** of the paper, geometry optimizations were performed at the BP86-D3(BJ)/def2-TZVP level and accurate electronic energies were calculated using the “gold standard” of quantum chemistry (CCSD(T)) at the DLPNO-CCSD(T)/def2-TZVP level of theory. *NormalPNO TIGHTSCF* were used. The RIJCOSX approximation was used to enhance computational efficiency during the DLPNO-CCSD(T)/def2-TZVP jobs. As such, a *def2/J*¹⁷ auxiliary basis set was used. As well, a *def2-TZVP/C* auxiliary basis set was used. ΔG°_{298K} energies were obtained using the electronic energy from the DLPNO-CCSD(T)/def2-TZVP calculations and thermally corrected with the BP86-D3(BJ)/def2-TZVP calculation. An SMD¹⁸ solvent model of THF was used at the BP86-D3(BJ)/def2-TZVP level of theory to account for solvation effects.

¹⁴ F. Neese, "Software update: the ORCA program system, version 4.0" *WIREs Comput. Mol. Sci.* 2017, e1327. doi: 10.1002/wcms.1327

¹⁵ a) S. Grimme, S. Ehrlich, L. Goerigk, *J. Comput. Chem.* 2011, **32**, 1456; b) S. Grimme, J. Antony, S. Ehrlich, H. Krieg, *J. Chem. Phys.* 2010, **132**, 154104;

¹⁶ F. Weigend, R. Ahlrichs, *Phys. Chem. Chem. Phys.* 2005, **7**, 3297.

¹⁷ F. Weigend, *Phys. Chem. Chem. Phys.* 2006, **8**, 1057.

¹⁸ A.V. Marenich, C.J. Cramer, D.G. Truhlar, *J. Phys. Chem. B.* 2009, **113**, 6378.

¹¹B NMR chemical shifts were calculated with reference to BF₃-OEt₂ at the BP86-D3(BJ)/def2-TZVP level of theory. A universal solvation model (SMD) of tetrahydrofuran (THF) was used for all ¹¹B NMR chemical shifts. *Grid6 NoFinalGrid* integral grid sizes were employed. An auxiliary basis set of *def2/JK*¹⁹ was employed as well. ORCA v. 4.2.1 employs the GIAO method for calculating NMR chemical shifts.

$$\delta = \delta_{\text{ref}} - \delta_{\text{targetmol}}$$

The starting geometry used for the PES scan was obtained from the structure of [5]⁺ with all Cy groups truncated to Me except on the boron of interest (Cy groups were maintained on this boron). The same method was used to construct a truncated model of [6]⁺.

Table S4. $\nu(\text{Co-H})$ calculated at the TPSS-D3(BJ)/def2-SVP (def2-TZVP on Co) level of theory.

Compound	$\nu(\text{Co-H}) / \text{cm}^{-1}$
[5] ⁺	2061
Truncated [5] ⁺	2042
Truncated [6] ⁺	2034

Table S5. Calculated ¹¹B NMR chemical shifts referenced to BF₃-OEt₂, calculated at the BP86-D3(BJ)/def2-TZVP level of theory with a universal solvation model of THF.

Compound	Individual ¹¹ B chemical shifts δ / ppm	Average δ / ppm
[5] ⁺	B _A	80
	B _B	78
	B _C	79
	B _D	79
		79

¹⁹ F. Weigend, *J. Comp. Chem.* 2008, **29**, 167.

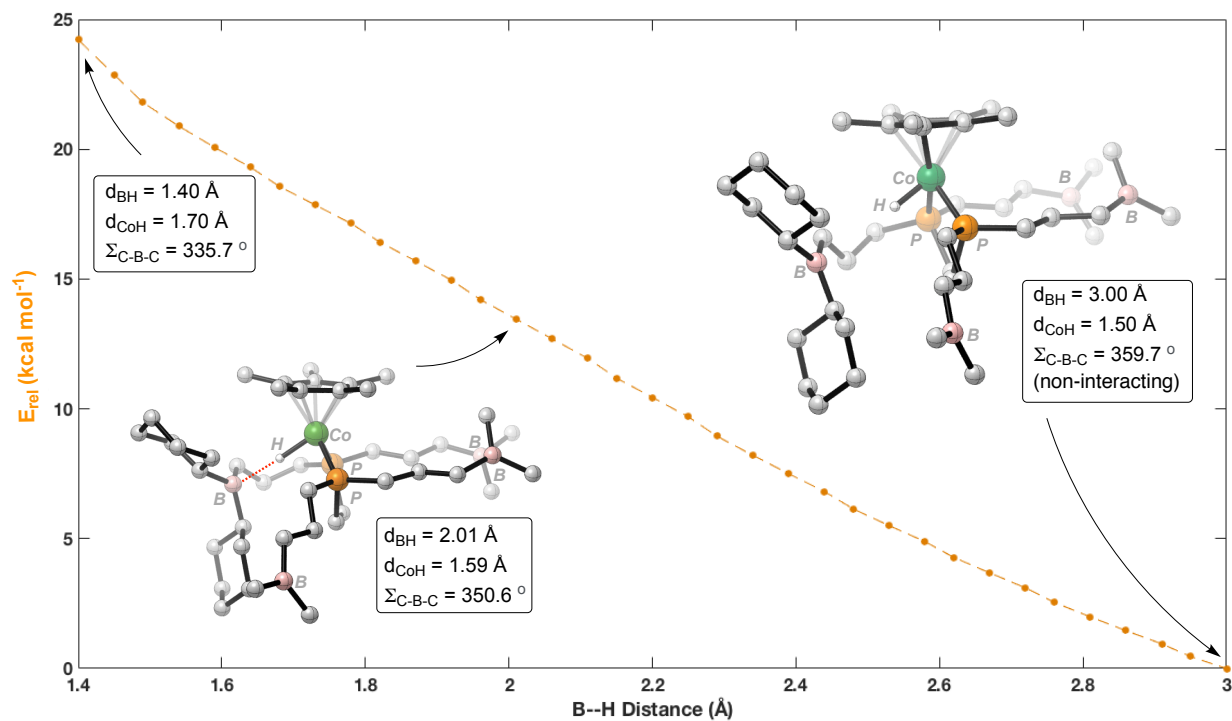


Figure 73. Potential energy surface (PES) obtained by varying the H--B distance from 1.40 to 3.00 Å. Truncated model using three non-interacting $-\text{BMe}_2$ groups and one interacting $-\text{BCy}_2$ group. Structures depicted using CYL view. Structure at 2.01 Å chosen arbitrarily.